Development and Application of Vegetative Buffer Width Modeling using Geographic Information Systems

A Thesis presented to the Faculty of the Graduate School

University of Missouri

In Partial Fulfillment

of the Requirements for the Degree

Master of Science

by

ASLAN ASLAN

Dr. Kathleen M. Trauth, Thesis Supervisor

JULY 2009

The undersigned, appointed by the dean of the Graduate School, have examined the thesis entitled

Development and Application of Vegetative Buffer Width Modeling using Geographic Information Systems

presented by Aslan Aslan,

a candidate for the degree of Master of Science,

and hereby certify that, in their opinion, it is worthy of acceptance.

Dr. Kathleen M. Trauth

Dr. Enos C. Inniss

Dr. Yingkui Li

Acknowledgements

After an amazing journey that spanned the last three years, I am finally here! Although it was slow and treacherous at times, with the blessing of Allah and the help of many people, I arrived with this M.S. Thesis.

Firstly, I would like to express my sincere appreciation to the staff in the Department of Civil and Environmental Engineering at the University of Missouri for their help and direction throughout my education. Many thanks go to my advisor Dr. Kathleen Trauth. Her guidance, assistance, understanding, and encouragement over the past three years have allowed me to progress until this point. I am forever grateful. To Dr. Richard McCuen who initially developed this model, thank you for your invaluable contribution and ideas. To both of my thesis committee members; Dr. Yingkui Li for his help and valuable suggestions in GIS analysis and Dr. Enos Inniss for reviewing my thesis and offering me helpful suggestions and references. I would also like to acknowledge Dr. Hani Salim for all of his advice especially guiding me in determining the equation for the model. My special thanks go to Dr. Allen Thompson for his guidance and friendship during my time here; I wish I could work with you someday, Sir! I would also deeply express my thanks to Dr. Margaret "Maggie" Kinnaird for her professional recommendation; I wish all the best go with you and Dr. Tim O'Brien.

To my "Water Resources" colleagues: Miriam, Matthew, Matt, Yee-Sook, and Jamie; thank you for your friendship. Special dedication and gratitude go out to Janggam, may Allah bless you and your family; Yoki for sharing his ideas in GIS; Isabella and Fernando for their kindness; Farouk, my Nigerian brother, for always saying "yes" when I need you, may Allah bless you and your family and preserve our brotherhood like Moses and Aaron. My profound gratitude goes to the Indonesian communities in Columbia and St. Louis, especially Mas Sri, Eka, Rilya, Akh Arief, and Uda Budzul. I wish each of you and your families all the best. I would like also to thank the "Keluarga" community and the Indonesian Muslim Student Association for their friendship and support, especially Akh Rudi, Akh Yusuf, and Kang Dena.

Finally, I wish to deeply thank my parents, especially ***my mother,*** and my family for their blessings and unfailing support and love, as well as my parents-in-law and their family who enabled me to overcome all the hurdles in my way. Last but not least, affectionately, my eternal gratitude goes to my blessed wife Eka Puspawati for all of her patience, support, and love, jazakillah and my cute children Amru, Faiq, and Dzkiri, for their tolerance, love, and unwavering support. "O my Lord! Grant unto us wives and offspring who will be the comfort of our eyes, and give us (the grace) to lead the righteous."

Financial support for this research was provided by an Environmental Protection Agency, Region 7, Water, Wetlands, and Pesticides grant under contract number CD-98753601.

Table of Contents

List of Figures

Figure

List of Tables

Table

Development and Application of Vegetative Buffer Width Modeling using Geographic Information Systems

Aslan Aslan

Dr. Kathleen M. Trauth

ABSTRACT

It has been widely accepted that vegetative buffers are effective in removing nonpoint source pollutants. However, problems focusing on vegetated buffers studies remain, especially in technical aspects (i.e., how to design appropriate buffers that can provide maximum performance and beneficial for people and ecosystems). In this research, a buffer width design methodology was successfully developed by transforming a graphical-based solution into a GIS-based solution using raster data models to integrate the physical parameters of slope, surface roughness, and soil. The GIS-based methodology will allow decision makers to move beyond rules-of-thumb for buffer requirements to incorporate site-specific parameters because a site-specific evaluation of performance could potentially require wider or narrower buffer widths in order to meet certain stormwater management criteria. This method was successfully demonstrated within the LaBarque Creek watershed located southwest of St. Louis, Missouri for three different scenarios: (1) utilization of GIS for delineating required buffer widths; (2) utilization of GIS for calculating trapping efficiencies for sediment; and (3) utilization of GIS for determining the volume of infiltrated stormwater per foot width of a buffer strip. The results show that the required widths from a variable buffer delineation respond dynamically to the changes in physical characteristics of the research sites.

Keywords: nonpoint source pollutants; buffer width modeling; physical parameters; GIS

Chapter 1:
INTRODUCTION

1.1 Background

Land alteration in the last few decades, such as extensive logging and urban development, has increased impervious surfaces, resulting in increased stormwater runoff rates and volumes (Wenger 1999; Freeman and Ray 2001). For example, studies regarding the effects of urban growth on surface runoff in the Zhujiang Delta of southern China found that the depth of surface runoff increased by 8-10 mm annually from 1989 to 1997 (Weng 2001). These developments will potentially influence water quality in streams, rivers and lakes by introducing nonpoint source pollutants that are transported along with stormwater runoff. Consequently, there is an urgent need to ensure that this development occurs with minimal impact on stream quality. One tool that local authorities have to help them keep waters healthy is the ability to implement land use regulations, i.e., to utilize vegetative buffers. Buffers can be used to cost-effectively control and minimize the effects of stormwater runoff, soil erosion, and nonpoint source pollution. Buffers can be effective because a buffer zone allows stormwater runoff and associated pollutants to be reduced before reaching surfaces waters via infiltration, adsorption, uptake, decay, filtering, and deposition (Tollner et al. 1976; Karr and Schosser 1978; Lowrance et al. 1985).

A buffer is defined as a vegetated zone located between natural resources (e.g., rivers, lakes, and coastal areas) and adjacent areas subject to human alteration. In addition to being an economical method to reduce stormwater runoff and the associated nonpoint source pollutants, buffers can be designed to provide other benefits to people and the

environment (Wong and McCuen 1982; Lowrance et al. 1998). For instance, most natural buffers are part of riparian ecosystems, which contain a diversity of plants and animals. This fact shows how important this land is not only for humans but also for plants and animals. Thus, managing these areas in concert with development is also an essential consideration in maintaining a harmonious relationship between humans and nature.

In general, vegetated buffer design consists of three zones (Figure 1) (Welsch 1991). Zone 1 begins at the stream edge and extends away from the stream for between 15 and 25 feet. It consists of a mature forest for shade and woody debris and deep root systems that provide streambank stabilization. Moreover, vegetation in this particular zone reduces flood effects and removes some sediment and nutrients. The extent of Zone 2 is from 10 feet up to several hundred feet, depending upon several factors: the objectives of the buffer, stream type, soil type, and topography. Vegetation in this zone consists of shrubs and slow growing trees with less deep roots with the primary function being the removal of sediment and pollutants from surface and groundwater. Zone 3 is the farthest zone from the stream with the primary function of providing initial protection for the buffer by splitting concentrated flow into sheet flow. Grass or herbaceous plants dominate the composition of vegetation in this zone.

Vegetated buffer zones have also been called streamside management zones (SMZ), stream protection zones (SPZ), and riparian management zones (RMZ) when applied to managing agricultural areas as a part of best management practices (BMPs) (Figure 2) (U.S. Environmental Protection Agency [USEPA] 1976; Hollabaugh 2006). However, in order to be effective, a vegetated buffer strip must be created in such a way that encourages sheet flow (the portion of precipitation that moves initially as overland flow

in very shallow depths before finally reaching a stream channel) and reduces the likelihood that concentrated flow will develop (Davis and McCuen 2005).

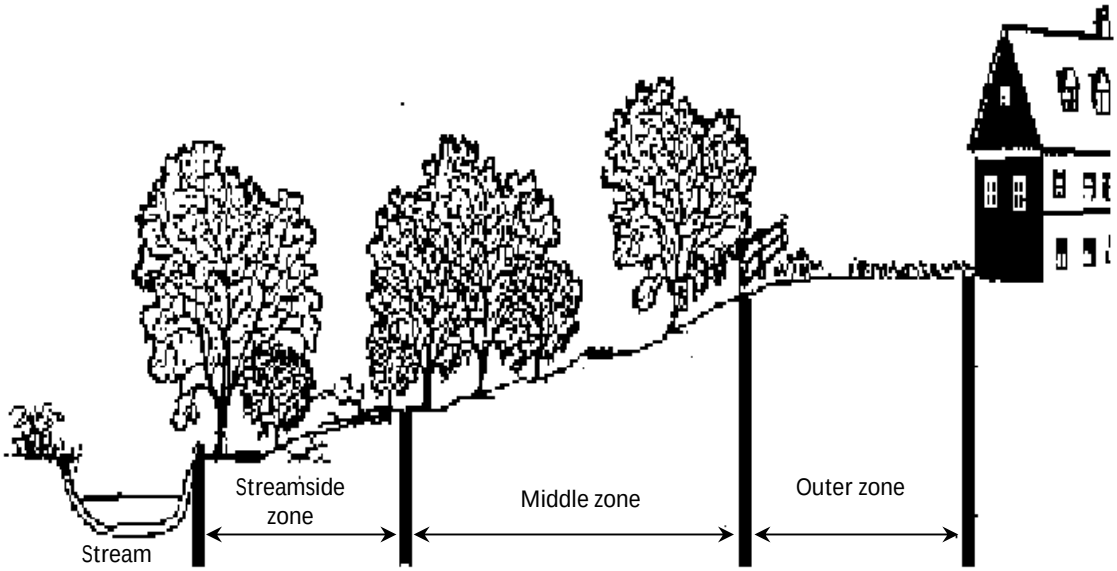

Figure. 1 A depiction of a three-zone buffer (EPA 2009, adapted from Welsch 1991)

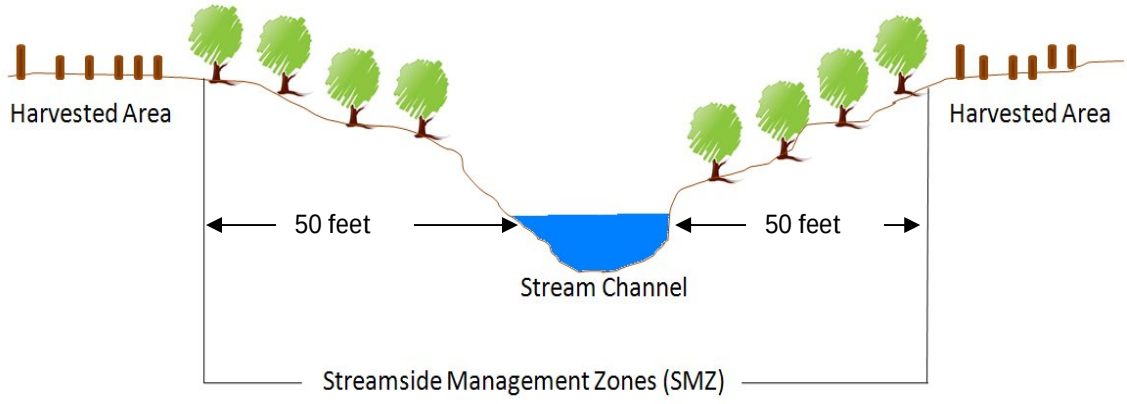

Figure. 2 Streamside Management Zones (after Hollabaugh 2006)

In the United States, vegetated buffers are regulated under Section 404 of the Clean Water Act (CWA) and/or Section 10 of the Rivers and Harbors Act of 1899 as a component of compensatory mitigation plans undertaken to meet permit requirements. The Rivers and Harbors Act of 1899 is the oldest federal environmental law in the United

States and was passed by Congress in 1882, while the Clean Water Act is a 1977 amendment to the Federal Water Pollution Control Act of 1972. The CWA is the primary federal law regarding discharges of pollutants to waters of the United States. In addition, although many activities covered by the Rivers and Harbors Act are regulated under the Clean Water Act, the 1899 Act retains independent vitality.

The U.S. Army Corps of Engineers (USACE) administers a CWA authorized permit program that requires proper and feasible compensatory mitigation to offset unavoidable impact to aquatic resources by replacing aquatic resource functions lost as a result of activities (National Wetlands Mitigation Action Plan 2009). Despite the fact that some local governments have developed their own stream buffer ordinances (e.g., Baltimore County, Maryland) others have not yet established them out of fear that without valid scientific support such regulations would not be legally defensible (USEPA 2009; Wenger 1999).

Nowadays, the rapid increase in computer modeling techniques and technologies including geographic information systems (GIS) has assisted scientists and engineers in conducting spatial analysis studies (e.g., buffer width-modeling studies). In general, any GIS model requires four components. The first component is the set of input parameters input in the form of geospatial data (i.e., data that have x and y coordinates). A second component is an empirical model that incorporates the input parameters. Third are the tools for spatial analysis (i.e., hardware and software for conducting mapping, analysis and visualization), while the fourth is the human input as to the type and method of spatial analyses to conduct, which is the most important factor in performing GIS analyses to address important issues. With regard to buffer modeling studies, the ability

of GIS to perform spatial analysis from different geospatial data inputs makes GIS undoubtedly a useful tool to analyze this problem.

1.2 Statement of problem

Even though vegetated buffers are regulated under section 404 of the CWA and/or Section 10 of the Rivers and Harbors Act of 1899 as a component of compensatory mitigation plans, problems focusing on vegetated buffers studies are still not yet solved. Problems remain from the technical point of view, and also with the regulations themselves. Nonetheless, among all those problems, the most interesting and important one is how to design vegetated buffers that can produce a win-win solution for the various parties associated with this issue (e.g., local authorities, landowners, and ecosystem managers).

As a part of the engineering process, one of the most common tools in any engineering analysis is to produce an efficient and accurate model. However, in regard to buffer modeling studies, most of the existing guidelines for buffer delineation assume that several factors including size and slope of the buffer, resistance to flow, and infiltration capacity that affects buffer effectiveness are constant (Phillips 1989). In fact, the physical characteristics such as soil properties, slope steepness, and surface roughness respond differently to overland flow. Therefore, at this point, the width of a buffer might not have to be constant along the flow path toward a stream in order to achieve the required consistent performance. Buffer widths are impossible to determine precisely, but by developing a design model that accurately incorporates and describes the physical characteristics of the landscape as well as hydraulic and hydrologic principles, one can significantly increase the probability of an appropriate buffer width determination.

Furthermore, the design model must also consider pre-development and post-development scenarios because problems can arise in the design process due to the fact that there may be a limited area for installing the buffer because of existing development. In addition, four questions should be addressed properly in designing a buffer width:

(1) How to determine the required buffer width based upon scientific principles rather than rules-of- thumb (e.g., 100 feet)?

(2) How effective is a given buffer strip in trapping sediment and infiltrating runoff?

(3) How wide should a buffer be to achieve a required level of trapping efficiency?

(4) What are the appropriate tools to achieve these goals?

Wong and McCuen (1982) developed a model to determine the effectiveness of buffer widths via a series of nomographs resulting from a combination of Manning's equation, Stoke's Law, and the minimum infiltration rates of hydrologic soil groups by considering the relative influence of different physical parameters (i.e., slope, surface roughness, and soil characteristics). This model was successfully demonstrated within a 47.7 acre watershed in Montgomery County, Maryland (Wong and McCuen 1982). Other student researchers at the University of Missouri have also demonstrated the basic use of this model within the LaBarque Creek watershed in Missouri by utilizing GIS based on discrete data inputs in a vector data model (i.e., point by point data). However, neither of these efforts was conducted over a continuous surface using a raster data model for evaluating the effectiveness of the model utilizing GIS analysis.

1.3 Objectives of study

The major goal of this research is to develop a GIS methodology for buffer width delineation by considering the physical parameter inputs of slope, surface roughness, and soil information on a continuous surface, the output of which can be used as guidance for decision makers in formulating stream buffer ordinances. This analysis of buffer width is based upon the criteria of stormwater runoff infiltration and the trapping efficiency for sediment removal. Further, this methodology will allow decision makers to go beyond rules-of-thumb for buffer requirements to incorporate site-specific parameters, because a site-specific evaluation of performance could potentially require a wider or narrower buffer width in order to meet certain stormwater management criteria. In addition, the major goal has been elaborated into two principal objectives.

1. To develop an empirical model derived from the nomograph created by Wong and McCuen (1982). Currently, a model can only work within the GIS environment if the model can be transformed into a mathematical equation because GIS analysis is arithmetically based. The transformation process will be further described in Chapter 3.
2. To demonstrate the use of the developed empirical model for vegetative buffer performance by applying it via a GIS analysis utilizing a raster data model in the LaBarque Creek watershed in Missouri. The design process could utilize either one of two approaches: first, determining the required buffer width to “treat” incoming stormwater runoff from specified contributing areas; or second, determining the treatment capacity for a given buffer width in trapping sediment and infiltrating stormwater runoff.

1.4 Thesis organization

Following this introductory chapter, Chapter 2 provides a literature review of past research pertaining to this study, including a brief history of buffer applications. It is a review of recent research regarding buffers and their effectiveness in removing pollutants, infiltrating stormwater runoff, and trapping sediment. This chapter also discusses GIS and potential applications in buffer modeling studies.

Chapter 3 describes the methodology used in this study. It begins with the description of study area (i.e., the LaBarque Creek watershed), followed by a discussion of the development of the GIS methodology using raster data analysis for applying the vegetative buffer strip model developed by Wong and McCuen (1982). The methodology includes three separate parts: (1) development of an empirical model describing sediment deposition and stormwater infiltration, (2) development of a spatial database, and (3) development of a GIS process for calculating appropriate buffer widths or determining the "treatment capacity" of an existing buffer.

Chapter 4 demonstrates the implementation of the analysis methodology developed in Chapter 3 for a specific watershed. It consists of three parts: (1) a determination of the required buffer width based upon an input of physical parameters and assumed trapping efficiency, (2) a determination of sediment trapping efficiencies based upon a given buffer width, and (3) a determination of the depth of stormwater infiltration based upon a given buffer width.

Chapter 5 presents the conclusions that have been derived from this research and includes a number of recommendations for future research.

1.5 Chapter summary

This chapter began with an overview of the historical impact of land alteration in the last few decades such as increases in the rates and volumes of surface runoff that potentially decrease water quality. The chapter then discussed the beneficial use of a vegetative buffer as a part of BMPs that can be implemented as one solution for such problems. The chapter also introduced the use of GIS, especially its spatial analysis capability, for conducting buffer modeling. The chapter continued by raising several important questions for designing buffer width, as well as introducing a vegetative buffer model that has been previously developed as a fundamental base of this research. A discussion of the major goals of this research were presented next, and finally the chapter ended by describing how this thesis is organized.

Chapter 2:
LITERATURE REVIEW

2.1 A brief history of buffer applications

Although the term agricultural buffer was not widely used until the 1970s, the concept of retaining uncultivated land between and within productive fields has been around for centuries. According to Vought et al. (1995), until the 19th century, agricultural landscapes throughout Europe contained features such as riparian forests, wetlands, and hedges. In the United States, many natural features also remained in rural landscapes even after much of the land was settled and developed for agriculture. Along with intensification of agriculture and introduction of clay drainage tiles in the mid-1800s, many of these natural ‘‘buffers’’ were removed and crops were planted in their place. In this period, at the same time that drainage tiles were increasingly adopted, soil erosion was becoming a problem in areas that had been continuously farmed (Vought et al. 1995).

In a book entitled Soil Conservation, Bennett (1939) introduced several soil conservation practices including vegetative control of gullies, vegetative waterways, and contour strip cropping. He also suggested retaining forest areas and planting trees to help control stream bank erosion. In the 1940s and 1950s, windbreaks, or shelterbelts, gained popularity for reducing wind erosion around farmsteads and fields. During that period, grassed waterways and vegetation along streams and roadsides were also promoted to combat soil erosion (Kohnke and Bertrand 1959). Prior to the 1970s, few studies evaluated water quality benefits from conservation buffers (Correll 1996). Furthermore,

since the mid-1970s, researchers have demonstrated the ability of buffers to remove nitrates (Osborne and Kovacic 1993), remove phosphorus (Lee et al. 2000), trap sediment (Karr and Schosser 1978), and remove herbicides (Correll 1996). Today, one can find a wide range of functions and designs that exist for the different conservation buffers in agricultural settings. Regardless of buffer type, the main goal of incorporating conservation buffers into agricultural landscapes has not changed, i.e., to improve ecosystem health.

2.2 The effectiveness of vegetative buffers strips

2.2.1 Sediment trapping

Sediment trapping efficiency can be defined as the capacity of a buffer to retain a fraction of sediment from the incoming runoff. A vegetative buffer should be viewed as an essential component of a comprehensive, performance-based approach to sediment reduction because suspended sediment affects stream habitat and water quality by reducing water clarity for sighted organisms and reducing light penetration for plant growth (Wenger 1999). The amount of sediment reaching a buffer strip not only depends on rain intensity and duration, but also soil type.

Scientific research has shown that vegetative buffers, especially riparian buffers, are generally very effective at trapping sediment from surface runoff and at reducing channel erosion; a buffer removes sediment by decreasing its velocity and allowing particles to settle (Wong and McCuen 1982; Wenger 1999). The effectiveness of a vegetative buffer is influenced by various factors, e.g., buffer width, vegetation types, slope gradient and length, flow convergence, source area, and pollutant concentration (Herron and Hairsine 1998). Further, trapping efficiency also depends upon the soil type from which sediment

was produced, rainfall energy as a primary force of aggregate dispersion, and sediment particle size, because the effectiveness of buffers is reduced as sediment size decreases (Lee et al. 2000).

Studies regarding buffer width and its efficiency in trapping sediment have yielded a range of recommendations. According to Wenger (1999), the absolute minimum width for a buffer cannot be less than 9 m (30 ft). For short-term periods, buffers as narrow as 15 ft (4.6 m) have proven effective, although wider buffers provide greater sediment control, especially on steeper sloped areas (Wenger 1999). Long-term studies recommend the need for wider buffers, and a 100 ft buffer is sufficient enough not only to trap sediments under most circumstances, but is also beneficial in maintaining healthy biota (Castelle et al. 1994; Wenger 1999). However, this width may be expanded by counting factors such as steep slopes and land uses practices that yield excessive erosion. Additionally, for maximum effectiveness, buffers must extend along all streams, including intermittent segments, because the effectiveness of a network of buffers is directly related to its extent. Governments that do not apply buffers to certain classes of streams should be aware that such exemptions reduce benefits substantially (Wenger 1999).

2.2.2 Stormwater infiltration

As mentioned previously, while the main function of a vegetative buffer is to trap sediment, the buffer also performs a secondary function, i.e., reducing the volume of stormwater runoff reaching a stream through infiltration of the water into the underlying soil (Wong and McCuen 1982). The infiltration capacity among areas within the buffer zone will vary depending upon four factors: type and condition of the vegetative cover,

the properties of the underlying soil, the intensity of rainfall, and antecedent soil moisture conditions (Wong and McCuen 1982; Phillips 1989; Lee et al. 2000). Furthermore, because the process of infiltration is complex (i.e., time variable and dependent on the hydraulic conductivity of the transmission zone), the rate at which a soil may absorb water will vary with time, decreasing in an exponential pattern until a final infiltration rate is achieved (Wong and McCuen 1982; Phillips 1989). In addition, the ability of vegetation within the buffer strip to decelerate flow has the effect of decreasing the velocity of runoff, resulting in increases in the detention time of overland flow. Thus, the increase in detention time results in increased opportunity for infiltration. Different types of vegetative cover will significantly influence the velocity of flow due to different values for Manning's n (Wong and McCuen 1982).

2.2.3 Nutrient removal

Large quantities of nitrogen and phosphorus can enter streams and wetlands areas from different sources such as agricultural runoff, sewage effluent, and runoff from fertilized areas. These and other sources are a major problem throughout the world (Sharpley et al. 2001; Melcher and Skagen 2005). Several factors effect the rates and extents of nutrient transport. Examples are the intensity and duration of precipitation, temperature, antecedent soil moisture, percent cover of residual vegetation, soil type, and slope (Melcher and Skagen 2005). According to Parkyn (2004), there is clear evidence that vegetative buffers, especially riparian buffers, can be effective at removing nutrients and sediment from surface and subsurface flow paths. The dense vegetation associated with a buffer reduces surface flow velocity, causes deposition of sediment and particulate nutrients, and promotes the infiltration of water and associated contaminants into the soil.

In addition, wetland areas adjacent to a stream, with the characteristic low-oxygen, organic-rich soils, help remove nitrate through the denitrification process where microbes convert nitrate to nitrogen gas. Furthermore, plants themselves take up dissolved nutrients to grow. Planted buffer zones have been shown to be most effective for dissolved nutrient removal when subsurface flow paths cross the root zone of trees before reaching the stream (Parkyn 2004).

2.2.3.1 Nitrates

A number of studies have shown impressive removal rates of over 90 percent of the soluble nitrate travelling through buffer zones (Parkyn 2004). Nitrogen removal by buffers strips depends on the complex interaction of spatially variable components of a buffers system including plants, buffer width, microbial communities, soil properties, and hydrologic flow paths (Wenger 1999). Buffers should be preserved along as many streams as possible, and it is especially important to preserve riparian wetlands, which are sites of high nitrogen removal. Even though the width required to optimize nutrient removal has been debated by scientists, a minimum 15 m (50 ft) of buffer width is probably necessary for most buffers to reduce nitrogen levels. However, wider buffers of 30 m (100 ft) or greater would be more likely to include other areas of denitrification activity and provide for more nitrogen removal (Wenger 1999). Another study (Fennessy and Cronk 1997) investigating the effectiveness of riparian buffer zones for removal of contaminants, especially soluble nitrate, found that a 20-30 m wide buffer can remove almost 100% of nitrates, while buffers of a 10 m (33 ft) width achieved over 70% retention of nitrogen.

There are conflicting reports on the ability of various plants to remove nitrate from stormwater runoff. For instance, Osborne and Kovacic (1993) found that on an annual basis, grass riparian buffers were less effective in removing nitrate than forested riparian buffers, partly through uptake by plants and denitrification. According to Borin and Bigon (2002), a narrow composition of buffer which consists of 5 m of a grass filter strip and a 1 m wide row of deciduous trees has been shown to reduce nitrate in subsurface flows underneath cropland in Italy. Furthermore, Corley et al. (1999), examining the effect of type and height of grassy riparian vegetation, found that there was no consistent difference among the species in the removal of nitrogen and phosphorus. According to Geyer et al. (1992), higher denitrification potential existed in the bottom of slopes; thus, indicating that there was a topographical control over nitrate removal. Moreover, by considering spatially variable attributes of buffer locations such as hydric soil status, geomorphology, and landscape controls, one can significantly improve nitrogen interception (Wenger 1999).

2.2.3.2 Phosphorus

In agricultural fields, phosphorus is one of the primary surface runoff pollutants. Phosphorus exists in many forms in soil, water, and sediment. When runoff occurs, the form of phosphorus is generally divided into particulate and dissolved fractions. Phosphorus from fertilizers and manure is commonly adsorbed by soil particles and organic matter in the runoff entering buffer strips; thus, its removal from runoff is closely associated with the retention of suspended sediment (Abu-Zreig et al. 2003).

Riparian buffers have been found to be effective in removing phosphorus from cropland runoff. For example, Lim et al. (1998) reported that phosphorus removal rates

from surface runoff leaving riparian buffers can be as high as 93%. However, a majority of studies conducted under a variety of vegetation types and widths of buffers reported rates of 60-90% (Line et al. 2000). According to Wenger (1999), riparian buffers do not provide long-term storage and are not effective at filtering soluble phosphate even though they can effectively trap phosphorus in runoff. As was the case for nitrate removal and sediment trapping, riparian buffer zones should be installed on all levels of streams. In terms of the effectiveness of plants in removing phosphorus, both forested and grassed buffers are similarly useful. Because of their limitations, riparian buffers should not be viewed as a primary tool for reducing phosphorus loading of streams; instead, every effort should be made to reduce phosphorus inputs at their sources (Wenger 1999). This objective can be accomplished through effective erosion control methods, proper placement of buffers, judicious application of fertilizers, inspection and maintenance of sewer lines, and restrictions on the land application of waste from concentrated animal feeding operations.

2.2.4 Other Pollutants

Other contaminants, including pesticides and heavy metals, vary tremendously in their degradation rates and toxicity levels. Every effort should be made to reduce these pollutants at their source, and it is wisest to prohibit sources within the floodplain, regardless of buffer width (Wenger 1999). Buffers alone are limited in their capabilities to protect streams within watersheds from these contaminants carried in stormwater runoff (Melcher and Skagen 2005). Buffers can normally handle stormwater runoff from small storms; however, larger events can exceed the infiltration and treatment capacity of the buffer. Therefore, additional stormwater control measures are often needed in highly

developed areas. The combination of buffers with other BMPs (such as conservation tillage, contour tillage, and mulching for agricultural areas, or grassed swales, and detention and retention basins for urbanized areas) is necessary to reduce the potential effects of pesticides and heavy metals from larger events of stormwater runoff. For example, studies conducted by Baker et al. (1995) found that conservation tillage (no-till) alone can reduce 60% of herbicide runoff on average.

2.3 General design consideration for buffer design

Criteria for determining the appropriate dimensions of buffer strips for some functions are not well established and recommended designs are highly variable. Improvements in design criteria for vegetative buffers in restoration projects are always needed, particularly for land managers throughout the world (Fischer et al. 2000). Political, economic, and legal aspects often take precedence over physical and ecological factors in designing and installing vegetative buffers (Wenger 1999; Fischer et al. 2000). As a result, the width recommendation is typically based on subjective information.

As mentioned earlier, landscape characteristics such as vegetation type, slope, soil type, flow length, velocity, and travel time of a proposed buffer play an important role in impacting a buffer width and its ultimate effectiveness (Clinnick 1985; Binford and Buchenau 1993; Osborne and Kovacic 1993; Fennessy and Cronk 1997). Furthermore, width, slope and vegetation have been recognized as important factors in determining effectiveness of buffer zones as sediment filters (Karr and Schlosser 1977; Herron and Hairsine 1998). The following is a brief discussion of each of these factors, including considerations for practical implementation into buffer width determinations.

2.3.1 Slope

The slope angle on either side of the stream and roughness of the surface are the primary determinants of the sediment trapping efficiency (Young et al. 1980; Dillaha et al. 1989; Magette et al. 1989; Phillips 1989). A study conducted by Wong and McCuen (1982) that developed a mathematical model over a 47.7 acre watershed in Montgomery County, MD found that a 150′ zone along a 3% slope reduced sediment transport to streams by 90%. In addition, a minimum buffer width of 50′ was recommended in buffer areas between logging roads and streams to reduce sediment load with the width increasing by 4 feet for each 1 percent slope increase (Trimble and Sartz 1957). However, this recommendation has been characterized as prediction rather than empirically defined widths (Karr and Schlosser 1977). The steepest slopes, those between 15 and 25 percent, are not effective in removing pollutants (e.g., sediments and nonpoint source pollutants) from overland flow (Wenger 1999). Ultimately, McCuen (personal communication, March, 2009) recommends that buffer slopes be limited to 10 percent because slopes greater than 10 percent are too steep to allow any significant detention of runoff and sediment regardless of buffer width.

2.3.2 Vegetation

Vegetation type may have a significant influence in terms of buffer effectiveness and the required width because the type of vegetation will determine the Manning's roughness coefficient (Wenger 1999; Davis and McCuen 2005). For instance, forested buffers are more effective in reducing nitrate, but are less effective than grass buffers in retaining total and dissolved phosphorus (Osborne and Kovacic 1993). Mannering and Johnson (1974) passed sediment-loaded water through a 49.2-foot strip of bluegrass and

found that 54% of the sediment was removed from the water. In addition, the type of vegetation planted over buffer zones impacts the response in removing nutrients. For example, according to James et al. (1990) cited in Gilliam (1994), the failure of a riparian buffer to reduce nitrate in Maryland was because of leguminous trees that actually increased the nitrate in groundwater. The age of vegetation, especially regarding whether it is in an active growth phase, may also influence nutrient removal efficiencies in buffer zones due to their capacity in the nutrient uptake process (Parkyn 2004).

2.3.3 Soil type

It is widely recognized that soil properties vary spatially, but the hydrologic characteristics of soil also vary with depth (McCuen 2005). The most important soil characteristic in relation to buffer effectiveness is its capacity to store water, because as precipitation and overland flow occur over saturated soils, the majority of the precipitation becomes runoff. The degree of saturation in a given soil within a buffer can be used to determine whether overland flow occurs (Wenger 1999). The volume of water that infiltrates is also a function of the physical characteristics of the buffer strip. The ability of the vegetation to delay flow has the effect of decreasing the velocity of the runoff, which increases the detention time of the overland flow, resulting in increased opportunity for infiltration (Wong and McCuen 1982).

2.3.4 Travel time

Most hydrologic designs in watersheds deal with the measurement of stormwater runoff discharge. Given that discharge has dimensions of volume per time (L^3/T), the time component is an important element in hydrologic design (McCuen 2005). For example, a given volume of water may or may not cause a flood hazard, where the nature

of the hazard will depend upon the time distribution of the flood runoff. Flood damages will occur if a significant portion of the total volume passes a given location at about the same time; conversely, if the total volume is distributed over a relatively long period of time, damage caused by a passing water wave may be minimal (McCuen 2005).

A number of time parameters are normally used with hydrologic design: the time of concentration, time lag, and travel time within a reach (McCuen, 2005). The time of concentration is often defined as the time required for water to flow from the most remote point of the drainage area to the point of interest. Travel time is closely related to the flow length and slope. Therefore, the velocity of flow can be estimated through the use of Manning's equation because the velocity is based on the concept that travel time for a particular flow path is a function of the length of flow and the velocity (McCuen 2005).

2.4 Soil erosion and vegetative buffer studies

Soil erosion and sedimentation because of land degradation play an important role in impairing water resources within runoff contributing areas (e.g., a watershed). According to Wang and Cui (2005), sediment is one of the main nonpoint source (NPS) pollutants in many watersheds. Therefore, by successfully predicting soil erosion, it is possible to identify protective land use practices as they relate to earth disturbing activities, estimate the efficiency of best management practices (BMPs) required to prevent the excess from sediment loading, and identify target areas for conservation efforts (Hickey et al. 2005).

A number of soil erosion models have been developed during the past decade, one of which is the Revised Universal Soil Loss Equation (RUSLE) (Renard et al. 1994). The RUSLE is the revised version of the former Universal Soil Loss Equation (USLE),

which provides soil loss in tons per acre per year for a given area based upon several parameters: rainfall factor (R), soil erodibility, slope and length of the contributing runoff area, and vegetative cover and management of the runoff area. In addition, Wong and McCuen (1982), used the USLE calculation when examining the effectiveness of 150′ vegetative buffer strips within a 47.7 acre watershed in Montgomery County, MD in trapping sediment for an assumed 90% trapping efficiency. They compared the tons/acre/yr of soil loss determined from field measurements with the total estimated annual loss and found that there is a disparity between those two measurements. The disparity occurs due to the degree of development that the watershed was undergoing when the observed sediment volumes were measured. In performing this simulation, they used a rainfall factor, R, of 175, which is equal to an average annual precipitation depth of 32.65 in/year and a soil erodibility factor, K, of 0.32. From this research, Wong and McCuen (1982) concluded that buffer strips alone would not be able to control sediment. Instead, they will have to be integrated with other stormwater control system.

2.5 Current status of buffer width design studies

Even though conservation buffers have been used for a long time (Vought et al. 1995), the performance of vegetated buffers to protect stream quality from the impacts of NPS pollutants and to prevent stream bank erosion is still a major concern of engineers. Hence, buffer design criteria, particularly buffer width, becomes an important issue for storm water management, especially for storm water ordinances in urban areas for determining the level of impact and the cost for installation (Dosskey et al. 2008). Ordinarily, a vegetative buffer is designed with a uniform width along a stream to intercept runoff. However, the relationship between the width of buffer strips and level of

impacts is not a simple one, and the percentage of a pollutant load that is trapped by a buffer varies with site conditions and the type of pollutant (Dosskey 2001). Further, spatial analysis of field conditions and runoff patterns indicates that more runoff is likely to flow to some locations within the buffer than to others which can substantially limit a buffer's effectiveness (Dosskey et al. 2005).

A number of studies regarding trapping efficiency for sediment as a function of buffer dimensions under laboratory controlled conditions concluded that vegetated buffers are very effective in preventing sediment loss. For example, Pearce et al. (1997) simulated erosion from a feedlot and cropland, finding that 4.6 m and 9.1 m of grassed strips removed 81 and 91 percent of sediment, respectively, from feedlot runoff and 63 and 78 percent from croplands. Furthermore, the design of vegetated buffer strips for controlling runoff and sediment is a function of both stormwater management policies and physical characteristics of the location (Wong and McCuen 1982). For instance, the required length of the buffer strip will depend upon the desired trapping efficiency, which is usually established through regulation. Trapping efficiency is the percentage of total collected sediment that can be settled out within the width of a buffer strip.

As mentioned earlier, the effectiveness of buffer strips depends on the spatial variability in the physical characteristics of the buffer location including land cover, slope, soil type and flow distance. One of the significant factors that determines the effectiveness of a buffer is its size. Numerous empirical models have been developed based on physical inputs providing an alternative approach to examining the relationship between buffer size and level of impact with a focus on buffer width. For example, the Vegetative Filter Strip Model (VFSMOD) is a computer-based model used to study

hydrology, sediment, and pollutant transport through vegetative filter strips (VFS) for given locations (Muñoz-Carpena and Parsons 2004). This model is intended for design purposes, utilizing a repetitive process of inputting different values of buffer width until the model predicts an impact that meets the desired levels. Furthermore, the model can also be applied to a broad range of geographical settings and is potentially quite accurate. However, there are some shortcomings, such as the fact that it requires large amounts of detailed input data on specific site conditions and also requires a high level of skill to properly parameterize, run, and interpret the results. Due to its high complexity, VFSMOD is not recommended for site planning (Dosskey et al. 2008).

Simpler models have been created for design and evaluation purposes. For instance, Phillips (1989) produced the Riparian Buffer Delineation Equation (RBDE) for assessing sediment and nitrate retention based on theoretical equations that account for slope, surface roughness, and soil hydraulic characteristics relative to those of a user-defined reference filter strip. A weakness of this model, however, is the fact that the user-defined reference buffer is questionable because the criteria for a reference buffer is based upon policy and expert opinion (i.e., that 100 feet is ideal). In addition, the reference for the physical inputs is established based upon the average parameters values of a particular study site. Another study conducted by Flanagan et al. (1989) derived a simple equation model from the Chemicals, Runoff, and Erosion from Agricultural Management Systems (CREAMS) Models developed by Knisel (1980) for assessing impacts of filter strips. CREAMS is a process-based model for predicting runoff, sediment transport, as well as plant nutrient and pesticide losses from field-sized areas. This model is intended to evaluate NPS pollution from watersheds. Several assumptions are used in this model to

define a field as a management unit such as having a single land use, relatively homogeneous soils, spatially uniform rainfall, and single management practices, such as conservation tillage or terraces.

Wong and McCuen (1982) introduced another buffer design model to determine the effectiveness of buffer widths, i.e., through a series of nomographs depicting a combination of Manning's calculation, Stoke's Law and the minimum infiltration rates of the four hydrologic soil groups. The physical factors of particle size, slope, and surface roughness were incorporated into this model. Moreover, in these nomographs, the sediment trapping efficiency can be determined using a combination of inputs of land cover types, slope, and flow path. In addition, a combination of inputs of flow path lengths, slope, land cover types, and hydrologic soil group were used to determine the minimum volume of runoff that will infiltrate into the buffer. One of the weaknesses of this model is its inability to address trapping efficiencies of less than 75% (Dosskey et al. 2008). The range of trapping efficiencies was limited because of the data from which this model was developed (McCuen 2009). Another recent study of buffer strip widths was conducted by Dosskey et al. (2008). Their research idea was similar to that of Wong and McCuen (1982), i.e., developing a graphical design aid for estimating the width needed to achieve target trapping efficiencies that can be applied to different pollutants under a broad range of agricultural conditions. The resulting design graph itself consists of a family of seven lines, is easy to use, and provides for a full range of possible relationships between buffer width and trapping efficiency.

2.6 Buffer regulations

2.6.1 Which water bodies should have buffer protection?

While individuals and agencies have conservatively placed more emphasis on the protection of larger rivers and streams, buffer protection should also apply to smaller streams (Wenger 1999). Protection of these smaller creeks and streams is critical for many reasons. First, small streams are so numerous across the landscape and are the most vulnerable because they respond most dramatically to changes in nearby land uses. For example, because small streams tend to be located on the steepest slopes and erosion-prone lands, the cumulative impacts of their degradation (e.g., because of land clearing and soil disturbance around small streams) is significant. Second, small streams and tributaries also often have the highest quality aquatic and terrestrial habitats and thus warrant riparian buffer protection. Third, they feed into larger streams and rivers.

Several policy options can be taken by municipalities when they have to determine which water bodies to include in their buffer ordinances. For example, a community can list specific streams, including all perennial and intermittent streams and apply specific buffer widths to each water body as long as streams are apparent on a map (e.g., the seven and one half minute (7.5') U.S. Geological Survey quadrangle map, surface water map, or fluvial erosion hazard map). The City of Columbia, MO has enacted their stream buffer requirements through a stormwater ordinance called “Land Preservation Act of the City of Columbia, Missouri” with the purpose of protecting streams in the city by establishing minimum stream buffer requirements (City of Columbia 2009). The ordinance is applied to three types of streams: Type I, Type II, and Type III. Type 1 streams are defined as perennial streams shown as solid blue lines on the U.S. Geological

Survey 7.5′ series topographical map. Type II streams are defined as intermittent streams shown as dashed blue lines on the U.S. Geological Survey 7.5′ series topographical map. Type III streams are defined as waterways or natural channels which are not shown on the U.S. Geological Survey 7.5′ series topographical maps as either solid blue or dashed blue lines, but which have drainage areas of greater than 50 acres. The required minimum width for all stream buffers is shown in Table 1.

Table 1. Required stream buffer width for Columbia, Missouri.

Waterway Type	**Required Width for Each Side**
Type 1	100 feet
Type II	50 feet
Type III	30 feet

Additionally, research has shown that stream damage can be minimized and water quality enhanced through reinstalling vegetative buffers where they have been previously removed (Parkyn 2004). Landholders can plant trees and shrubs in the areas where there is a gap in the buffer to begin restoration. However, most plans to restore a vegetative buffer involve more than just planting trees and should be coordinated with the local authority and an agency experienced with stream restoration practices. Native species of vegetation are preferred over nonnative species in order to preserve the terrestrial ecosystem of the area. On the other hand, the manipulation of stream channels using small dams, grade control structures, porous fence revetments and channel crossings was recommended to affect flow regimes, channel stability, and water quality. Furthermore,

channel treatments can also be useful in supporting denitrification as a means to manage nutrients (Groffman et al. 2005).

2.6.2 Protection of private property rights and regulatory riparian areas

According to Presler (2006), if a community decided to protect riparian areas through land use ordinances, then the regulation may possibly raise concerns or challenges based on the concept of constitutional "takings." In the past, regulations to protect water quality have been viewed by courts as advancing a legitimate state interest; regulations lacking a legitimate state interest would constitute a taking (Presler 2006). Regulatory taking actually commences when the landholder challenges the validity of the land use regulation and specifically seeks to use the property for a purpose inconsistent with the regulation at issue (Slagter and Yoakum 2002). For example, based on a land use regulations case in Ohio, the Ohio Supreme Court found that residential zoning of the property did not advance a legitimate state interest and, therefore, constituted a regulatory taking. Moreover, because a taking occurred, the Court also found that a property owner was entitled to compensation for the period the property owner was unable to use the property due to the zoning. In addition, the government may not acquire private property through possessory taking (i.e., physical appropriation) or through regulatory taking (i.e., substantial interference with the property's use), except if the acquisition is for a public purpose and the government fairly compensates the owner (Presler 2006).

According to the National Research Council (NRC) (2002), riparian area protection must not restrict the use of property so that it constitutes a regulatory taking. First, it cannot require owners to grant public access to the property. Second, it cannot prohibit use of the entire parcel so that the landowner cannot make economically viable use of the

property. Buffer ordinances should include some flexibility; for example, existing land uses should be exempt in order that the second condition above does not occur (Presler 2006). Landowners must be encouraged to apply for and obtain a waiver from buffer requirements in the case of economic difficulties. At the same time, appeals processes should also be defined so that a landowner may appeal if the government denies the waiver request (Schueler 1995).

2.6.3 Public awareness

Because of the complexity of riparian buffer issues, a challenge that a community faces in designing and implementing a buffer program is achieving public awareness and understanding, which is vital to a successful effort (Presler 2006). Public involvement can help ensure a successful program because members of an informed community give greater support to a program they understand and value and are thus more likely to comply with its provisions (USEPA 2005). Moreover, a sense of urgency and importance for riparian buffer preservation must be conveyed to the community because such activities cannot be an afterthought implemented once water quality and erosion problems arise (Presler 2006).

As an example, the City of Lenexa, Kansas has successfully implemented a riparian area protection regulation, called the Stream Setback Ordinance. One of the factors that may make this program a success is the support from the general public and the economic development community (Presler 2006). Briefly, the stream setback ordinance applies to all land or new development along stream segments. The ordinance requires a three-zoned buffer along stream segments mapped by the city. The following is the description of each zone.

- "Streamside Zone: 25 feet from the edge of the stream, and measured horizontally from the edge.
- Middle Zone: Variable-width zone determined by stream segment type and order, and measured horizontally from the outer boundary of the streamside zone to the inner boundary of the outer zone, provided, however, that the minimum width of the middle zone on each side of the stream is at least half of the minimum total width of the middle zone as set forth in Table 2. The middle zone includes a distance that comprises all lands with slope greater than 15% and floodplains, provided that these features occur, in part, within the streamside or middle zone.
- Outer Zone: 25 feet from the outer boundary of the middle zone, measured horizontally from that boundary."

Table 2. Minimum total corridor widths for Lenexa, Kansas.

Stream Order	Types 1-2 (Sensitive Streams)	Type 3 (Restorable Streams)	Type 4-5 (Impacted Streams)
1	150 feet	125 feet	100 feet
2	250 feet	200 feet	150 feet
3+	300 feet	250 feet	200 feet

Note: Width of the middle zone will be expanded if necessary, to include flood plains and lands with slope greater than 15%

2.7 The role of GIS for buffer width modeling

Recognizing that hydrologic processes can vary in space and time, the need to incorporate this larger-scale variability and spatial heterogeneity of the environmental landscape exists. This need has necessitated the use of geo-spatial technologies and

distributed databases because many environmental models require large amounts of spatial and non-spatial data for each interacting process (Bajwa and Tim 2002). Geographic information system (GIS) concepts and technology have gained widespread use in a variety of engineering applications, including its application for buffer width modeling studies. These applications are appropriate because information about water resources and the environment (e.g., soil, land use, and topography) occurs in a spatial context (Johnson 2009). Furthermore, GIS technology that offers the combined power of geography and information systems is an ideal solution for effective management of water industry infrastructure (Shamsi 2005). The position of GIS within water resources planning and design processes is shown in Figure 4.

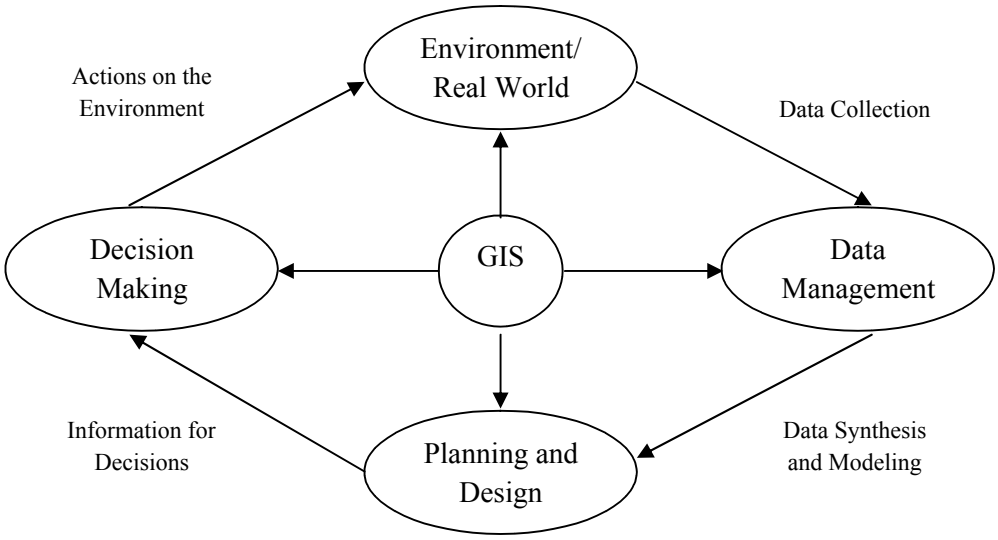

Figure 3. GIS within water resources planning and design (modified from Johnson 2009).

From Figure 3, one can see that GIS holds an important place in water resources planning and design studies. The function of GIS began with its ability to assist in data collection from real world conditions and continues with its capability to manage the collected data as well as assist in the planning and design process by performing data synthesis and spatial modeling. Finally, the role of GIS comes full circle with its

capacity to provide accurate information through series of maps for decision makers in order that they can take the right actions for the environment.

A GIS can be defined as a computerized system that is designed to collect, store, manipulate, analyze, and display data that is spatially referenced. Thus, based upon its definition, five elements are required for developing a GIS: data, computer hardware, computer software, procedures, and people (Dangermond 1988; Goodchild 1996). Since the late 1980s, GIS has been implemented for water resources primarily for the purposes of mapping, modeling, facilities management, and work-order management for developing capital improvement programs and operations and maintenance plans by federal, state, and local government agencies (Morgan and Polcari 1991).

Conventionally, there are two common data models in GIS to represent real world features: a *vector* data model and a *raster* data model, both of which have advantages and disadvantages (Figure 4). *Raster* data models appear in finite difference models and represent two-dimensional spatial variation by assigning values to cells in a fixed rectangular array. A *vector* data model represents the spatial variation of points, lines, and areas in an irregular distribution fashion (Goodchild 1996). Furthermore, in *vector* data models, lines and area boundaries are represented as connected sequences of straight segments (i.e., polylines and polygons, respectively). However, in *raster* data models, lines and area boundaries are often conceived as smoothly varying (e.g., elevation data), in which typically each cell in an array has its own value (Goodchild 1996).

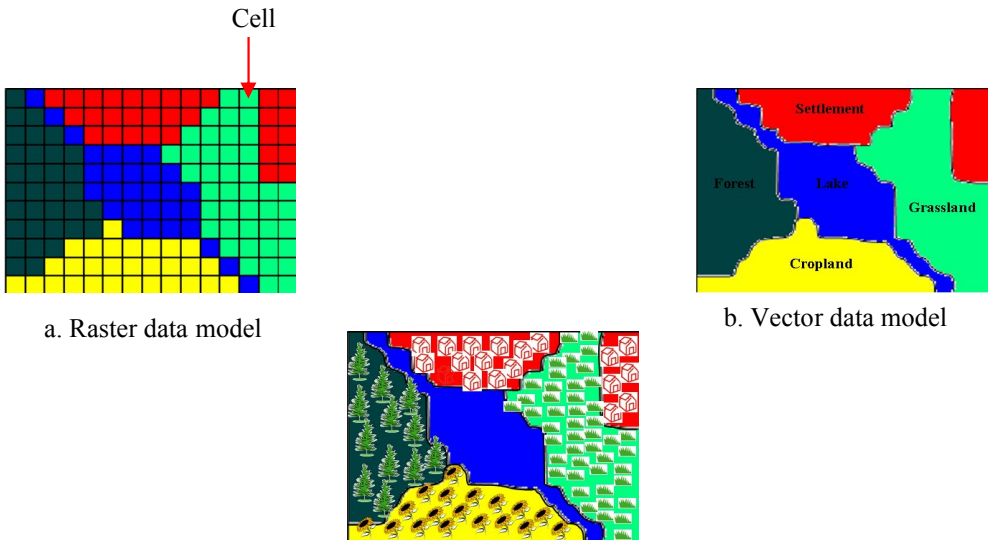

a. Raster data model

b. Vector data model

c. Actual features

Figure 4. Raster and vector data model representations of actual features.

In order to determine which data model is most suitable be used in a GIS analysis for planning and engineering design purposes, factors such as the scale of the input data and the procedures or models that will use the GIS output are important because these data and models will represent real-world conditions and will guide decision-making (Johnson 2009). Vector data models are often used for local scale analyses because it is recommended where there is user concern regarding the precision of a final map. Alternatively, a raster data model is commonly used in regional scale analyses, which are intended to provide the user with a rough depiction of conditions or predictions of phenomena in the study areas; for example, climate change analysis and land use/land cover change analysis.

In site-specific vegetated buffer applications, GIS analysis and database functions provide an integrating data and modeling environment for determining buffer width (Johnson 2009). The measurement of area, distance, flow velocities, slope gradients, and surface roughness determinations are generally handled in digital formats and easily

achieved in a geospatial database utilizing GIS software (e.g., ArcGIS) (ESRI 2009). The spatial analysis functions allow the overlaying of multiple layers and the attribute database can then be used to produce maps and reports in support of decision making between design alternatives. Moreover, while a map has the capacity to be presented interactively (e.g., time series analysis of land use change), maps can be an effective communication medium to communicate the GIS analysis results in public forums so that citizens concerned with planning and design choices can better understand and be more involved in the process prior to promulgation of a final regulation (Johnson 2009).

A number of previous experiences in modeling buffer width utilizing GIS have been accomplished. For example, since 1993, a variable buffer delineation has been successfully applied to several North Carolina watersheds based upon the Riparian Buffer Delineation Equation (RBDE) developed by Phillips (1989) and utilized by multiple researchers (Xiang 1993; Xiang 1996; Xiang and Stratton 1996). In Hawaii, a study concerned with improving water quality through site selection for a riparian restoration project also used the RBDE model (Lavalle 2007). The RBDE model is based upon a mathematical model that considers the detention time capabilities of a buffer in retaining a pollutant within its vegetated area. The RBDE was designed to calculate the appropriate width of a proposed vegetated buffer by comparing the proposed buffer's current physical properties to a user-defined reference buffer that often is comprised of ideal buffer conditions but can also be typical conditions for the area of interest (Xiang 1996). The effectiveness of this model is measured by its capability to delay or infiltrate stormwater, or remove pollutants in runoff (Phillips 1989). Nevertheless, although the RBDE model is a widely accepted means for calculating a variable buffer width based upon site-specific

parameters, the effectiveness of riparian buffer determinations based on this model have not been verified through experimental research (Halley 2002).

2.8 Chapter summary

This chapter began by looking at the historical applications of vegetative buffers strips in Europe and in the United States that was mainly intended for supporting agricultural activities as a part of conservation practices (i.e., protecting agricultural land from wind and water erosion). The chapter then discussed the effectiveness of buffer strips in removing pollutants, trapping sediments, and promoting stormwater infiltration as well as general design considerations prior to installing vegetative buffers in order to obtain maximum performance of the buffers. The current status of buffer width modeling studies was presented by describing various empirical and process-based models developed by engineers, followed by a discussion of some legal aspects in buffer regulation. Finally, the chapter ended with a discussion of the role of GIS in water resources planning and design, specifically buffer width-modeling studies.

Chapter 3:
METHODOLOGY

3.1 General description of the study area

The LaBarque Creek watershed is located in northwestern Jefferson County, Missouri, within the coordinates 38˚23'- 38˚27' North latitude and 90˚37'- 90˚44' West longitude (Figure 5). The entire area of the watershed is 8,392 acres or about 13 square miles with 6.6 miles of stream length that drains to the Meramec River 42 miles upstream from the confluence with the Mississippi River. The watershed is categorized as Ozark land where more than 60% of the land is considered as having a steep slope, and about 89% of the area is dominated by deciduous forest. At least 42 species of fish live in the Creek, which indicates that this watershed is a very healthy ecosystem. The geology of the area is primarily sandstone that allows flowing water to carve caves, waterfalls, bowls and overhangs, and provides habitats for several state listed rare plants (Missouri Dept. of Conservation 2007).

Currently, the population density in the area is about 100 people per square mile, where most of the population is concentrated on only 20% of the watershed land. However, even though a low population density can result in a low impact to the watershed ecosystem, local authorities must consider the potential effects of rapid development and population growth in neighboring areas. For example, based on information from the U.S. Census Bureau (2000), the population in the City of Eureka (on the north side of the watershed) and the population growth in the City of Pacific (just west of the watershed) increased by 83 and 27 percent, respectively, from 1990 to 2000.

These high growth rates can result in high demand for development within the watershed and surrounding areas. As a result, a combination of high diversity of ecological value and development patterns can make the watershed an excellent candidate for conservation efforts.

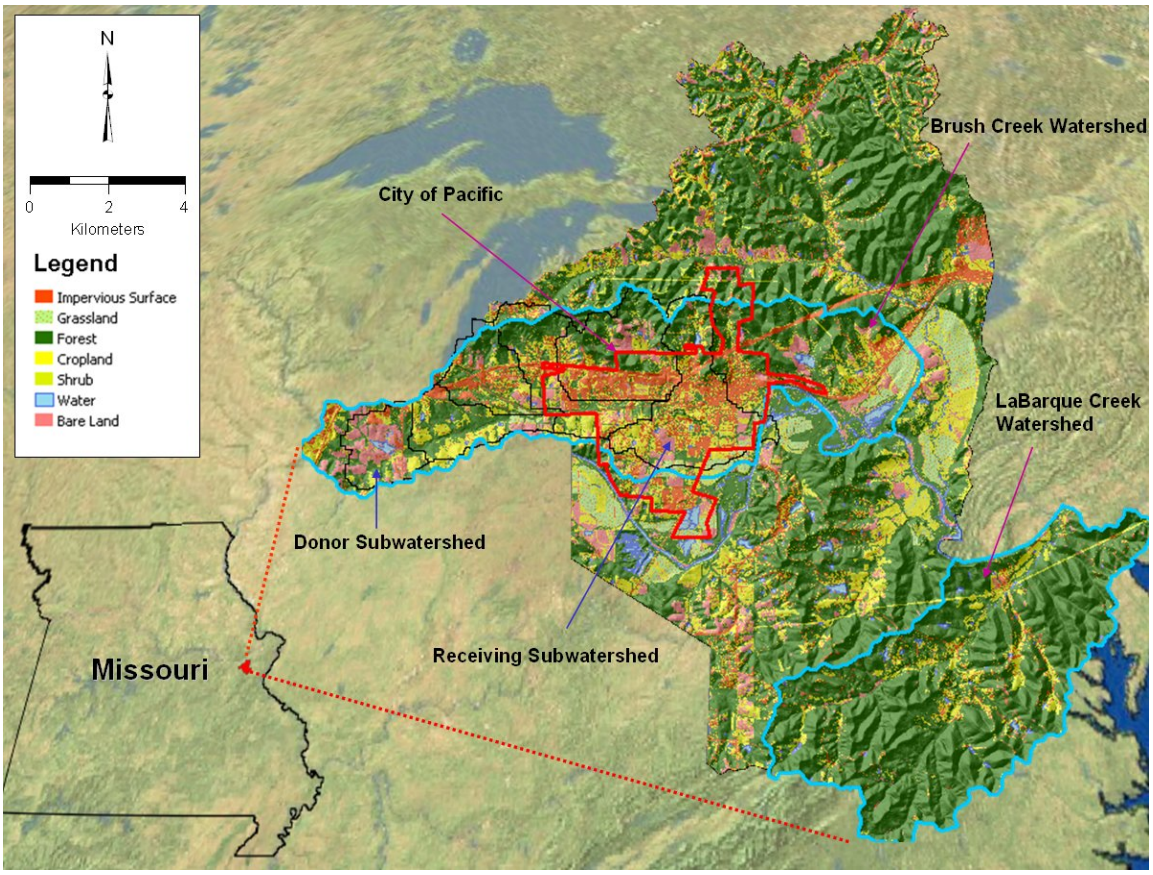

Figure 5. Location of the LaBarque Creek watershed.

3.2 Buffer modeling development

The analytical framework for generating a vegetative buffer strip model and evaluating its performance to address the objectives of this research is comprised of 3 phases:

1. development of an empirical model,
2. development of a spatial database, and
3. development of methods using GIS.

General information regarding each phase of the methodology is shown in Figure 6. First, the development of empirical vegetative buffer strip models consists of two parts; sediment control and stormwater infiltration, and was developed based upon a series of nomographs created by Wong and McCuen (1982). The nomographs themselves were created from a combination of the Manning's equation, Stoke's Law, and the minimum infiltration rates of the four hydrologic soil groups (i.e., particle size, slope, and surface roughness). In this particular phase, four equations were created (one for calculating runoff velocity, one for determining the effectiveness of a buffer, one for calculating travel time, and one for determining the volume of infiltrated stormwater per foot width of buffer strip). Second, following the creation of empirical models, a spatial database was prepared that relates to the components of the model (i.e., physical parameters): the digital elevation model (DEM) for slope, land cover for Manning's n, soil type, soil texture, and hydrology of the study site. The development of methods utilizing GIS is the third phase of the methodology framework. In this particular phase, GIS flow charts were devised that apply the empirical vegetative buffer strip models in the GIS environment.

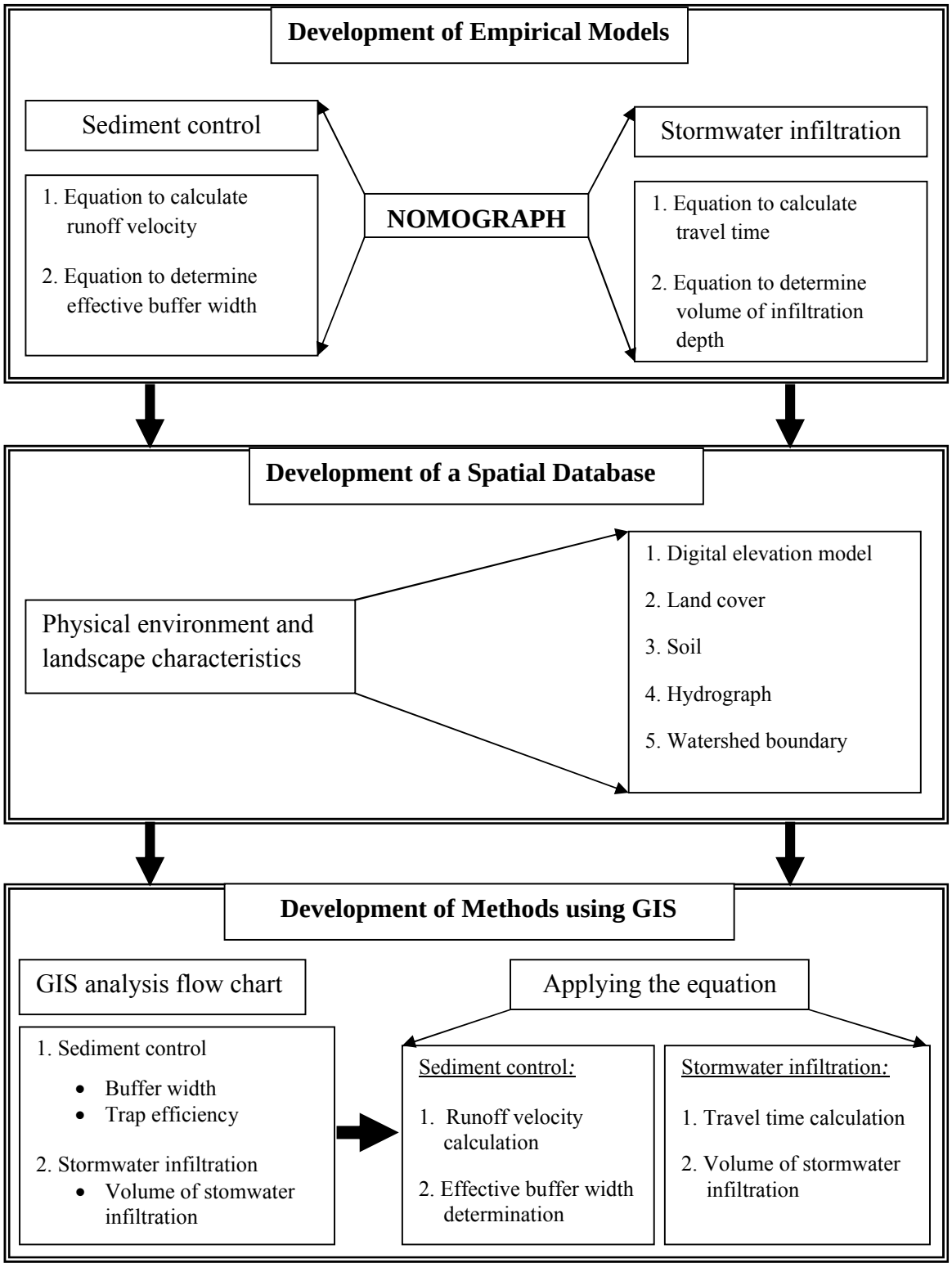

Figure 6. Research methodology in developing and implementing the empirical models.

3.2.1 Development of empirical models

In phase 1, an empirical vegetative buffer strip (VBS) model for sediment control was first developed followed by a stormwater infiltration model based on the nomographs from Wong and McCuen (1982).

3.2.1.1 Establishing a mathematical model for sediment control

In developing the model, a combination of GIS software (i.e., ArcGIS) and Microsoft Excel has been applied to generate and validate the model through a process of digitization and statistical analysis. The following steps were used to generate and validate the VBS model:

1. Divide the nomograph into two parts,
2. Scan the nomograph,
3. Rectify the nomograph,
4. Digitize the nomograph,
5. Perform a regression analysis,
6. Create a procedure to apply the regression equations, and
7. Validate the model.

These steps are now described in detail.

1. The nomograph is divided into two parts as shown in Figure 7. Part 1 is a runoff velocity (ft/sec) versus slope (percentage) relationship and part 2 represents runoff velocity (ft/sec) versus effective buffer width (ft).

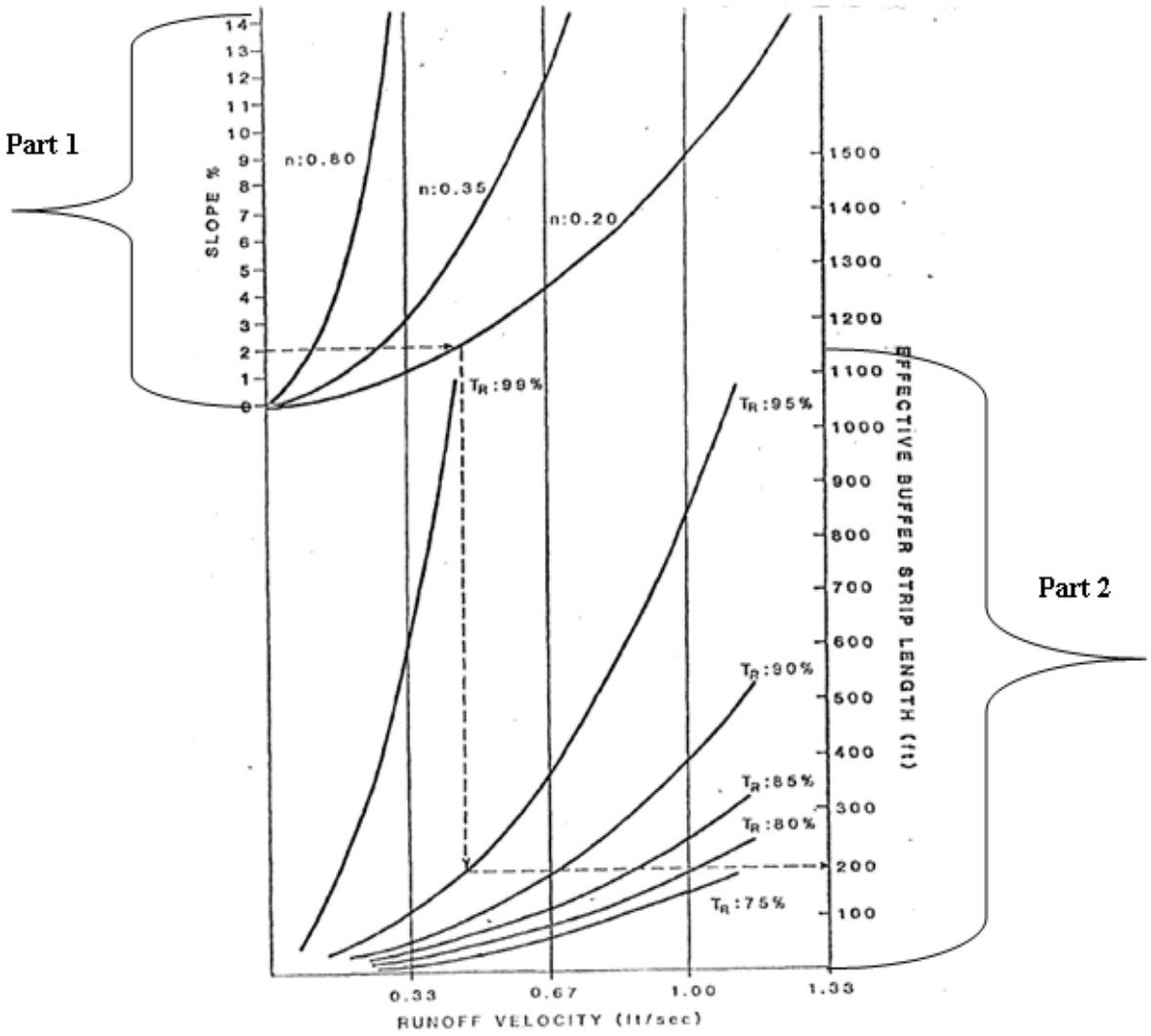

Figure 7. Separation of the effective buffer width determination nomograph into two parts.

2. The nomograph is scanned in this step so that it can be digitized in step 4.
3. The scanned nomograph is loaded and rectified into its real "coordinate" by using georeferencing tools in ArcGIS. For part 1, the "x" axis represents runoff velocity and the "y" axis represent slope, while for part 2, the "x" axis represents runoff velocity and the "y" axis represents buffer width.
4. The digitizing process is performed for each of the nomograph lines.

Part 1:

Generating 100 points from the curves that represent Manning's n values of 0.2, 0.35, and 0.8, as shown in Figure 8.

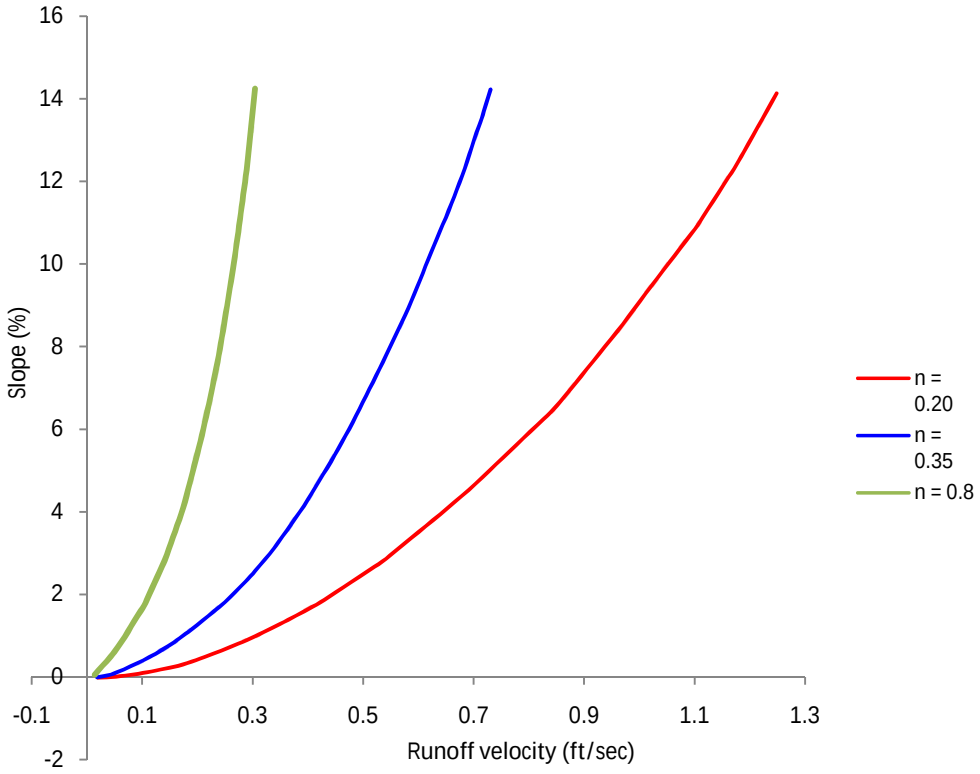

Figure 8. Manning's n curves resulting from the digitizing process in ArcGIS.

Part 2:

Generating 100 points from the curves that represents trapping efficiency values of 75%, 80%, 85%, 90%, and 95%, as shown in Figure 9.

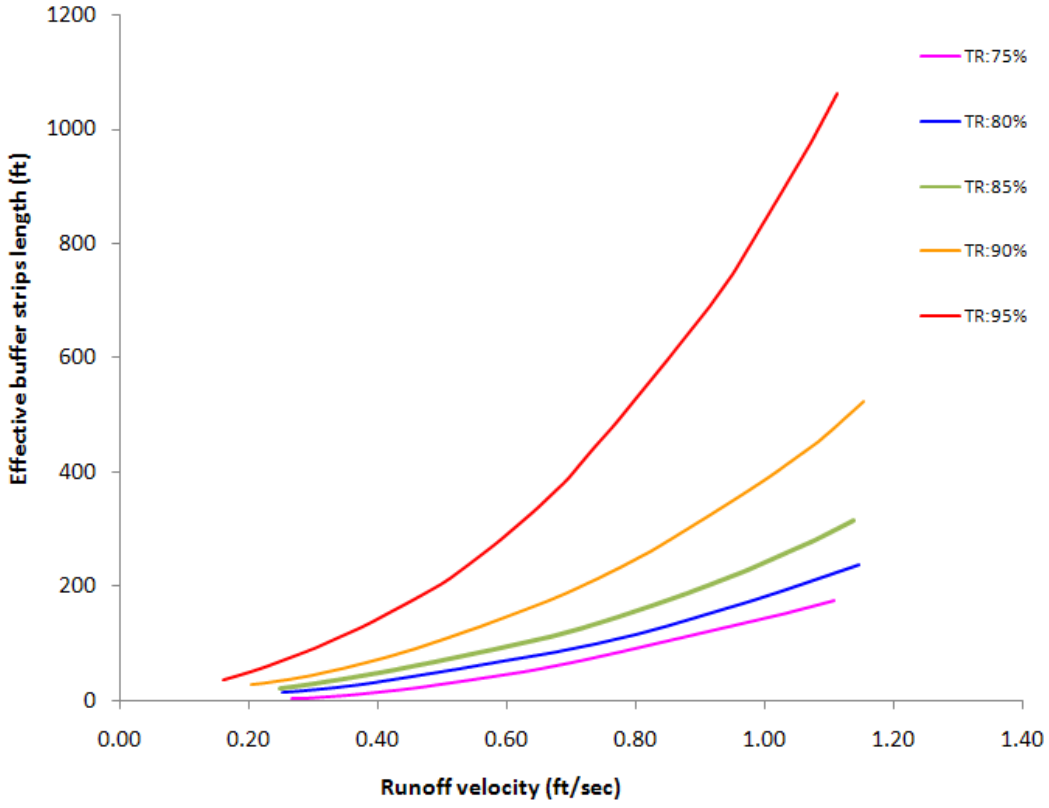

Figure 9. Trapping efficiency curves resulting from the digitizing process in ArcGIS.

5. Regression analysis

To create an equation for part 1 and part 2 of the nomograph, all the attribute points collected through the digitizing process were exported to a Microsoft Excel file as shown in Tables 3 and 4. Negative values of slope in Table 3 occur due to human error during digitizing of the nomograph. The complete dataset can be found in Appendices A and B.

A regression analysis was performed to produce prediction equations for both parts of the nomograph. In part 1, the character of the prediction equation for calculating velocity is that the equation can be applied for different Manning's n values between 0.2 and 0.8. In part 2, the prediction equation to determine the

width of a vegetative buffer can be used for trapping efficiencies between 75% and 95%.

Table 3. Sample data recorded from digitizing for Manning's n = 0.2 (Part 1).

Point ID	Runoff velocity (ft/sec)	Slope (%)
1	0.0197	-0.0181
2	0.0360	-0.0090
3	0.0524	0.0069
4	0.0687	0.0322
5	0.0849	0.0608
.	.	.
.	.	.
100	1.24847	14.13125

Table 4. Sample data recorded from digitizing for a trapping efficiency of 85% (Part 2).

Point ID	Runoff velocity (ft/sec)	Buffer Width (ft)
1	0.2473	23.1300
2	0.2586	24.8663
3	0.2698	26.6063
4	0.2811	28.3425
5	0.2923	30.1200
.	.	.
.	.	.
100	1.1378	315.9600

Generally, the process of developing prediction equations is through "trial and error," but principally all the Manning's n curves in part 1 and all the trap efficiency curves in part 2 must be fit to one curved line each, as shown in Figure 10 and Figure 11. This process can only be achieved by utilizing a "dimensionless" function whereby the value of the "y" axis is divided by the value of each curve. From this point, the prediction equations for part 1 (Equations 1 and 2) and part 2 (Equations 3 and 4) can be estimated through regression analysis by determining a simple trend line that best fits all fitted curve lines.

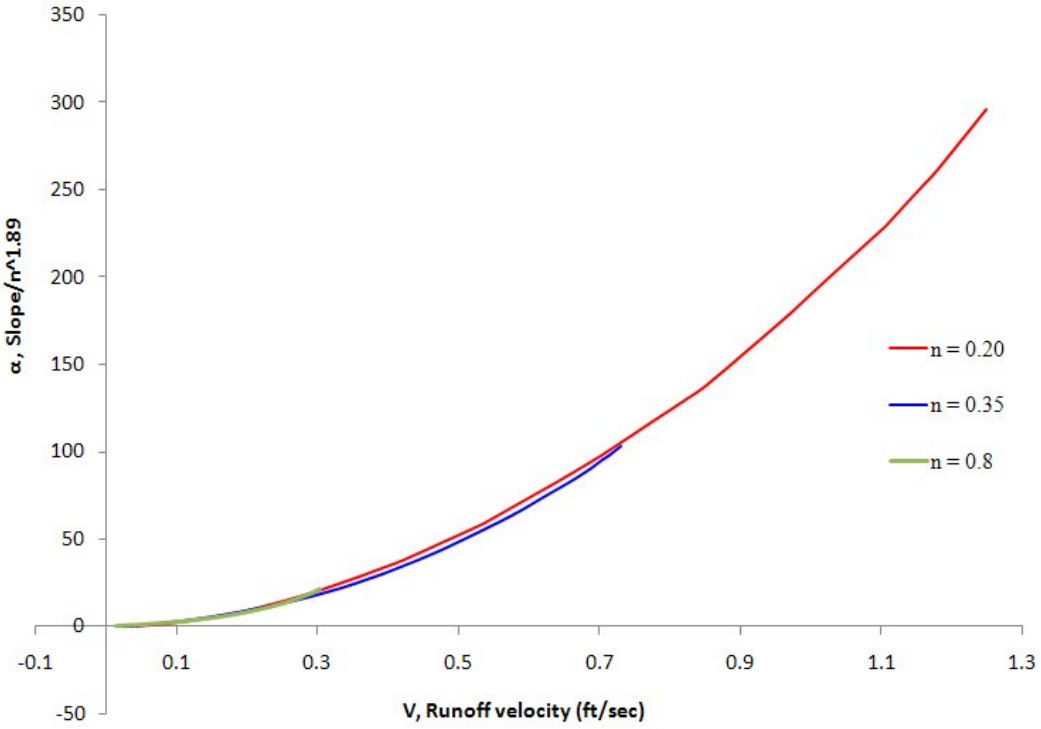

Figure 10. Utilization of dimensionless curve in part 1 to produce Equations 1 and 2.

$$\alpha_i = -\frac{S_i}{n^{1.89}} \qquad \text{(Equation 1)}$$

$$S_i = 174.45V_i^2 + 14.234V_i + \alpha_i \text{ (used to calculate velocity)} \qquad \text{(Equation 2)}$$

where:

S = slope (%),

V = runoff velocity (ft/sec),

n = Manning's n from different land cover types, and

i = cell in raster data from 1,…, n.

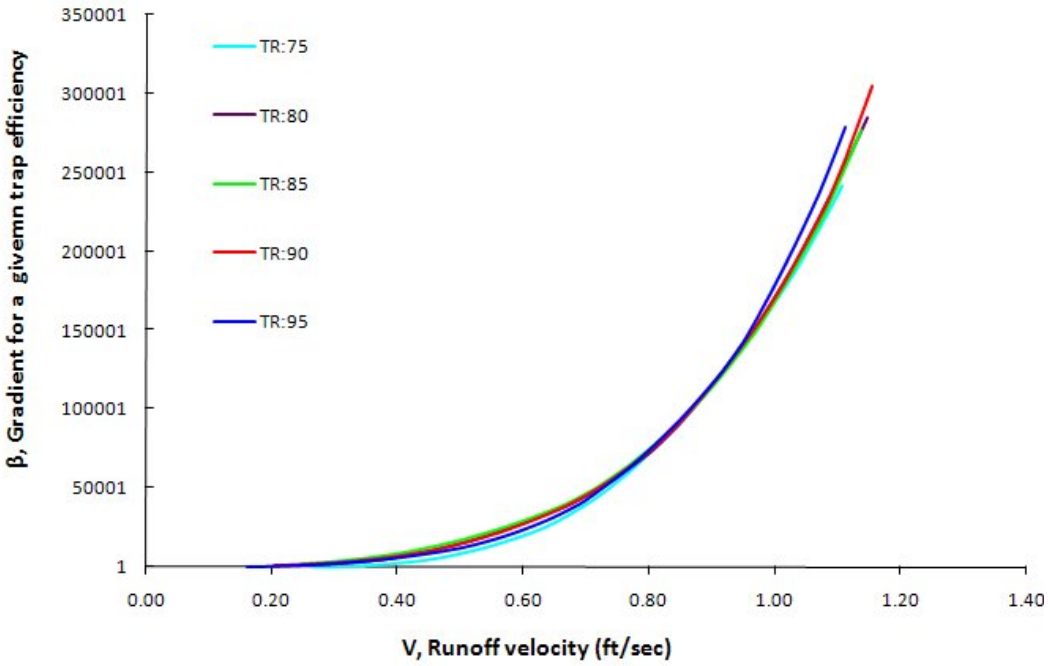

Figure 11. Utilization of dimensionless curve in part 2 to produce Equations 3 and 4.

$$\beta_i = 0.00002\lambda_i^4 - 0.00649333\lambda_i^3 + 0.7909\lambda_i^2 - 42.81267\lambda_i + 868.95 \quad \text{(Equation 3)}$$

$$L_i = (321331V_i^4 - 405658V_i^3 + 354609V_i^2 - 111311V_i + 12585)^{0.5283*\beta_i} \quad \text{(Equation 4)}$$

where:

L = buffer width (ft),

V = runoff velocity (ft/sec),

β = gradient for a given trapping efficiency,

λ = trapping efficiency (%), and

i = cell in raster data from 1,…, n.

The α coefficient in Equation 2 and the β coefficient in Equation 4 result from the dimensionless process. In addition, in part 2 prior to the creation of the prediction equation, there is a certain procedure to estimate the gradient equation (i.e., Equation 4) that will be incorporated into the prediction equation for

determining buffer width (Figure 12). First, points were collected at a runoff velocity of 0.8 ft/sec from each trapping efficiency curve. The 99% trapping efficiency curve was eliminated from consideration because that curve did not intersect the vertical line of 0.8 ft/sec velocity. The next process was to find the relationship among those coordinate points by producing the gradient equation (Equation 4) utilizing a regression analysis, where the x-axis is trapping efficiency and the y-axis is buffer width.

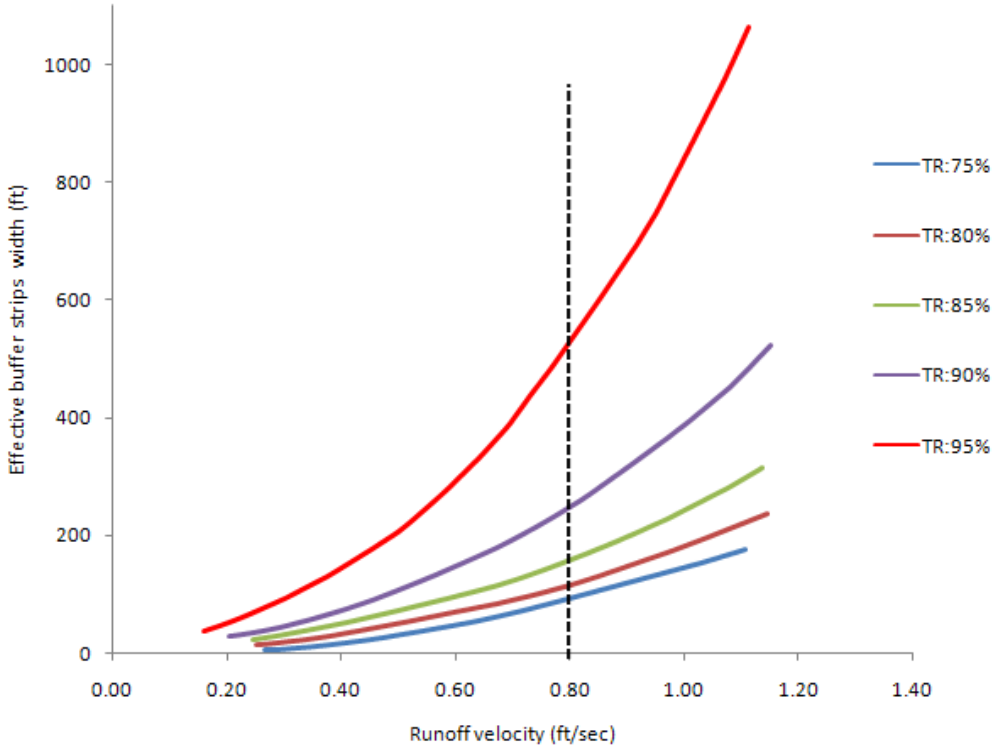

Figure 12. Coordinate sample extraction as an aid in producing the gradient equation.

6. Procedure for applying regression equations

The regression equations developed above are used in the following process to calculate the buffer width for each cell (i).

- Step 1: substitute the value for S_i and n into Equation 1 to compute α_i,

- Step 2: substitute α and S into Equation 2 to solve for runoff velocity (V_i),
- Step 3: assume an efficiency value λ_i in order to calculate β_i from Equation 3, and
- Step 4: substitute V_i and β_i from steps 2 and 3, respectively, to calculate buffer width (L_i) from Equation 4.

7. Model validation

A double mass plot through equation "y = x" was used to validate the prediction model for runoff velocity and buffer width determinations by comparing observed values data derived from the nomograph and prediction values derived from the numerical model (i.e., Equations 1- 4). Sample analyses for slopes and buffer widths are shown in Tables 5 and 6, respectively. Complete sets of values can be found in Appendices C and D.

Table 5. Comparison of slope calculations between modeled and observed values for Manning's n = 0.35.

ID	Modeled Slope (%)	Observed Slope (%)	Percentage Difference
1	0.13	0.06	116.67
2	0.18	0.12	50.00
3	0.23	0.19	21.05
4	0.29	0.26	11.54
5	0.36	0.33	9.09
.	.	.	.
.	.	.	.
100	13.51	14.22	4.99

Table 6. Comparison of buffer width determinations between modeled and observed values for a trapping efficiency of 90%.

ID	Modeled Buffer Width (ft)	Observed Buffer Width (ft)	Percentage Difference
1	33.94	32.63	4.01
2	35.11	35.10	0.03
3	37.02	37.75	1.93
4	39.47	40.73	3.09
5	42.41	43.73	3.02
.	.	.	.
.	.	.	.
100	520.27	522.69	0.46

A coefficient of determination (R^2) derived from the double mass plot was then used to estimate the accuracy of the prediction model. In part 1, based on the regression analysis, the coefficients of determination between modeled and observed velocity values for Manning's n values of 0.2, 0.35, and 0.8 were 0.999, 0.999, and 0.974, respectively. In part 2, from the regression analysis, the coefficients of determination between modeled and observed buffer width values for trapping efficiencies of 75%, 80%, 85%, 90%, and 95% were 0.983, 0.999, 0.999, 0.999, and 0.997, respectively. Representative analyses for validating runoff velocity calculations and buffer width determinations are shown in Figures 13 and 14, respectively. Complete data can be found in Appendix E.

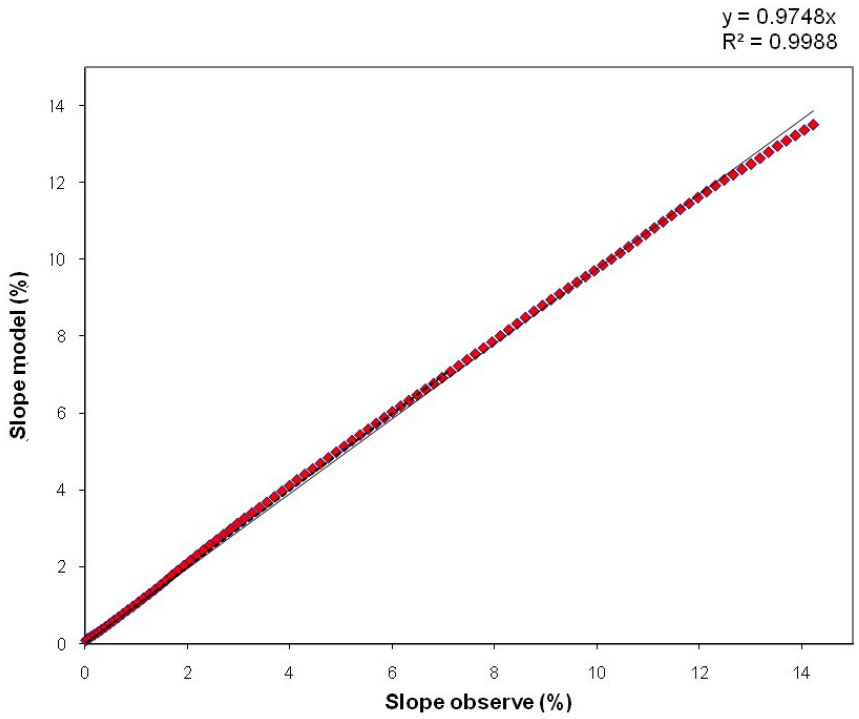

Figure 13. Double Mass Plot between modeled and observed data for slope calculation (%) for Manning's n = 0.35.

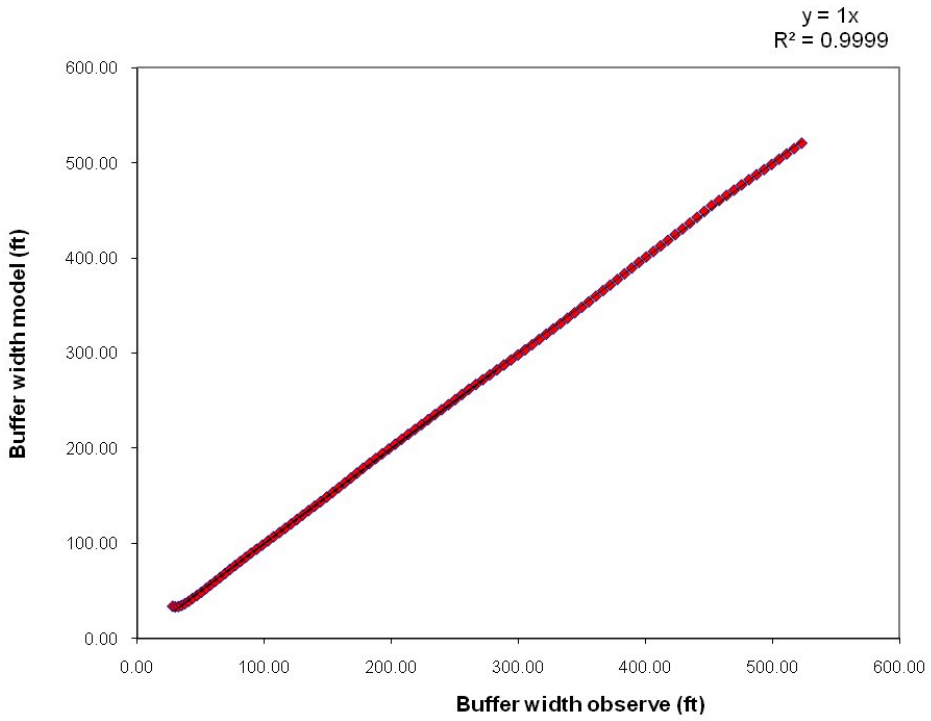

Figure 14. Double Mass Plot between modeled and observed data for buffer width determination (ft) for a trapping efficiency of 90%.

The process of validation is also presented visually by overlaying the predicted curve over the curve derived from the nomograph, as shown in Figures 15 and 16.

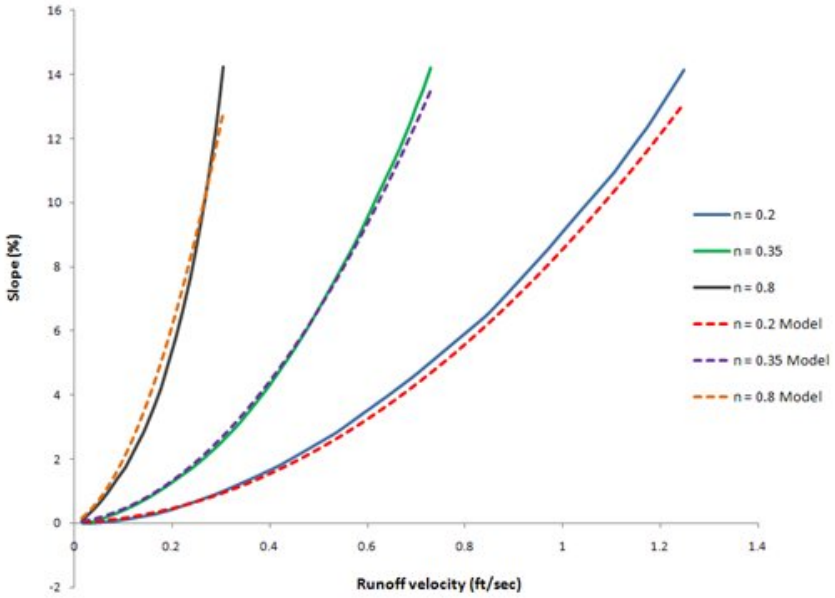

Figure 15. Manning's n curve comparison between modeled and observed data.

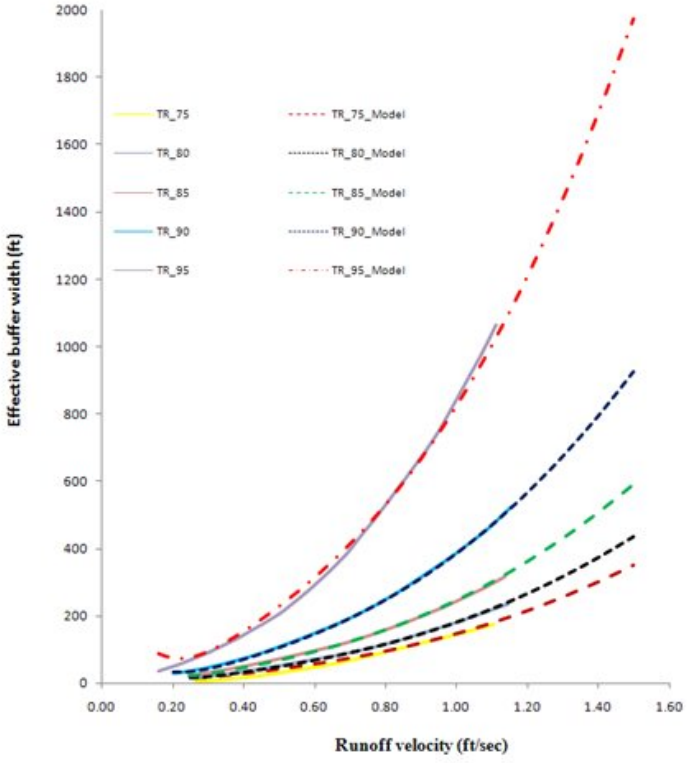

Figure 16. Trapping efficiency curve comparison between modeled and observed data.

3.2.1.2 Establishing a mathematical model for stormwater infiltration

For the relation between depth of infiltration and buffer width, the travel time (T_t) for a particular flowpath is calculated based on the simple relationship between the length of flow (L) (i.e., pixel length) and the velocity (V), as shown in Equation 5

$$T_t = \frac{L}{3600V} \qquad \text{(Equation 5)}$$

where T_t, L, and V have units of hours, ft, and ft/sec, respectively. In addition, recognizing that the infiltration losses may be small, the volume of infiltrated depth from a vegetative buffer is calculated based on the simple equation developed by Wong and McCuen (1982) (Equation 6).

$$V_L = \frac{f_c T_t L}{12} \qquad \text{(Equation 6)}$$

in which V_L is the volume of infiltrated water per width of buffer strip in cubic feet per foot, f_c is the equilibrium or minimum infiltration rates in inches per hour, L is the buffer width in feet, and T_t is the overland flow travel time over a buffer strip in hours. For Equation 6, soil types are classified using the Natural Resources Conservation Service (NRCS) (2004) hydrologic soil groups A, B, C, and D, which are associated with different equilibrium, or ultimate, infiltration rates, f_c, as shown in Table 7. The following is the description of soil properties according to the NRCS (2004) classification.

Table 7. Minimum infiltration rates (f_c) of four NRCS soil groups modified from Wong and McCuen (1982).

NRCS Soil Groups	f_c used by Wong and McCuen (1982) (in./hr)	Actual range of f_c (in./hr)
A	0.43	0.3-0.45
B	0.26	0.15-0.30
C	0.13	0.05-0.5
D	0.03	< 0.05

- "Group A soils have a low runoff potential due to high infiltration rates even when saturated. These soils primarily consist of deep sands, deep loess, and aggregated silts.
- Group B soils have a moderately low runoff potential due to moderate infiltration rates when saturated. These soils primarily consist of moderately deep to deep, moderately well to well drained soils with moderately fine to moderately coarse textures (shallow loess, sandy loam).
- Group C soils have a moderately high runoff potential due to slow infiltration rates. These soils primarily consist of soils in which a layer near the surface impedes the downward movement of water or soils with moderately fine to fine texture such as clay loams, shallow sandy loams, soils low in organic content, and soils usually high in clay.
- Group D soils have a high runoff potential due to very slow infiltration rates. These soils primarily consist of clays with high swelling potential, soils with permanently high water tables, soils with a claypan or clay layer at or near the surface, shallow soils over nearly impervious parent material such as soils that swell significantly when wet or heavy plastic clays or certain saline soils."

3.2.2 Development of a spatial database

Environmental Systems Research Institute (ESRI) (2009) software (i.e., ArcGIS) was used to run the simulations for this project. For example, ArcCatalog was used to manage, manipulate, re-project, create, and delete data layers for this project. ArcMap, with its extensions (e.g., Spatial Analyst) was used to view, develop, edit, query and analyze the project's data layers. Hydrology tools in ArcToolbox were used to analyze the data as well as to develop the spatial data due to its capabilities in geo-processing.

Following the steps in Figure 7, a GIS database was developed that contains information needed for applying the buffer model in the study area. The data consists of digital soil data, elevation data, land cover data, hydrography data, and the watershed boundary. All these data used in the demonstration of the methodology were collected from state and federal agencies, as well as from university and commercial sources with varying scales. The spatial and tabular Soil Survey Geographic (SSURGO) database from NRCS (2004) has a scale of 1:24,000 and was used to generate hydrologic soil group and texture of the soil as shown in Figure 17 and Figure 18, respectively. The land cover map for LaBarque Creek watershed (Figure 19) was derived from QuickBird satellite imagery from Digital Globe (2006) with a 2.4-meter pixel resolution through an image classification scheme. The land cover map consists of seven classes (i.e., forest, shrubs, cropland, grassland, barren land, impervious, and water). The map was then used to generate the Manning's n factors. DEM data with a 10-meter cell resolution, established by the U.S. Geological Survey (USGS) was obtained from the Missouri Spatial Data Information Service (MSDIS) (2006), and provided the elevation data in Figure 20. The watershed boundary was obtained from the East-West Gateway Council of Governments

(2006) (Figure 21). Hydrography was downloaded from MSDIS (2006) and is also shown in Figure 21. In addition, because the input data were provided at varying scales, the datasets then needed to be standardized into a raster data model with a 10 meter pixel resolution (i.e., based on the resolution of the DEM) and projected into a similar projection system (i.e., NAD 1983 Zone 15 North). The purpose of standardizing these data is to ensure that all spatial data obtained from data sources is in the correct projection system.

The following subsections outline the process for creating the basic GIS layers that are required for the demonstration of the model (e.g., slope, Manning's n value, settling velocity for a given particle size, and minimum infiltration rates). These layers were derived from base GIS data (i.e., DEM, land cover, and soil).

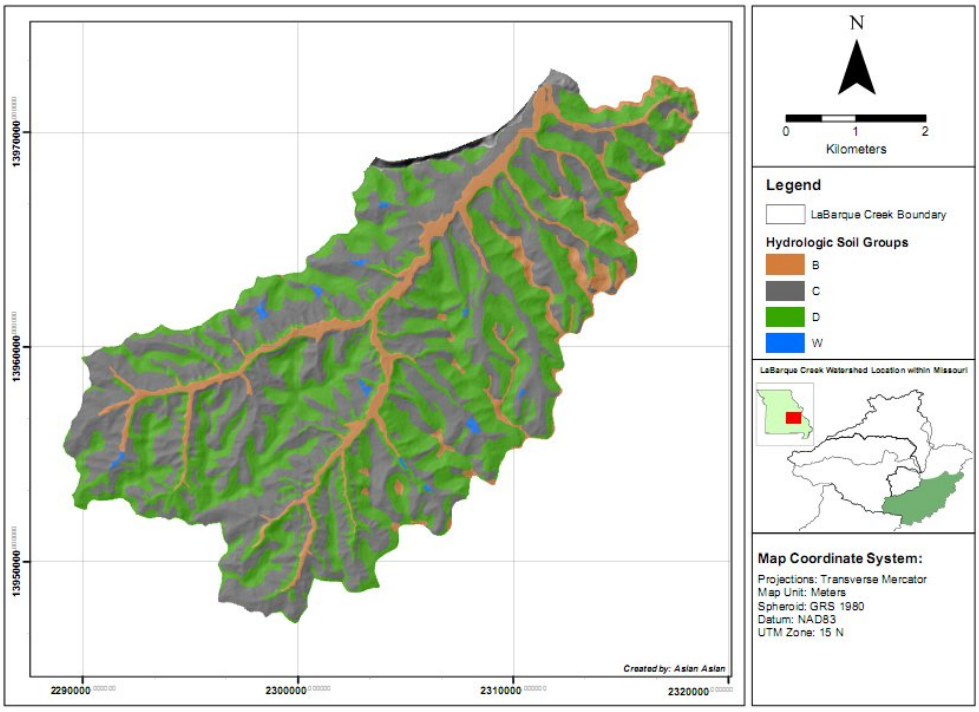

Figure 17. Hydrologic soil groups for the LaBarque Creek watershed.

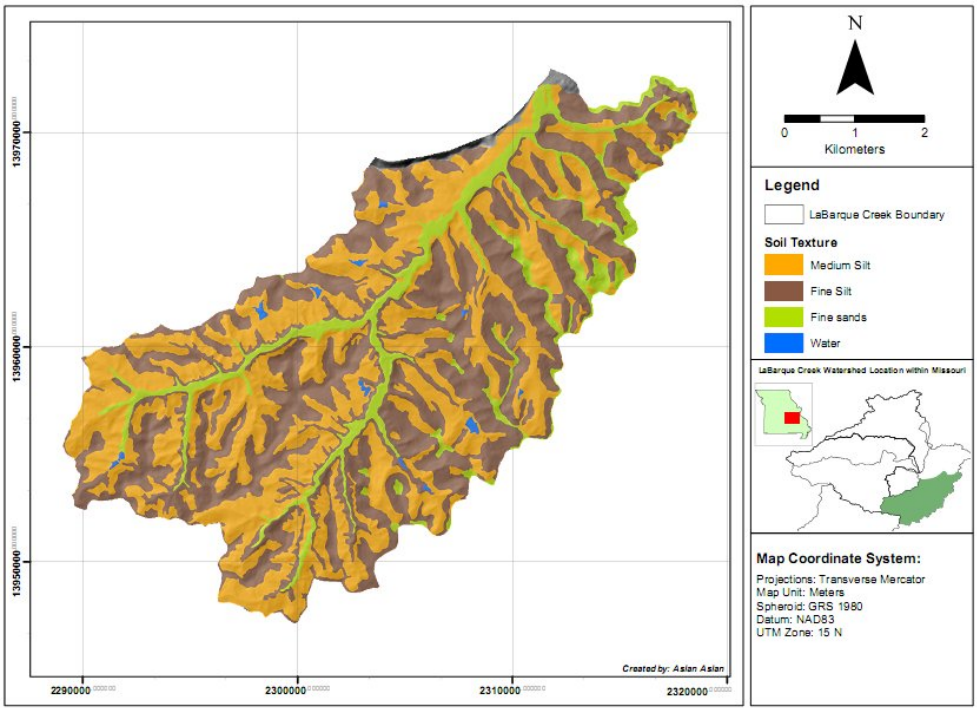

Figure 18. Soil textures for the LaBarque Creek watershed.

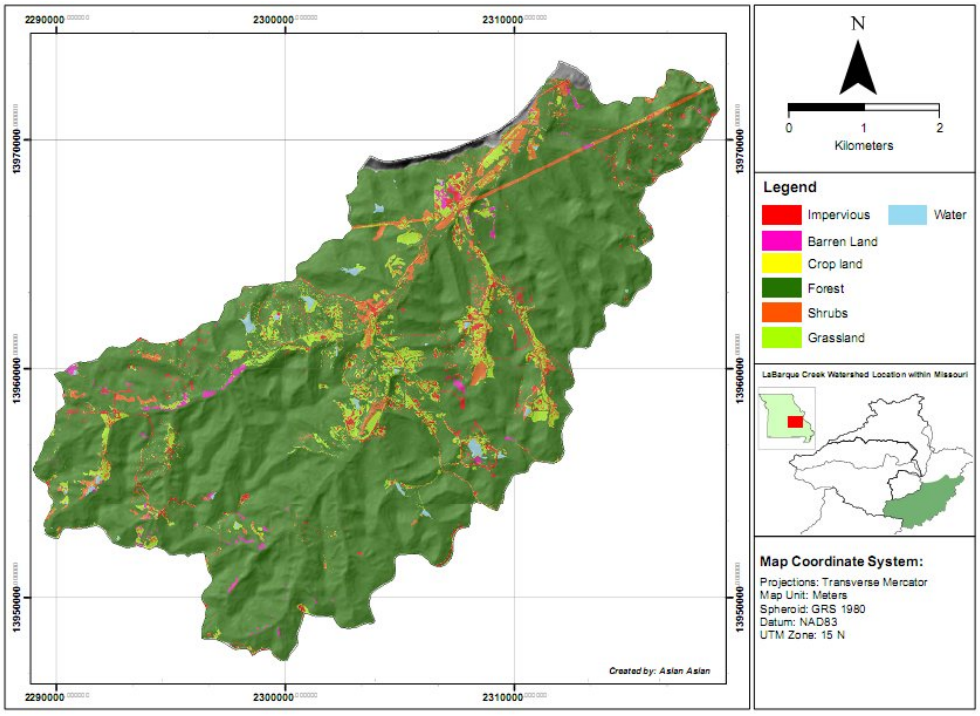

Figure 19. Land cover for the LaBarque Creek watershed.

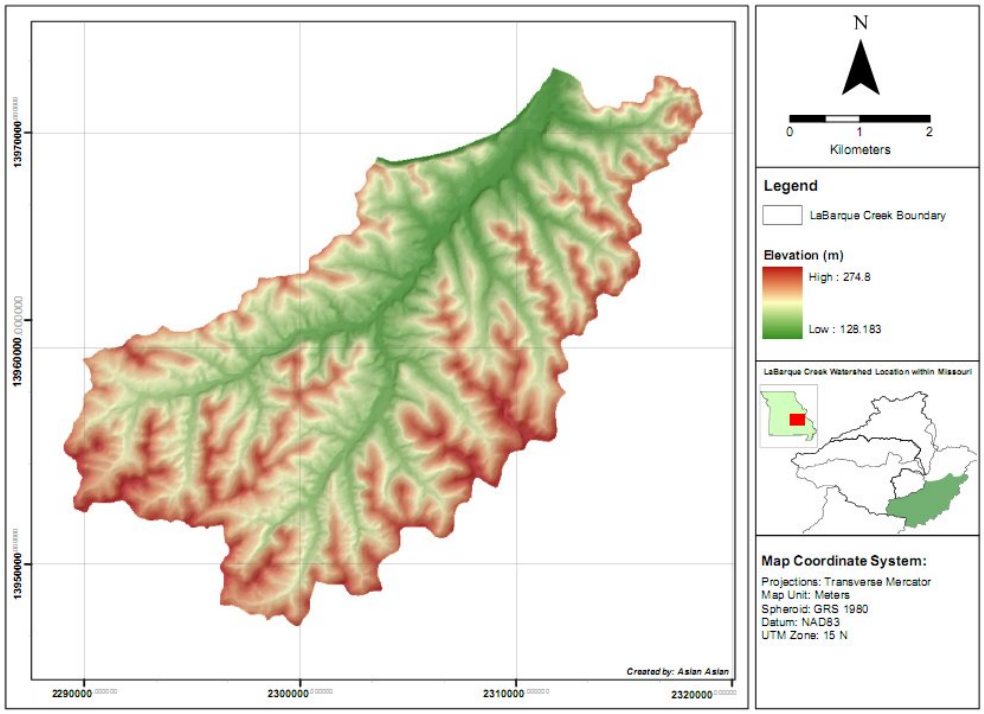

Figure 20. Elevation range for the LaBarque Creek watershed.

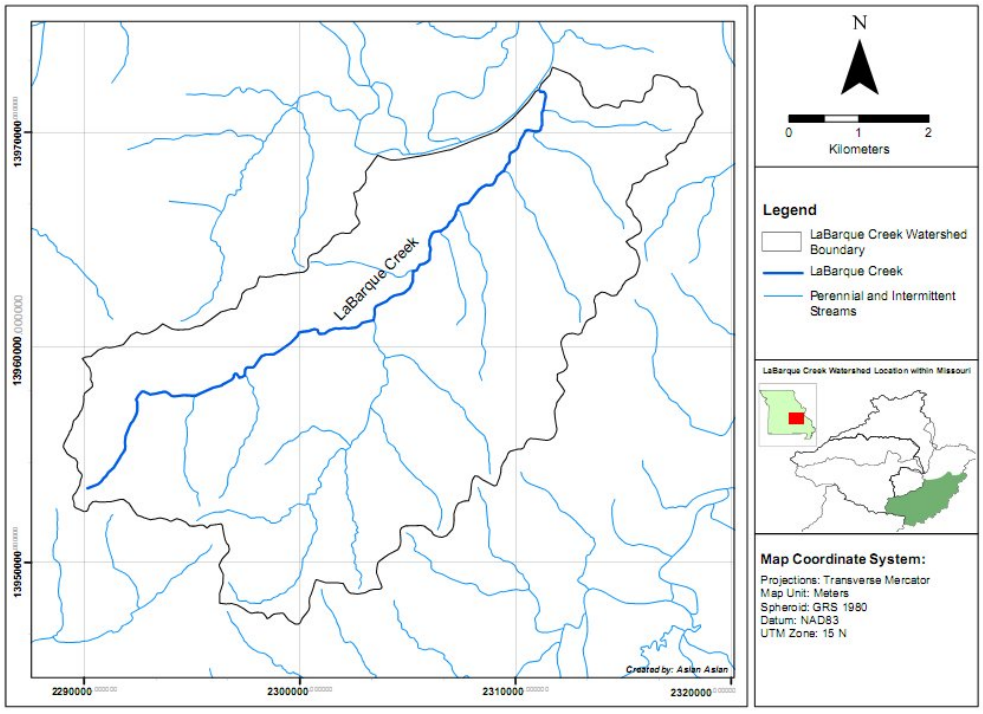

Figure 21. Boundary and hydrography for the LaBarque Creek watershed.

3.2.2.1 Basic GIS layer creation

3.2.2.1.1 Slope

Similar to other water resources studies, slope is an important factor in these models because from it runoff velocities can be calculated. Slope identifies the steepest downhill path for a location on a surface. In a raster data model, it is the maximum rate of change in elevation over each cell and its eight neighbors where the lower the slope value, the flatter the terrain and vice versa. In relating slope to runoff velocities, steeper slopes may result in higher runoff velocities. In addition, the output of raster slope can be calculated as percent slope or degree of slope. Mathematically, slope is a rise over a run. When the slope angle equals 45 degrees, the rise is equal to the run and if it expressed as a percentage, the slope of this angle is 100 percent. In these models, slope is input as a percent slope. A depiction of the slope within the LaBarque Creek watershed can be seen in Figure 22. In ArcMap, slope is easily calculated by utilizing the Surface Analysis module in 'Spatial Analyst' menu.

Based on Figure 22, one can see that slopes in the study area vary from 0 to 98.5 percent with slopes less than 30 percent dominating the watershed.

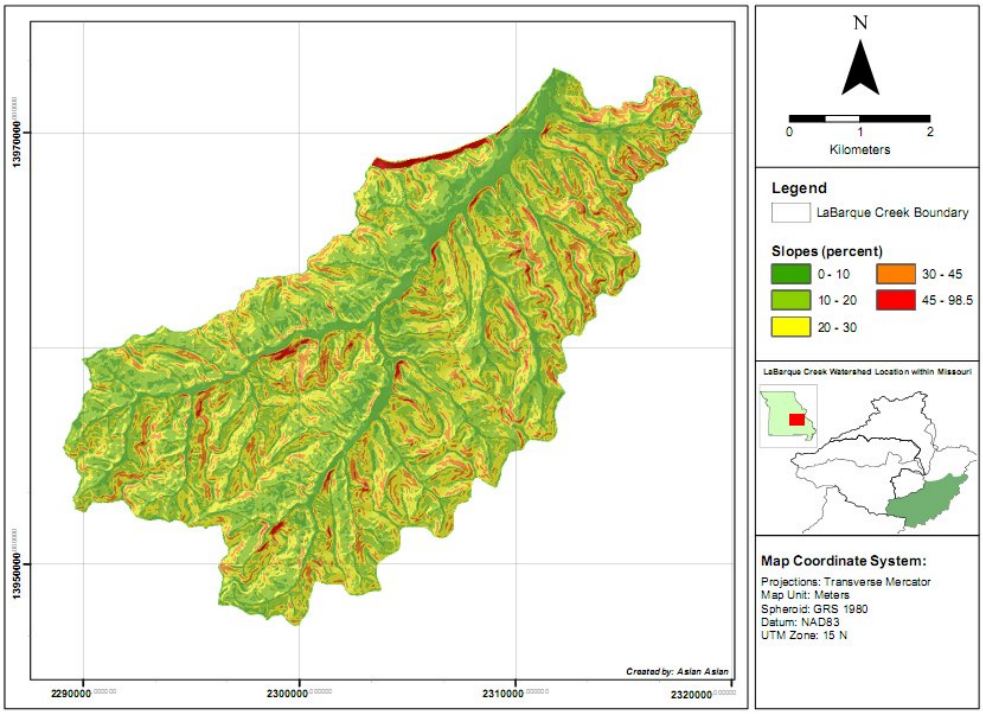

Figure 22. Slope layer for the LaBarque Creek watershed.

3.2.2.1.2 Manning's n

Similar to slope, surface roughness is also an important factor in hydrologic design, especially for these models because the roughness of a surface affects the characteristics of overland flow. For example, a grass surface is hydrologically rougher than an impervious surface; therefore, the grass retards the flow greater than does the impervious surface. Manning's roughness coefficient (n) is the most widely used by engineers and scientists to represent surface roughness for hydrologic models. For example, Wong and McCuen (1982) used Manning's roughness coefficients of 0.2, 0.35, and 0.8 to represent light turf, dense turf, and conifer/deciduous forest with dense grass understory, respectively, to generate a runoff velocity. In this research, the Manning's n layer was derived from land cover data as shown in Figure 23. Further, values of Manning's n for hydrologic overland flow surface are provided in Table 8.

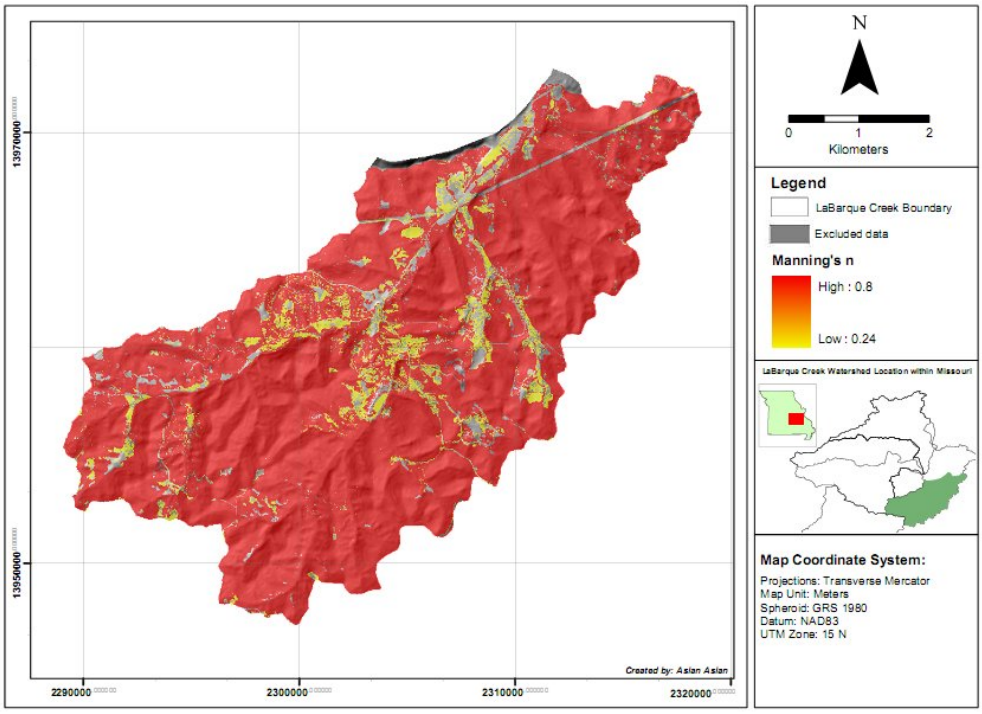

Figure 23. Manning's n layer for the LaBarque Creek watershed.

Table 8. Manning's roughness coefficient (n) extracted from land cover types.

Land cover type	Manning's n	Manning's n source
Impervious	0.011	Engman (1986)
Bare land	0.02	Engman (1986)
Cropland	0.24	Engman (1986)
Grassland	0.41	Davis and McCuen (2005)
Shrub	0.13	Prakash (2004)
Forest	0.8	Davis and McCuen (2005)
Water	0.01	Engman (1986)

However, due to the limitation of these models, the land cover classes that have Manning's n values less than 0.2 (e.g., impervious, water, and shrub) were not used by Wong and McCuen (1982) and will be excluded from this simulation (and are shown in gray). Therefore, the land cover classes that will be used in this simulation consist of grassland (n=0.41), cropland (n=0.24), and forest (0.8).

3.2.2.1.3 Settling velocity

In this research, the settling velocity of particles is another significant factor in regard to the determination of the width of a vegetative buffer, as well as in determining the effectiveness of a buffer in trapping sediment. The greater the settling velocity, the higher the removal efficiency per length of buffer strip (Wong and McCuen 1982). According to Stoke's law, as can be seen on Equation 7, soil particles settle at different rates based upon their diameters and specific gravities. For instance, larger particles such as medium sands will have higher rates of settling velocities. However, very small particles, such as colloidal clay particles and fine silts, have extremely slow settling velocities

$$v = \frac{1}{18}\left[\frac{(\rho_s - \rho_F)gd^2}{\mu}\right] \qquad \text{Equation 7}$$

where

v = settling velocity (ft/s),

g = gravitational acceleration g (32.2 ft/sec^2),

ρ_s = density of dropped object (lb/ft^3),

d = diameter of dropped object (ft),

ρ_F = density of fluid (lb/ft^3), and

μ= kinematic viscosity (ft^2/sec^2).

Specific to this model, settling velocities of sediments are based on a soil texture of coarse silt with a mean settling velocity rate of 0.002 feet per second through a buffer strip (Wong and McCuen 1982). Therefore, settling velocities for other soil textures may

also be estimated by knowing the settling velocities ratios of the coarse silt to the other soil textures. For instance, the ratio of the settling velocities for coarse silt to medium silt is 1.3:1. Thus, the width of buffer strip obtained from this model should be multiplied by this ratio (i.e., 1.3) to obtain the required width for a medium silt. To implement that formula in a raster data model, if the required buffer width for coarse silt conditions is 3 cells (i.e., about 100 feet) then the required buffer width for the medium silt will be 3.9 cells, rounded up to 4 cells or 133 feet. Figure 24 shows the factors to apply to the coarse silt-based buffer widths to account for the differences in buffer widths required for materials that settle out faster or more slowly than coarse silt. It was derived from the soil texture data in ArcMap (Figure 17) (Personal communication with Bryan Mayhan, May 10, 2009). Fine sand is shown in red, and its greater settling velocity results in a smaller required buffer width. The light green areas in the watershed represent locations with medium silt, where a slightly larger buffer width is required. Blue areas indicate fine silt, the settling velocity for which is so low that the required buffer width is almost five times that of coarse silt. Values of the ratio of settling velocity for different soil textures to coarse silt are given in Table 9 (Wong and McCuen 1982).

Table 9. Settling velocity ratios of soil textures to coarse silt (Wong and McCuen 1982).

Soil texture	**Settling velocity ratio**
Fine silt to coarse silt	1: 4.9
Medium silt to coarse silt	1: 1.3
Fine sands to coarse silt	1: 0.02
Medium sands to coarse silt	1: 0.005

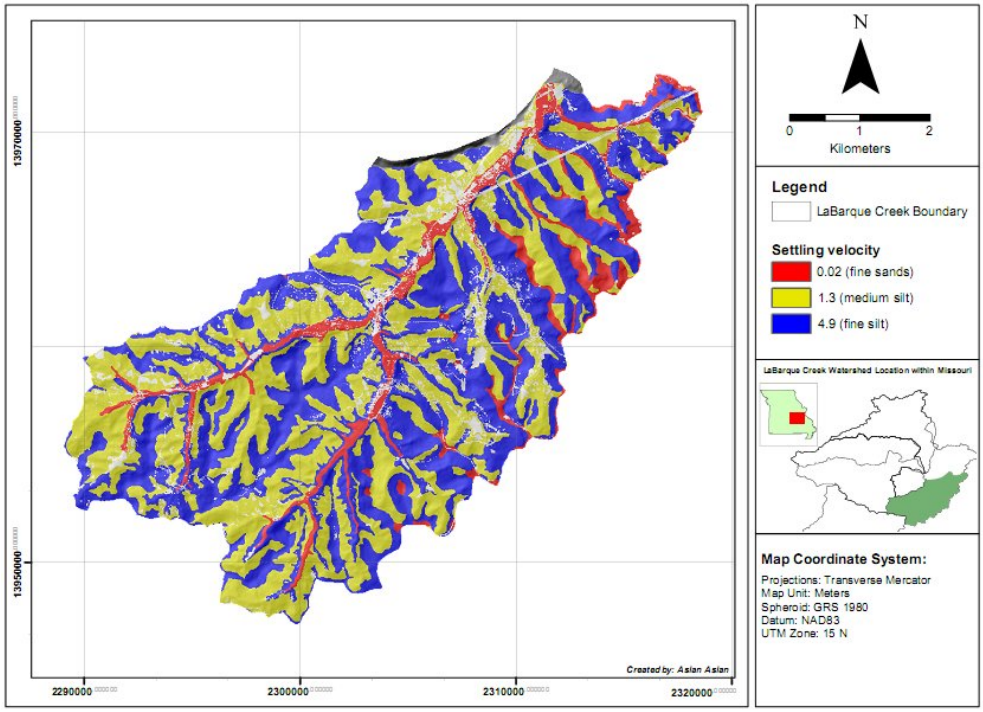

Figure 24. Buffer width factors to be applied to coarse silt buffer widths for the LaBarque Creek watershed.

3.2.2.1.4 Minimum infiltration rate

Creation of the minimum infiltration rates layer from the soil layer is essential for the infiltration model, because it can be used to determine the volume of water infiltrated within buffer strips from stormwater runoff. Values for minimum infiltration rates can be determined based the NRCS hydrologic soil groups (i.e., A, B, C, and D) (Wong and McCuen 1982). As stated previously, group A soils are normally coarse, sandy, well-drained soils, with the highest rates of infiltration and the lowest potential for runoff. On the other end, group D soils are normally heavy, clayey, poorly drained soils, with the lowest rates of infiltration and the highest potential for runoff to occur. The characteristics of group B and C soils are intermediate between groups A and D soils.

Values of minimum infiltration rates are listed in Table 7. Similar to creating the settling velocity layer, the minimum infiltration rates layer (Figure 25) was derived from hydrologic soil group data in ArcMap (Figure 18).

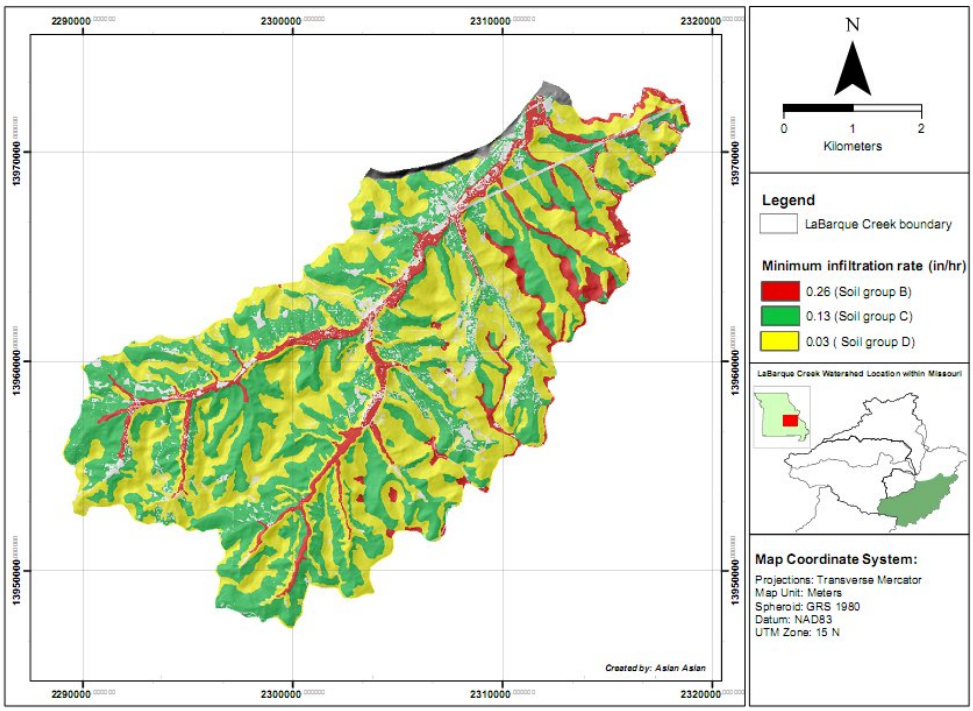

Figure 25. Minimum infiltration rates layer for the LaBarque Creek watershed.

3.2.2.1.5 Flow direction, reverse DEM, and reverse flow direction

Layers representing the flow direction, the reverse DEM, and the reverse flow direction are needed in these models for several reasons. The flow direction layer from the normal DEM is useful in the process of calculating cumulative travel time from uphill down to the streams, while the reverse flow direction layer from the reverse DEM is necessary when delineating the buffer width in the final process. The reverse DEM layer assumes that the river centerline is the highest point from which all water will drain, while in a normal DEM layer, the centerline of the river is the lowest point. In ArcMap, the process of creating a reverse DEM layer is accomplished by using the 'Negate' tool in

ArcToolbox. Moreover, based on the reverse DEM layer, a reverse flow direction layer can be derived by using the 'Hydrology' tool also in ArcToolbox.

Theoretically, the direction of flow across a surface will always be in the steepest downslope direction according to the D8 algorithm developed by O'Callaghan and Mark (1984). The D8 algorithm is the most frequently used method for approximating flow directions on a topographic surface using GIS software, where all areas that have accumulated upstream of a given grid cell drain to only one of eight neighboring grid cells, that with the steepest angle of descent. The flow direction value for each cell will consists of values between 1- 255 according to the direction. Moreover, to assign a flow direction value to a cell, the "distance weighted drop" to each of eight neighboring cells is calculated by taking the difference in elevation values and dividing by $\sqrt{2}$ for a diagonal cell and one for a non-diagonal cell (O'Callaghan and Mark 1984). The flow direction for a cell is assumed to be in the direction with the greatest distance weighted drop. In GIS software, the eight possible flow directions are assigned to have unique numbers according to the following convention (East = 1; Southeast = 2; South = 4; Southwest = 8; West = 16; Northwest = 32; North = 64; Northeast = 128). A sample depiction concept of the D8 algorithm can be seen in Figure 26 (parts a through d), where Figure 26a shows an example elevation grid, Figure 26b shows the flow direction assignment convention, Figure 26c shows the numerical values assigned to cells in the flow direction grid, and Figure 26d shows the flow directions symbolically with arrows (National Oceanic and Atmospheric Administration (NOAA) 2009). The resultant layers of the flow direction from the normal DEM, reverse DEM, and reverse flow direction, can be seen in Figure 27, Figure 28, and Figure 29, respectively.

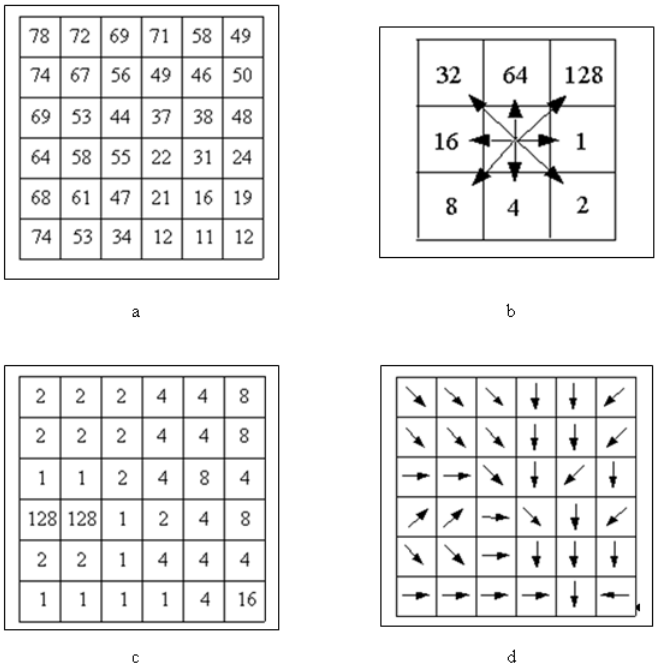

Figure 26. A depiction of the flow direction concept using the D8 algorithm: a. elevations; b. flow direction codes; c. flow direction grid values; d. symbolic representation of flow directions (Adopted from NOAA 2009).

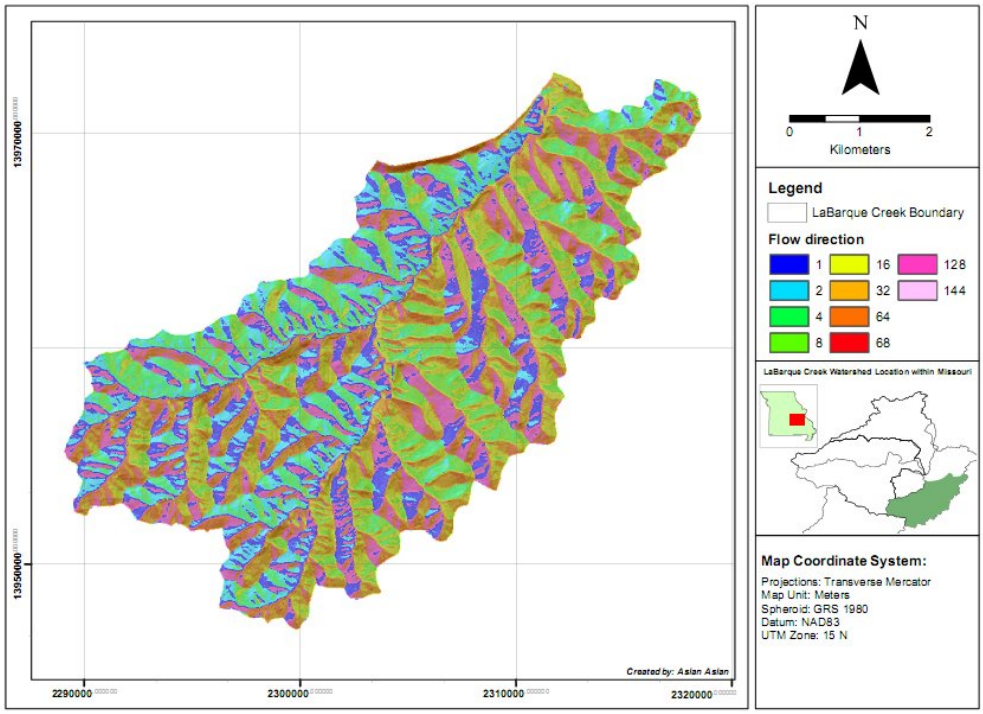

Figure 27. Flow direction layer for the LaBarque Creek watershed.

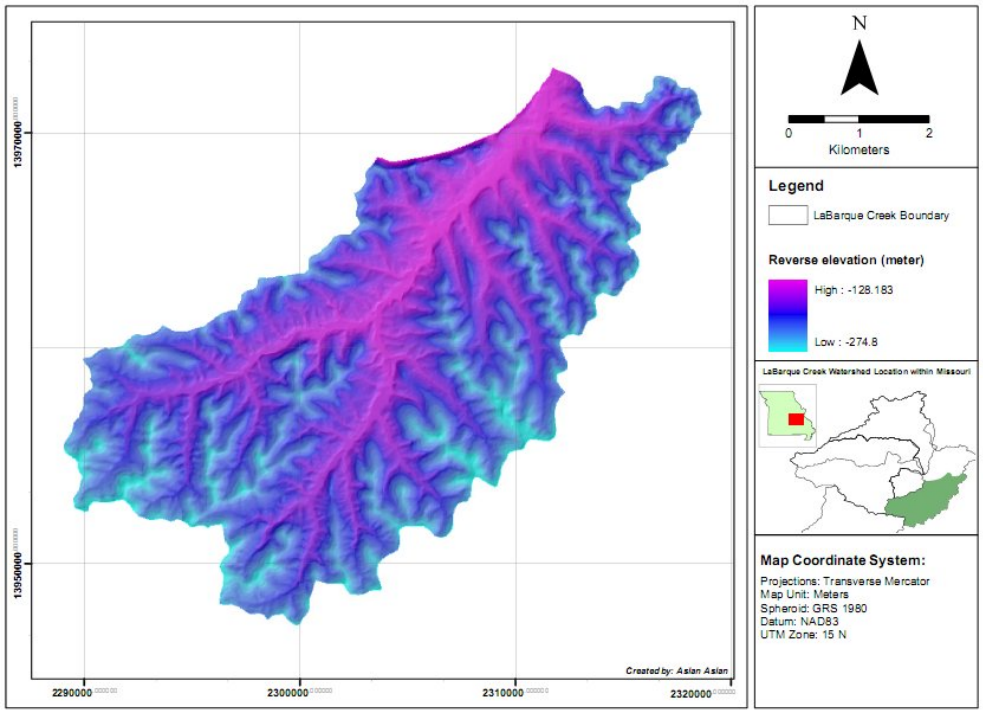

Figure 28. Reverse DEM layer for the LaBarque Creek watershed.

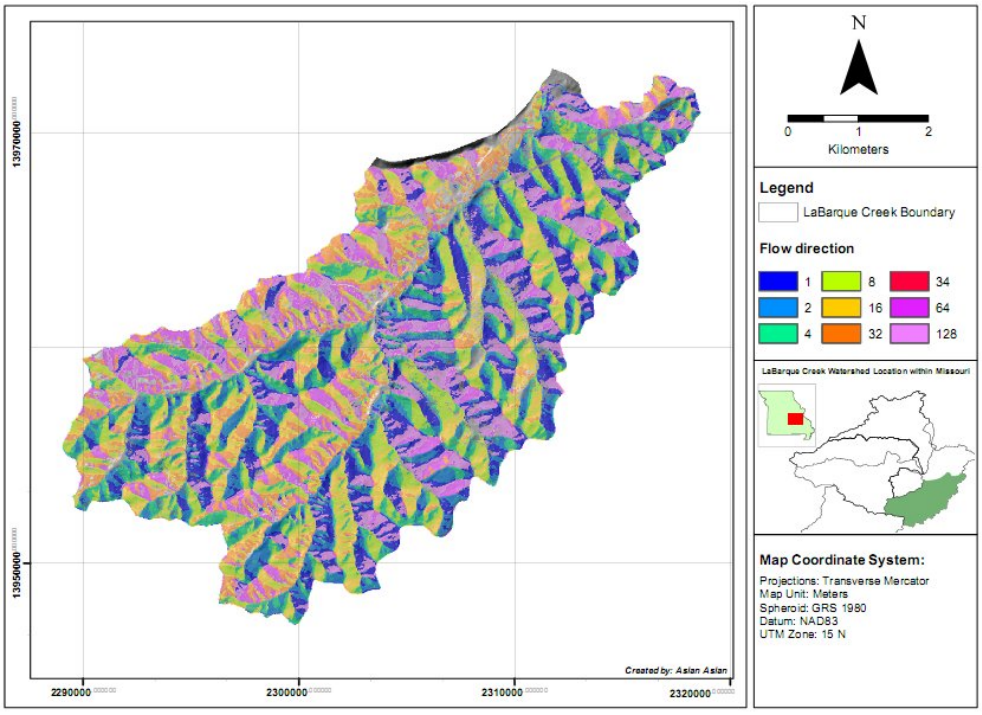

Figure 29. Reverse flow direction layer for the LaBarque Creek watershed.

3.2.3 Development of methods using GIS

In phase 3, a GIS procedure to implement the methodology established in phase 1 was developed through development of a GIS analysis flow chart plan. In total, three flow charts were developed to represent the implementation of the vegetative buffer strip models using GIS raster data analysis on a cell-by-cell basis. First, for sedimentation, the new layers are those of runoff velocity and buffer width required for a specific removal efficiency and by using a simple summation over the segments, the total buffer width required can be determined. Second, the removal efficiency for sedimentation can be estimated by knowing the buffer width and the runoff velocity. Third, for infiltration, the calculation utilizes data layers of the site-specific parameters that account for the fact that physical parameters (e.g., hydrologic soil type) can vary spatially independently of each other. New data layers of travel time and depth of infiltration are created through equations that relate the physical parameters to an assessment of how much time is available for infiltration as storm water runoff travels over a finite segment between the source (e.g., a parking lot) and the receiving stream.

3.2.3.1 GIS flow chart for delineating buffer widths

The following process is the procedure to determine the buffer width for each cell (i), according to the GIS flow chart in Figure 30.

Step 1:

Substitute the value for slope (S_i) (from the DEM) and Manning's n (from the land cover) into Equation 1 to compute α_i.

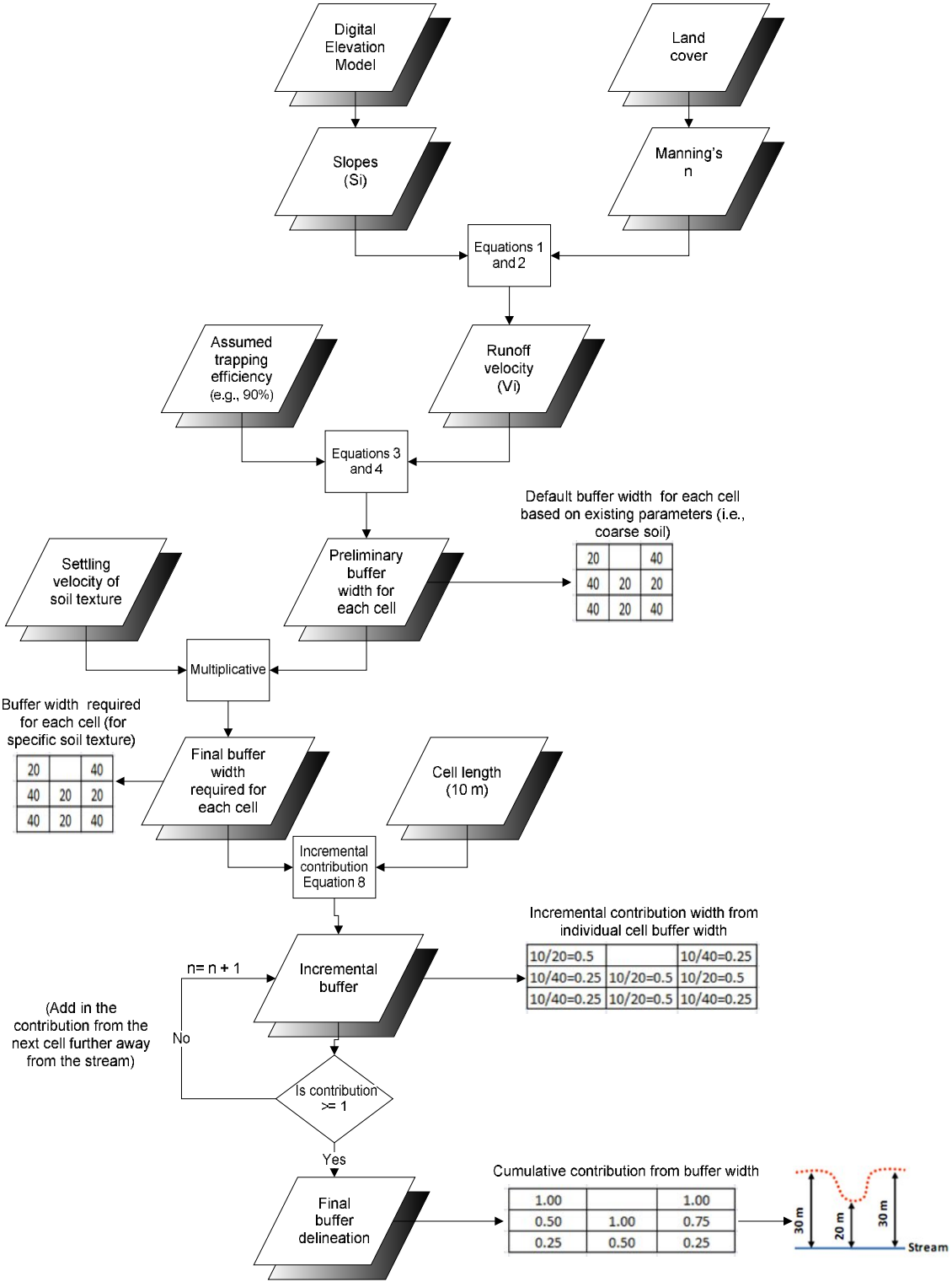

Figure 30. A GIS flow chart for determining the required buffer width based upon an input of physical parameters and an assumed trapping efficiency.

Step 2:

Substitute α_i and S_i into Equation 2 to solve for runoff velocity (V_i). Additionally, because Equation 2 is a quadratic equation, the runoff velocity can be determined by using the quadratic formula:

$$V_i = [-b + \text{sqrt}(b^2 - 4ac)\ ] / (2a) \qquad \text{Equation 8}$$

where V_i = runoff velocity ft/sec, a = 174.45, b = 14.234, and c = α .

Step 3:

Assume a trapping efficiency value (λ_i) (e.g., 90%) in order to calculate the gradient trapping efficiency (β_i) from Equation 3.

Step 4:

Substitute V_i and β_i from steps 2 and 3, respectively, into Equation 4 to calculate the preliminary buffer width (L_i). The resultant buffer width in this stage is a buffer width for the default model (i.e., based on the settling velocity for coarse silt soil).

Step 5:

Multiply the buffer width from step 4 by the settling velocity ratio to obtain the required buffer width for each cell for different soil textures. A detailed discussion for how to implement the GIS in this particular step is presented in Chapter 4.

Step 6:

Calculate the incremental contribution of the individual cells to the overall buffer performance. Mathematically, the incremental contribution is calculated using Equation 9:

$$\text{Cell}_{\text{contribution}} = \left(\frac{A}{B}\right) \qquad \text{Equation 9}$$

where A = actual width of pixel (feet), and B = calculated width needed (feet).

In this particular simulation, the actual width of the pixel is 32.8 feet (10 m). For example, if the values of B for three consecutive cells are 40 m, 40 m, and 20 m, then the values of incremental cell contribution are 0.25, 0.25, and 0.5. This means that the first and second cells each only contribute 25% of the total required buffer width, while the third cell contribute 50% of the total requirement of buffer width.

Step 7:

Determine the final buffer width by calculating cumulative contribution of each individual cell. This is an iterative process accomplished by summing up each cell along a flow path (i.e., from the centerline of the stream) with two conditions. First, if the value of the cumulative cell contribution is greater than or equal to 1, then the summation process stops because it has already reached the 100% requirement for buffer width. Second, if the value of cumulative cell contribution is less than 1, then the summation process continues because the requirement for buffer width for particular cell has not yet been achieved.

3.2.3.2 GIS flow chart for calculating sediment trapping efficiencies

The process for calculating sediment-trapping efficiency is a reverse process of the process of delineating buffer width because both of them use similar equations (i.e., Equations 1 – 4). The following process is the procedure to calculate sediment-trapping efficiency for each cell (i), according to the GIS flow chart in Figure 31.

Step 1:

Substitute the value for slope (S_i) (from the DEM) and Manning's n (from the land cover) into Equation 1 to compute α_i.

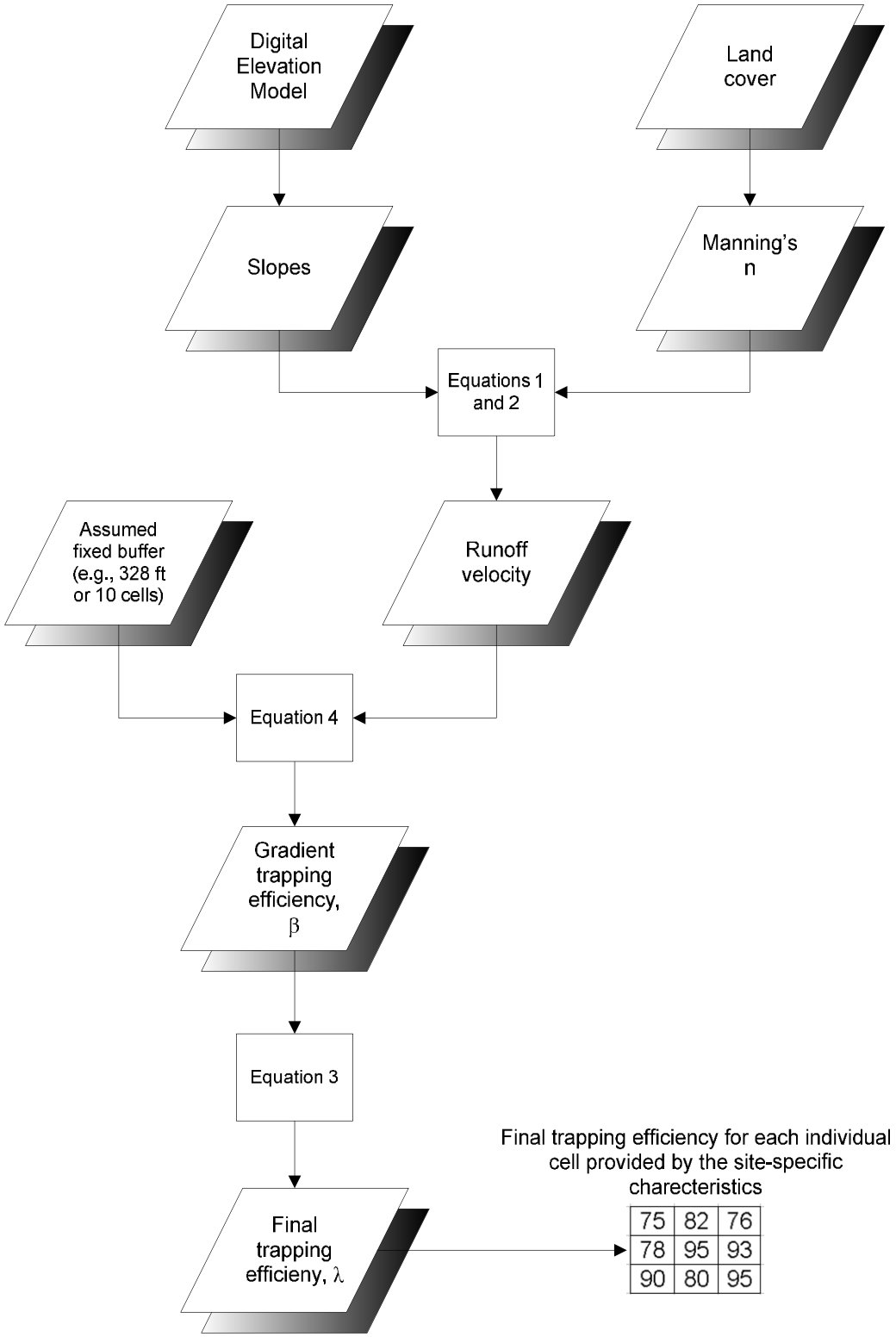

Figure 31. A GIS flow chart for determining the sediment trapping efficiency for individual cells based upon an input of physical parameters and a given buffer width.

Step 2:

Substitute α_i and S_i into Equation 2 to solve for runoff velocity (V_i). Additionally, because Equation 2 is a quadratic equation, the runoff velocity can be determined by using the quadratic formula:

$$V_i = [-b + \text{sqrt}(b^2 - 4ac)\ ] / (2a) \qquad \text{Equation 8}$$

where V_i = runoff velocity ft/sec, a = 174.45, b = 14.234, and c = α .

Step 3:

Assume a fixed buffer width (L_i) (e.g., 328 ft or 10 cells) in order to calculate gradient trapping efficiency (β_i) by rearranging Equation 4

$$\beta_i = \left(\frac{\text{Log}(L_i)}{\text{Log}(321331V_i^4 - 405658V_i^3 + 354609V_i^2 - 111311V_i + 12585)} \over 0.5283 \right) . \quad \text{(Rearranged Eq. 4)}$$

Step 4:

Determine the final sediment trapping efficiency of each individual cell (λ_i) by utilizing β_i and Equation 3. Because Equation 3 is a 4th degree polynomial, it is difficult to calculate λ_i in ArcGIS. Therefore, the process was conducted in Microsoft Excel by creating a look-up table with values of trapping efficiency (from 75 to 95 percent [i.e., according to the limitation of the model] in 0.1 increments) in the first column and the corresponding gradient of trapping efficiency from Equation 3 in the second column. Table 10 shows a partial list of both the trapping efficiency and the corresponding gradient. The complete data can be found in Appendix G.

Table 10. Sample calculation of trapping efficiency and its gradient.

Trapping Efficiency (%)	Gradient of Trapping Efficiency
75.00	0.251
75.10	0.251
75.20	0.251
75.30	0.251
75.40	0.251
75.50	0.251
75.60	0.251
75.70	0.252
75.80	0.252
75.90	0.252
76.00	0.253
.	.
95	1.413

3.2.3.3 GIS flow chart for determining volume of stormwater infiltration

The following process is the procedure to determine volume of stormwater infiltration for each cell (i), according to the GIS flow chart in Figure 32.

Step 1:

Substitute the value for slope (S_i) (from the DEM) and Manning's n (from the land cover) into Equation 1 to compute α_i.

Step 2:

Substitute α_i and S_i into Equation 2 to solve for runoff velocity (V_i). Additionally, because Equation 2 is a quadratic equation, the runoff velocity can be determined by using the quadratic formula:

$$V_i = [-b + \text{sqrt}(b^2 - 4ac)\ ] / (2a) \qquad \text{Equation 8}$$

where V_i = runoff velocity ft/sec, a = 174.45, b = 14.234, and c = α. .

Step 3:

Assume a fixed buffer width (L_i) (e.g., 328 ft or 10 cells) in order to calculate the incremental travel time (Tt_i) for an individual cell by using Equation 5.

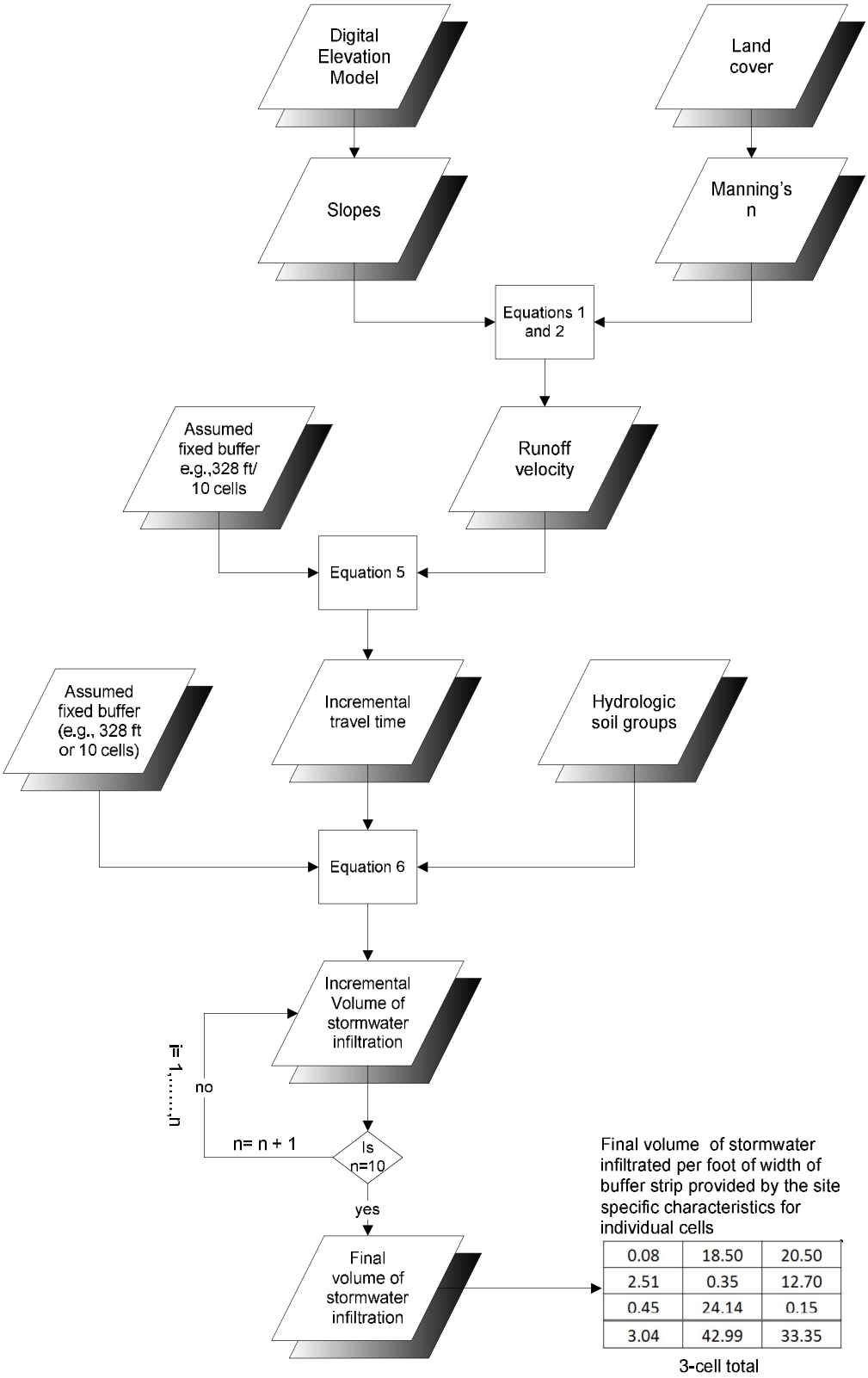

Figure 32. A GIS flow chart for determining the volume of water infiltrated based upon an input of physical parameters and a given buffer width.

Step 4:

Calculate the volume of stormwater infiltration for each individual cell (V_L) by using Equation 6, using the assumed fixed buffer (L_i) (e.g., 328 ft or 10 cells), incremental cell travel time (Tt_i) from step 3, and minimum infiltration rates for each cell (fc_i) (from the hydrologic soil group map).

Step 5:

Determine the final volume of stormwater infiltration by calculating the cumulative contribution of each individual cell from step 4. This is an iterative process achieved by summing down each cell along a flow path (i.e., from the edge of the buffer to the centerline of the stream) with two conditions. First, if the cumulative cell number is greater or equal to the number of cells of the given buffer (e.g., 10), then the summation process is stopped because the contributions from all cells in the buffer have been added in. Second, if cumulative cell number is less than the number of cells in given buffer (e.g., 10), then the summation process continues because all cells have not yet been accounted for.

3.3 Chapter summary

This chapter began with a general description of the study site (i.e., the LaBarque Creek watershed) including the ecosystem, geology, and demographics of the area. The chapter then discussed the development of a GIS methodology using raster data analysis for applying a vegetative buffer strip model developed by Wong and McCuen (1982). The methodology was constructed from three subsequent parts: (1) development of empirical models (for sediment control and stormwater infiltration), (2) development of a spatial database, and (3) development of GIS flow charts to implement the models. In the

development of the mathematical models, statistical analyses were performed utilizing Microsoft Excel to produce the equations and validate the models. In developing the spatial database, GIS datasets were collected from various organizations and the data then standardized into raster data formats with similar projection systems. Further, in this particular section, basic GIS information was derived from the GIS data because they were required for the demonstration of the model. Finally, the chapter concluded with an explanation of the development of the flow charts used to implement the vegetative buffer strip models within the GIS environment.

Chapter 4:
RESULTS AND DISCUSSION

4.1 Overview

It has been shown that the spatial placement of buffer strips within a study area (e.g., a watershed) can have a significant effect on water quality. A GIS as a tool can assist decision makers in determining where the most benefit can be accrued from placing buffers on a landscape through its spatial analysis function as well predict how effective the installed buffers will be. In addition, because an analysis via GIS is arithmetically based, each cell within each layer that will be used in the GIS analysis should have its own value. For example, values of 1 and 2 can be assigned to forest and grassland classes, respectively, in a land cover map layer. The process of integrating between layers in GIS in order to produce a new layer is called overlay. This process occurs when there are two or more map layers of discrete features for the same area and one desires to generate a new map layer which shows the intersection of the different layers.

As stated previously, one of the objectives of this research is to demonstrate the development of a buffer strip design framework using GIS raster data (i.e., with a continuous surface) with a 10 meter (32.8 feet) cell size in the LaBarque Creek watershed. Therefore, to address the research objectives, a GIS analyses was performed using the framework for three different scenarios based upon the flow chart plan developed in Chapter 3: (1) utilization of GIS for delineating buffer widths; (2) utilization of GIS for calculating the trapping efficiencies for sediment; and (3) utilization of GIS for determining the volume of infiltrated stormwater per foot width of buffer strip.

4.2 Utilization of GIS for delineating buffer widths

A simulation of buffer width delineation for each cell in a continuous surface layer was performed by following the flow chart (Figure 30) as found previously in Chapter 3. Before the simulation was begun, the map units in the ArcMap frame were converted from meters to feet because the models were developed using English units.

4.2.1 Calculating α

The calculation of the α layer (Figure 33) was performed by overlaying slope layer (Figure 22) and Manning's n layer (Figure 23) using Equation 1. Based on Figure 33, it can be seen the value of α in the study area is varies from 0.0246096, which represents the mildest slopes, to the value 462.01, which represents the steepest slopes.

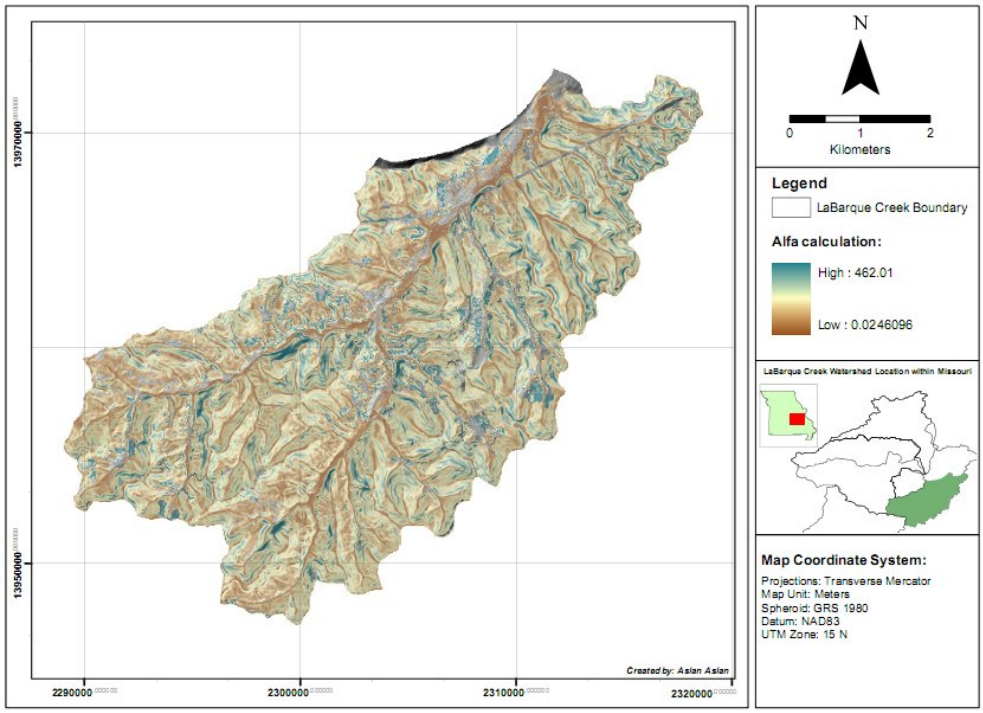

Figure 33. α layer for the LaBarque Creek watershed.

4.2.2 Calculating runoff velocity, V

The calculation of the runoff velocity layer (Figure 34) was conducted by substituting the values of α and slope into Equation 2 in GIS analysis. From Figure 34, one can see that the velocity of runoff in the LaBarque Creek watershed varies from 0.08 ft/sec on the milder slopes to 1.67 ft/sec on the steeper slopes. These overland flows velocities are logical because steeper slopes provide greater energy to produce high runoff velocities. Additionally, the model itself was developed by using measured data input of runoff velocity from 0 ft/sec to 1.4 ft/sec. Therefore, it can be seen that the runoff velocity range resulting from the model simulation is consistent with the input used to create the models. The runoff velocity layer will be used further as an input layer in delineating buffer width, determining trapping efficiency, and determining volume of stormwater infiltration.

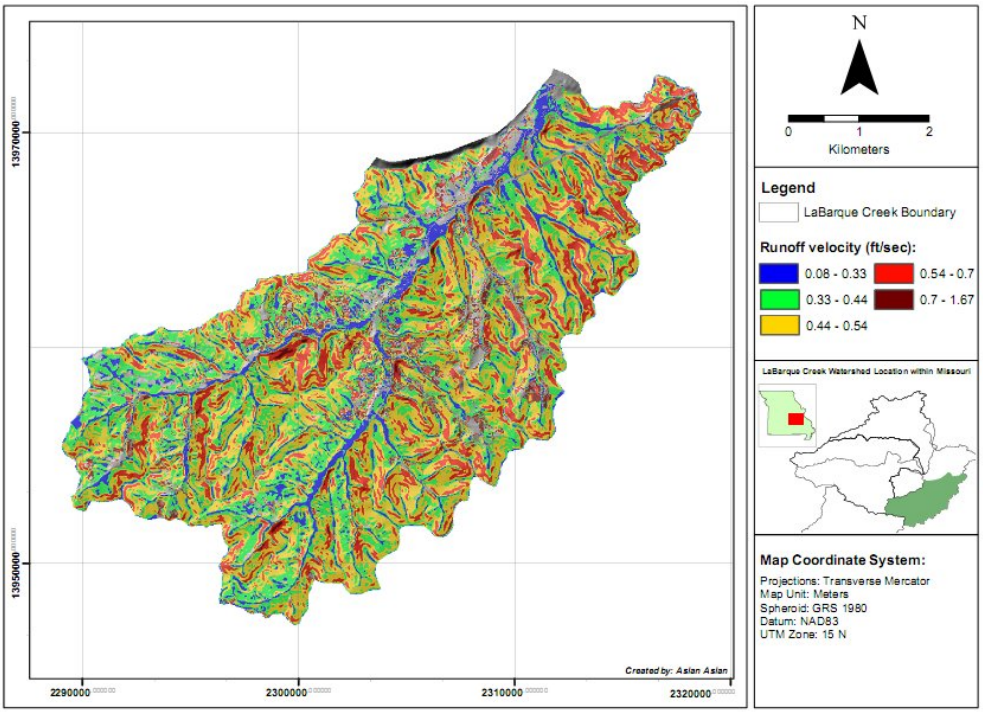

Figure 34. Runoff velocity layer for the LaBarque Creek watershed.

4.2.3 Calculating the trapping efficiency gradient, β

The calculation of the gradient layer, β, for a given trapping efficiency, λ, was performed using Equation 3. In this particular case, a trapping efficiency of 90% was chosen to be tested in the model for the entire study area. Based on the calculations, the resultant value of β is 0.66213, as can be seen in Figure 35.

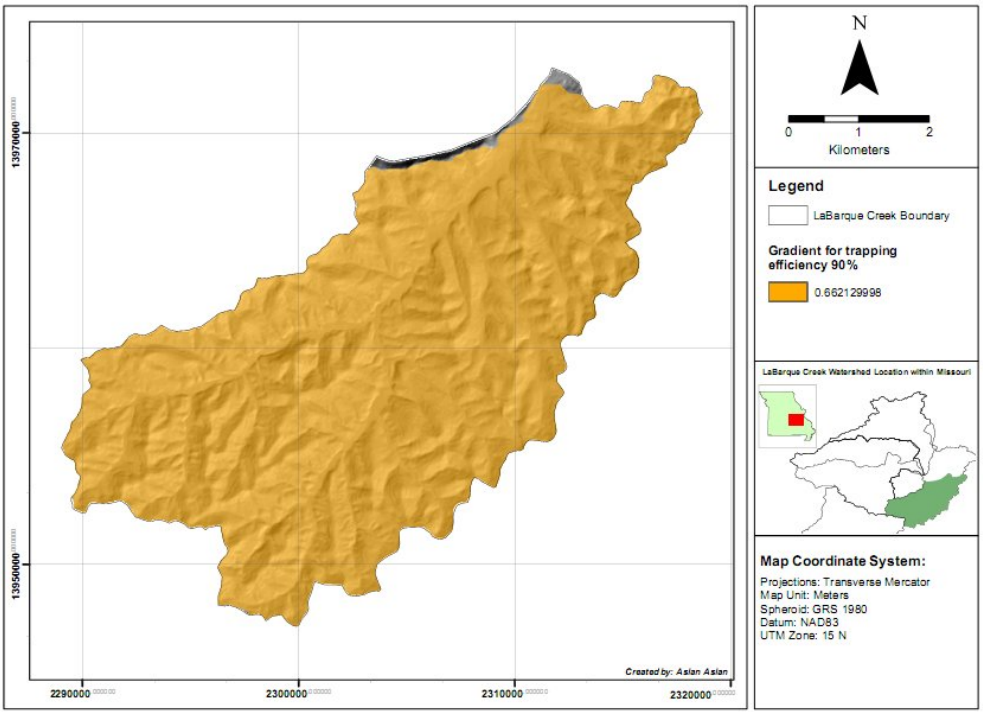

Figure 35. Gradient layer, β, for trapping efficiency, λ = 90%, for the LaBarque Creek watershed.

4.2.4 Calculating preliminary buffer width, L

The calculation of the preliminary buffer width layer (Figure 36) was conducted by overlaying the runoff velocity layer in step 2 and the gradient layer (β) in step 3 utilizing Equation 4. The preliminary buffer width contains information about the required buffer width in the study area for each cell, considering physical parameter input and assuming a soil texture of coarse silt with a settling velocity of 0.002 ft/sec (Wong and McCuen 1982). In order to achieve a similar sediment trapping efficiency (i.e., 90%) for another

soil texture, a derivative layer from this preliminary buffer layer is created by overlaying with the settling velocities layer (Figure 24) in order to obtain the final buffer width map.

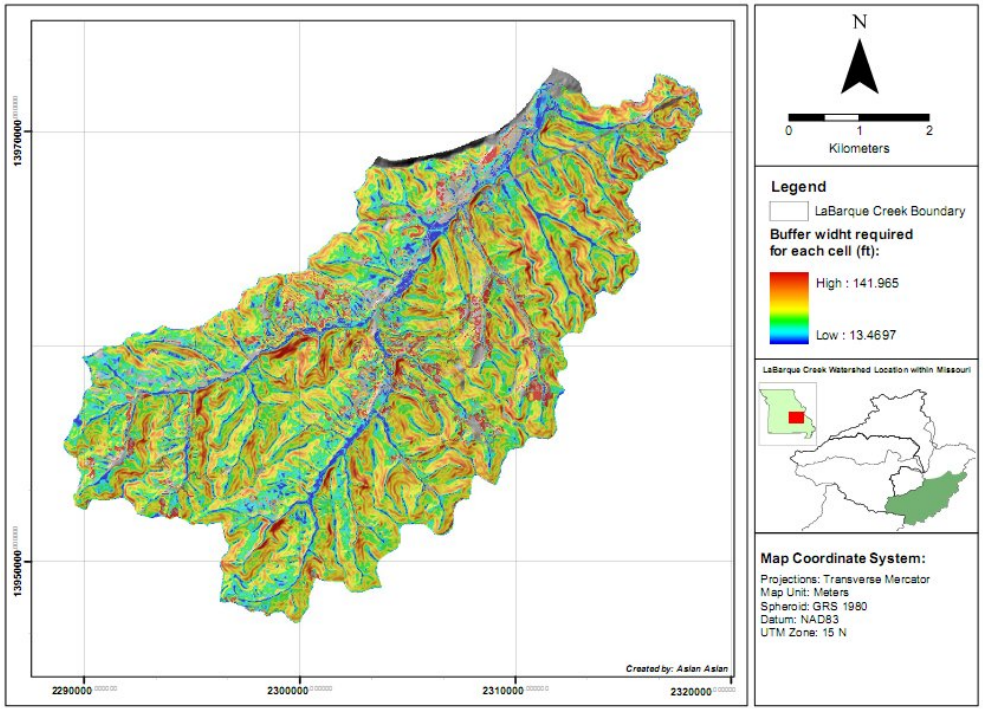

Figure 36. Preliminary buffer width required for each cell for the LaBarque Creek watershed (based on assumed coarse silt).

From Figure 36, the required buffer width for each cell in the study areas was calculated to vary from 13.4697 to 141.965 feet, where the lower values represent areas with milder slopes and vice versa. One should remember that this required buffer width is for coarse silt. Therefore, in order to obtain buffer width needed for other soil textures that can remove 90% of sediment, the preliminary buffer layer was overlaid with the buffer width factor layer (Figure 24). Mathematically, the process is multiplicative where the value of each cell in the preliminary buffer width layer was multiplied by the value of each cell in the buffer width factor layer. The output of this process is a required buffer width layer based on the soil texture conditions in the watershed. The resulting layer can be seen in Figure 37.

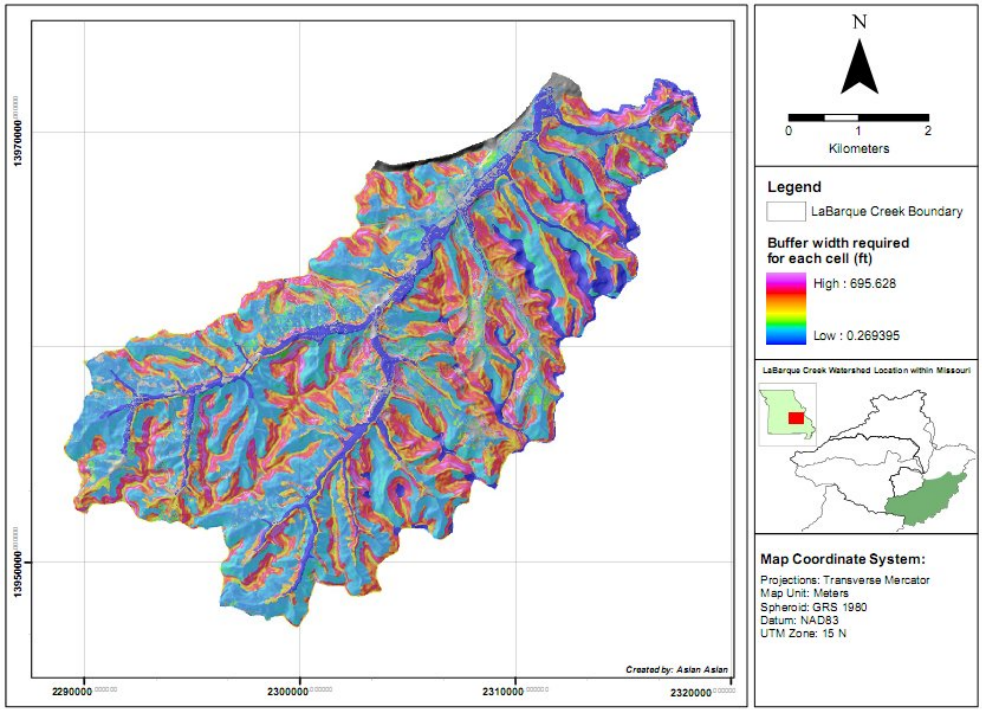

Figure 37. Buffer width required for each cell based on the soil texture condition for the LaBarque Creek watershed for a 90% trapping efficiency.

From Figure 37, one can see that after overlaying the preliminary buffer width with the buffer width factor layer, the range of new required buffer widths changed significantly from 13.5 to 0.3 feet for the lower bound, and from 142.0 to 695.6 feet for the upper bound. Moreover, this significant change proves that the settling velocity layer cannot be disregard in these models. For example, for upper limits, the ratio of 695.6 feet to 142.0 feet is 4.9, which is the ratio of the coarse silt to the fine silt soils. This means that it takes 4.9 times the length of a buffer where the runoff is carrying fine silt in order for the fine silt to be removed at the same rate as the coarse silt would be. The fact that the buffer width required can be greater than the size of a cell means that one cell cannot provide the necessary buffer size.

4.2.5 Calculating the incremental contribution of a buffer cell

Once the required buffer width per cell has been calculated, the individual cell contribution to overall buffer performance can be calculated using Equation 9 to produce an incremental contribution layer for each individual cell. This incremental contribution layer will be used in the 'flow accumulation' process to calculate the cumulative contribution of all cells up to a given location in order to create a final buffer width delineation. The resultant layer of the incremental contributions of each individual cell can be seen in Figure 38. All values greater than or equal to 1.0 are given the same color because they require only one cell to meet the buffer requirements. In other words, locations with contributions greater than 1.0 (indicating that less than 32.8′ would be needed for a buffer to trap sediments) would still be required to have a buffer the size of one cell.

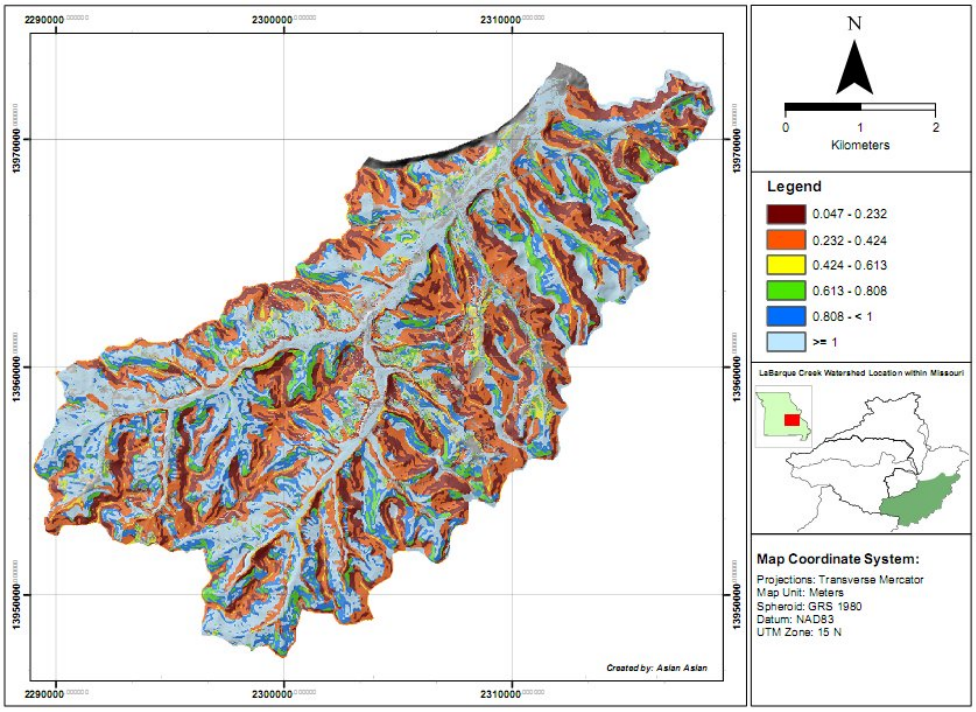

Figure 38. Incremental contribution of each individual buffer cell to sediment removal for the LaBarque Creek watershed.

The calculation of cumulative buffer contribution to buffer performance from successive cells in this simulation was conducted by using the 'Flow Accumulation' function in the 'Hydrology Tool" in ArcToolbox following the D8 algorithm principles (O'Callaghan and Mark 1984). The flow accumulation function is normally used in hydrologic analysis using GIS software to delineate the boundary of the watershed, where the highest values in the output raster layer represent streams. In GIS terms, flow accumulation can be calculated in an unweighted (i.e., accumulation with equal cell contribution) or a weighted manner (i.e., each cell has different contribution values) where the accumulation may not only be a function of topography but also be a function of precipitation depth, for example. In this particular case, the flow accumulation process follows the weighted principle; two layers were used as input: (1) the reverse flow direction layer; and (2) the incremental contribution of each cell layer as the "weighted" layer. This is an iterative process with the objective of delineating the final buffer width by calculating the cumulative contribution from cells by summing from the cell nearest the stream and progressing upslope. The resultant layer from this process can be seen in Figure 39.

As can be seen in Figure 39, the cumulative values of cell contribution was varied from 0 to 50911.9, where the zero values typically represent the centerline of streams and 50911.9 represents locations on the ridges of the study area. Further, in the final process of delineating buffer width, the threshold values between 0 and 1 become the actual buffer width needed for the watershed considering an input of physical parameter layers.

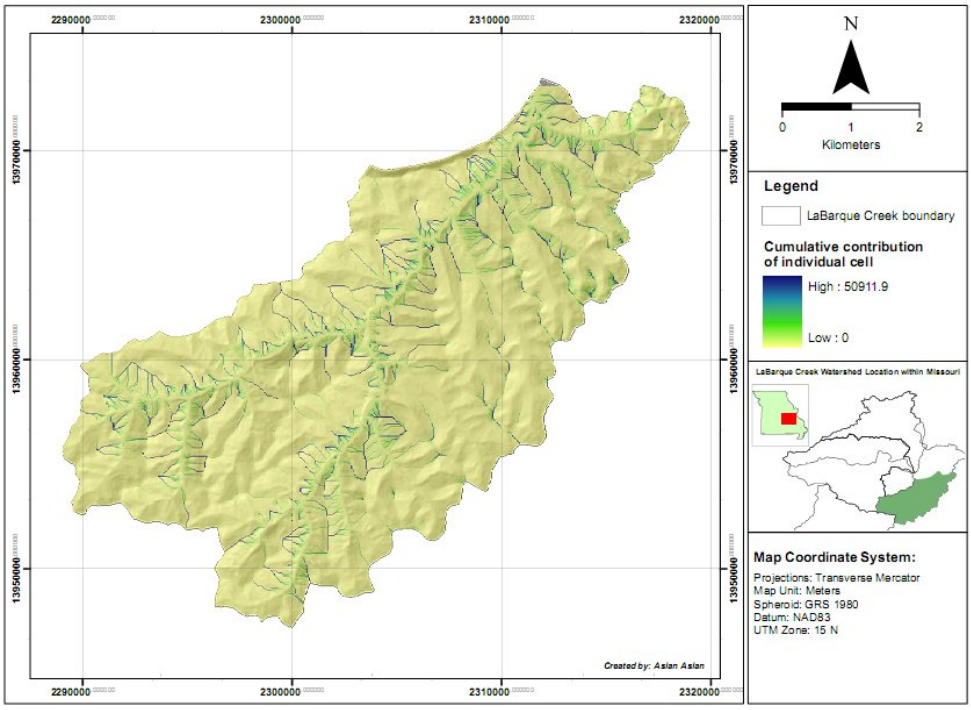

Figure 39. Cumulative contribution layer for the LaBarque Creek watershed.

4.2.6 Final buffer width delineation

The last process in delineating the buffer width was performed by applying the "Cut Off" operation using this syntax (i.e., [accumulative value] <= 1) in ArcMap for threshold values between 0 and 1 by using the 'Raster Calculator" tool in the Spatial Analyst menu to the cumulative contribution layer. Ultimately, the final delineation map of buffer width using this model is shown in Figure 40.

Figure 41 shows the difference between the delineation of required buffer width based on the default model (i.e., assuming coarse silt as the soil) and the actual delineation of buffer width needed considering actual soil types for the watershed, after overlaying with the buffer width factor layer. It can be seen within the black circle that the widths of actual buffer needed vary from lower order streams to higher order streams

while the widths of buffer from the default model did not varying between the lower streams and the higher order streams.

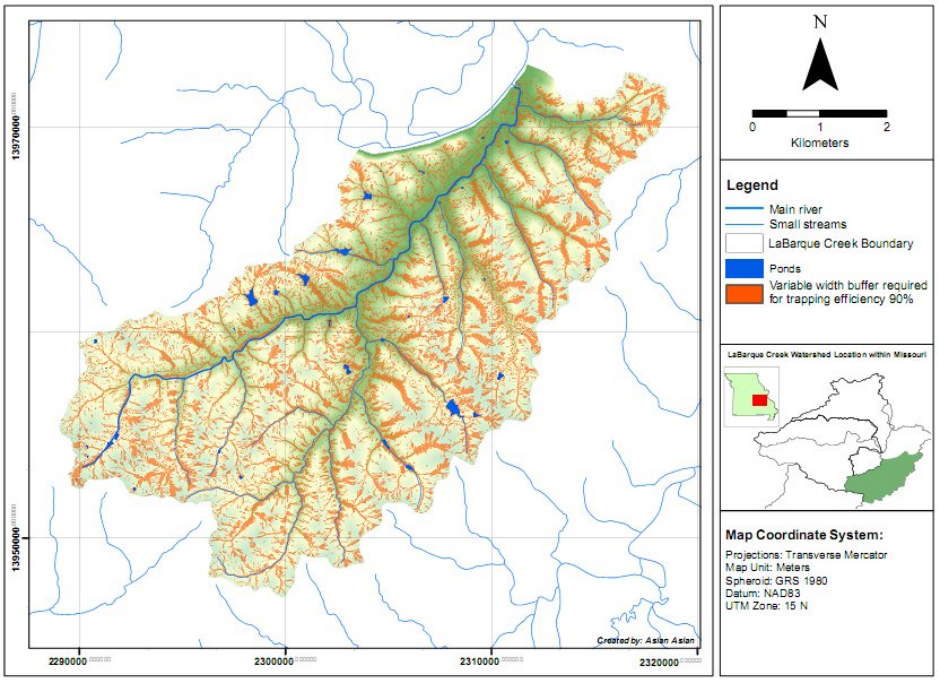

Figure 40. Variable buffer width delineation for the LaBarque Creek watershed.

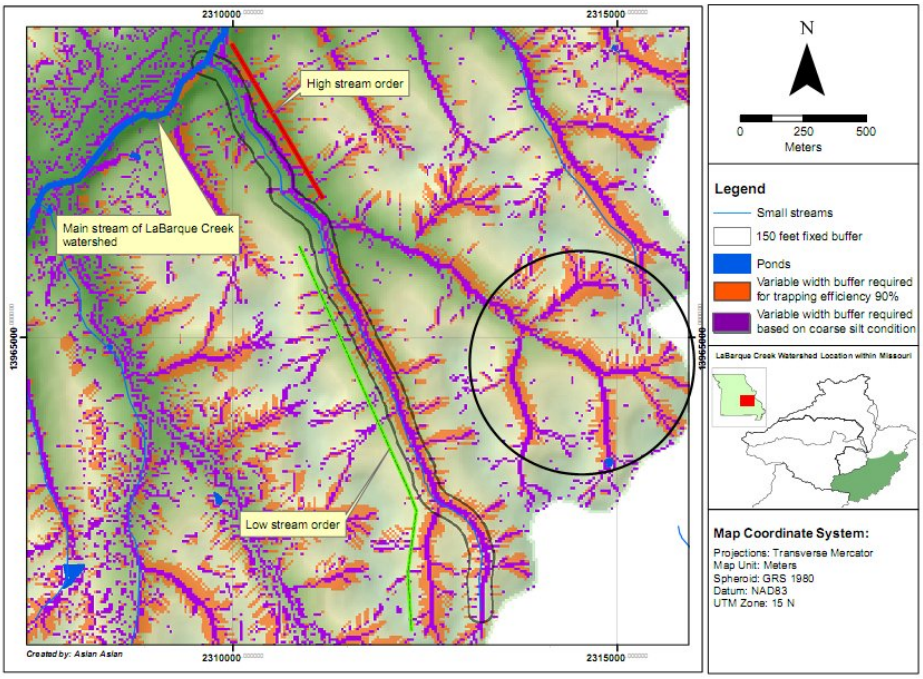

Figure 41. Variable buffer width delineation based on the default model (coarse silt) vs. the actual buffer width needed within the LaBarque Creek watershed.

4.2.7 A comparison between variable buffer width and fixed buffer width

The resulting buffer from Figure 40 can be compared to a fixed buffer width that is required by some municipal ordinances. In this case, a 150 foot fixed buffer width (150 ft on each side of the stream) was created for a small stream in the eastern part of watershed and overlaid with the variable buffer width derived from the model as shown in Figure 42.

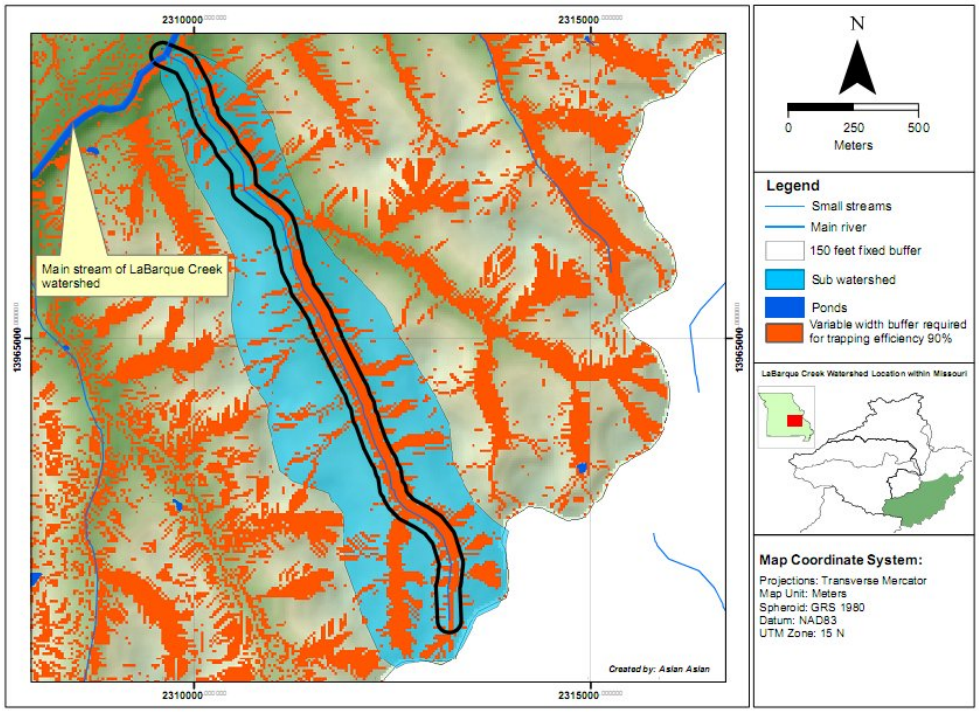

Figure 42. Variable buffer width delineation vs. a 150 foot overall fixed buffer width within the LaBarque Creek watershed.

Based on the actual required buffer width delineation using the model as shown in Figure 42 above, it can be seen that these buffers have widths that change corresponding to changes in land cover, slope, and soil condition compared to the fixed 150′ buffer width. Moreover, from distance measurements in ArcMap, the width of required buffers varied from 2 cells to 8 cells (i.e., 50 ft to 260 ft) in extent. It can also be seen that the widths of buffers are much wider along lower order streams when compared to higher

order streams. This fact shows that buffer delineation derived from this model follows the common rule in establishing buffers along the streams. Normally, buffer ordinances require wider buffers on lower order streams because they serve the functions of protecting water quality from erosion as well as preserving the ecosystem in those areas. Therefore, from this point of view, it can be concluded that buffers zones that result from the use of this model are both site-specific (and can be used as guidance for decision makers) and are consistent with the common direction of recommended buffer regulations.

The significant differences between a variable buffer widths delineation (i.e., 2 to 8 cells) and a fixed 150′ buffer width will affect not only the total area required for buffers placement, but also the proportion of land that is available for various land uses. For instance, based on calculations for the width of buffer from the model, the land requirement for installing a vegetative buffer zone in the LaBarque Creek watershed to obtain 90% removal of sediment in the portion of the watershed shown in Figure 42 is about 28.8%. Conversely, by using a 150′ fixed buffer width, the required land for installing vegetative buffer zone in the same location is 20.5%. Therefore, there is about an 8.3% difference between those two methods. Consequently, this fact could affect significantly the decisions of policy makers, especially when it comes to establishing riparian buffer ordinances.

When examining Figure 42, one can see that there are also some errors in the resulting buffers created by using this model. For example, on each side of the stream where fixed and variable buffers occur, the delineation of the buffer zones are not placed appropriately along the streams (i.e., there is a displacement between the main stream

channel and the buffer created from the model). This displacement may occur because of two factors. First, the 10-meter resolution of the DEM data is not sufficient to be used in this model because its cell size is too large, resulting in the centerline of streams not being precisely determined when running the simulation. As was stated previously, the reverse DEM data of this model assumes that the centerline of the stream is the highest point whenever the process of accumulating contribution from each cell is undertaken. Therefore, to solve this problem, it will be necessary to use a higher pixel resolution for creating an accurate DEM (e.g., with 1-meter resolution). A higher resolution DEM should result in the centerline of streams being determined appropriately when the simulation begins. A second source of error may be from the vector line data (i.e., the location of the streams within the LaBarque Creek watershed). An error possibly occurs because the source of the streams data was derived from the USGS topographic map that has a smaller scale than the DEM data (i.e., 1:24,000). Therefore, in this case, the stream location should be updated by refining the line through digitizing based on satellite imagery or an aerial photo that has a similar or higher resolution than the 10-meter DEM data. Finally, from this case it can be concluded that obtaining accurate data is an important factor prior to performing a GIS analysis.

4.3 Utilization of GIS for calculating sediment trapping efficiencies

The simulation process for calculating sediments trapping efficiencies for a given buffer width for each cell was performed by following the flow chart as found in Figure 31. The map units in the ArcMap frame were converted from meters to feet. The process of calculating trapping efficiency used equations presented earlier (i.e., Equations

1-4) and several intermediate layers such as runoff velocity (Figure 34) and fixed buffer widths.

4.3.1 Creating fixed width of buffer, L

The process of calculating sediment trapping efficiency begins with a fixed buffer width. In this particular case, the width of the buffer being analyzed was arbitrarily set to 328 feet (i.e., ten times the pixel size or 10 cells) for each side of the stream and for this simulation the buffer was only created for small streams located on the eastern side of wastershed. In ArcMap, the process of creating a 328 foot fixed buffer in the raster data format was performed by using the 'Straight Line' function in the Spatial Analyst menu. The resulting layer from this process can be seen in Figure 43.

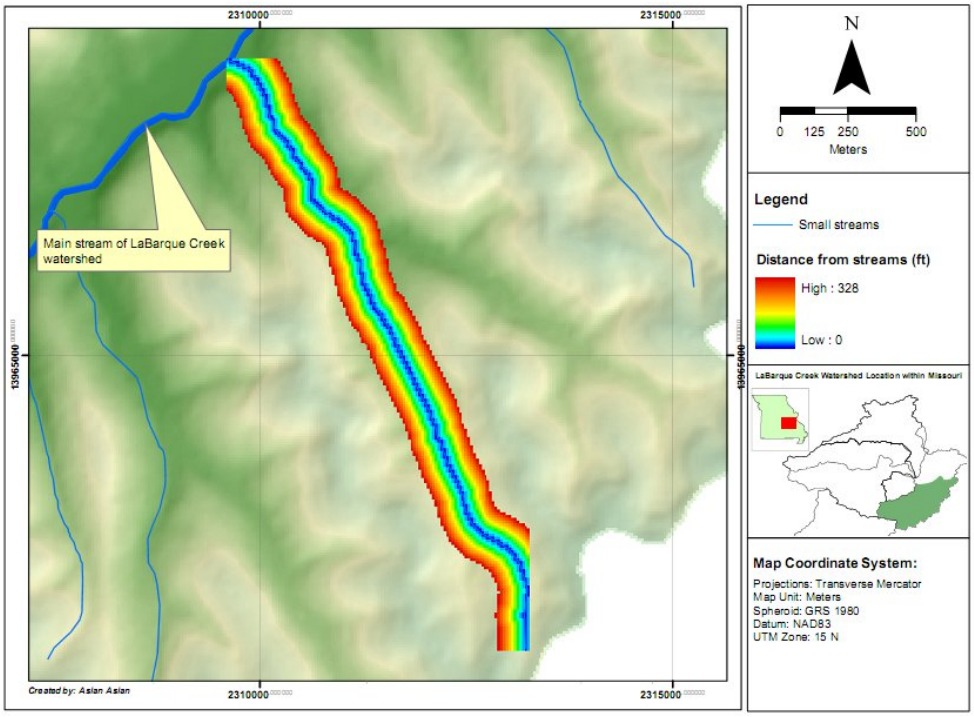

Figure 43. A 328 feet assumed buffer width for the simulation area within the LaBarque Creek watershed.

4.3.2 Calculating runoff velocity, V

The simulation uses the previously determined runoff velocity layer (Figure 34). The runoff velocity layer for the analysis area within the LaBarque Creek watershed can be seen in Figure 44. From Figure 44, one can see that for the area of interest, the runoff velocity varies from 0.12 ft/sec to 1.1 ft/sec.

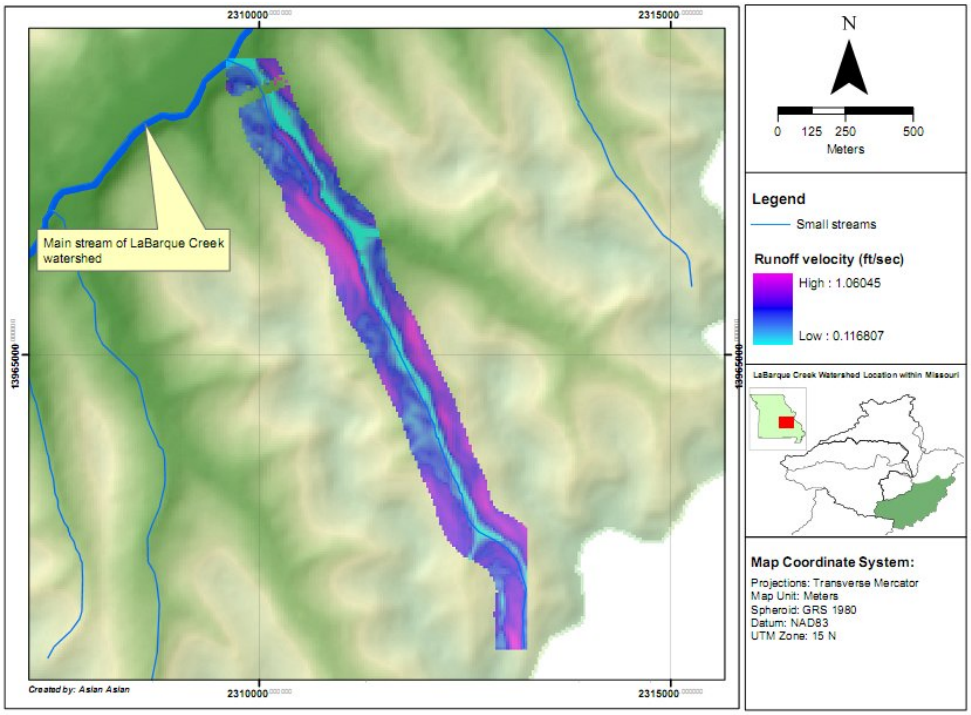

Figure 44. Runoff velocity layer for the simulation area within the LaBarque Creek watershed.

4.3.3 Calculating trapping efficiency gradient, β

The calculation of the trapping efficiency gradient was accomplished by overlaying the runoff velocity layer (i.e., Figure 44) and the 328 foot fixed buffer width layer (Figure 43) by utilizing a rearranged form of Equation 4. The resulting trapping efficiency gradient can be seen in Figure 45.

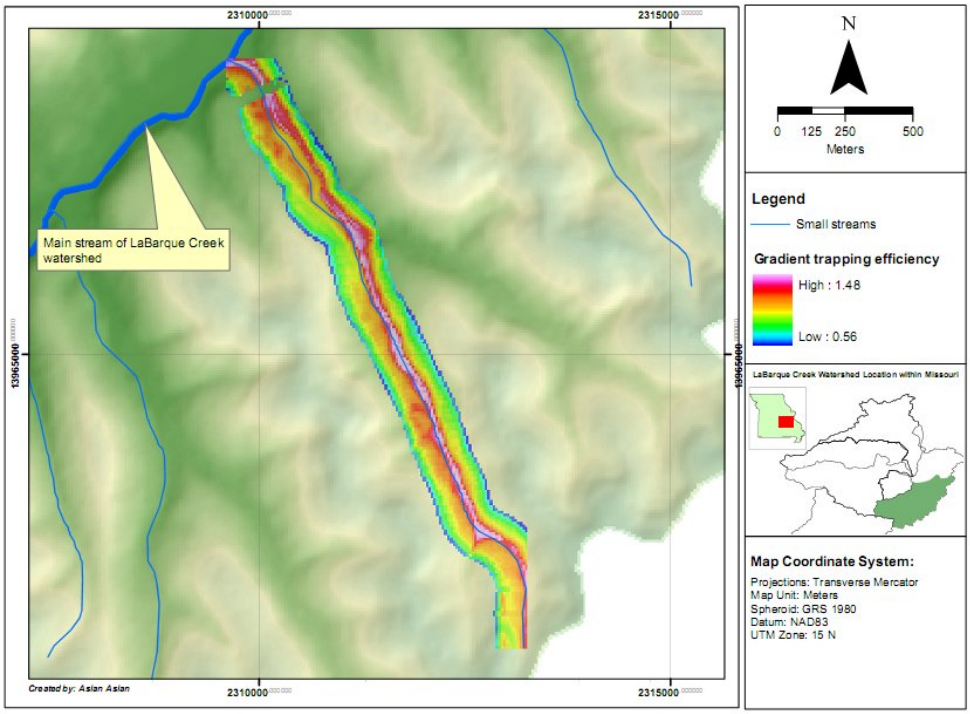

Figure 45. Trapping efficiency gradient for the 328 foot fixed buffer width for the simulation areas within the LaBarque Creek watershed.

4.3.4 Calculating trapping efficiency, λ

The last process of this simulation was to determine the trapping efficiency of a particular fixed buffer utilizing Microsoft Excel. Equation 3 was used to determine the trapping efficiency for each cell within the fixed buffer as implemented through Table 10 (see Figure 46).

Based on Figure 46, trapping efficiencies from 93% to 95% dominate the area of the fixed buffer followed by trapping efficiencies of from 92% to 93%. One can also see that the trapping efficiency gradually increases in a logically manner from the outer bound of buffer zone to the centerline of streams. Moreover, the trapping efficiency responds to the variation of physical conditions in the study areas.

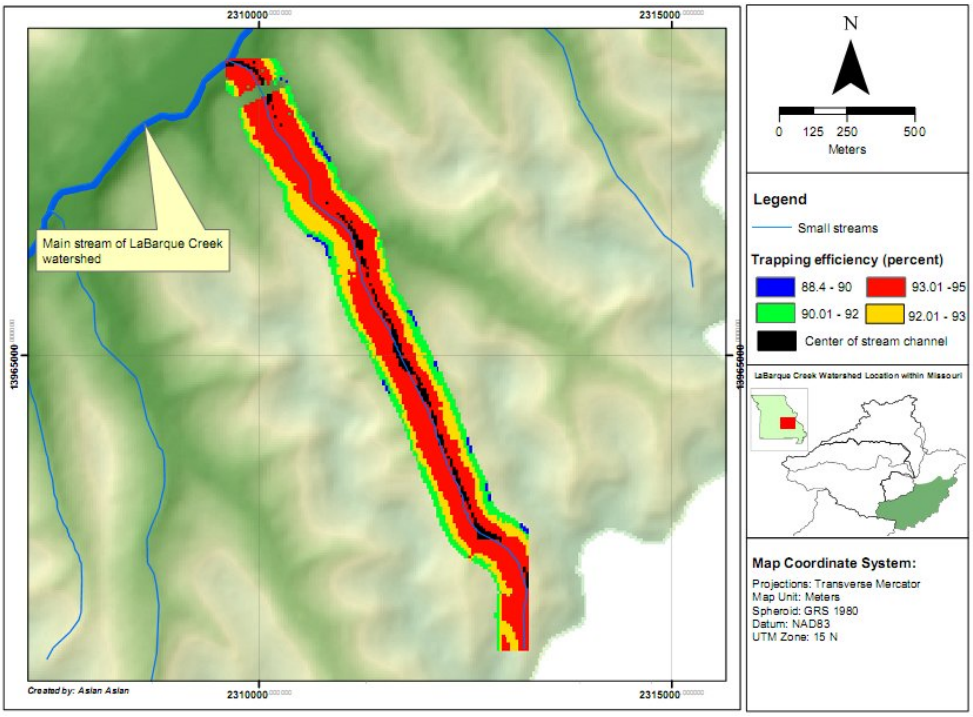

Figure 46. Trapping efficiency map for the simulation area within the LaBarque Creek watershed.

4.4 Utilization of GIS for determining volume of stormwater infiltration

The simulation process for determining the depth of stormwater infiltration through a given buffer width was performed by following the flow chart in Figure 32. Map units in ArcMap were converted to feet from meters. The process of calculating the stormwater infiltration depth used Equations 5 and 6, as well as several layers developed previously: fixed buffer widths (Figure 43), runoff velocity (Figure 44), flow direction from the normal DEM data (Figure 29), and minimum infiltration rates (Figure 25).

4.4.1 Creating fixed width of buffer, L

The process of determining of volume of infiltrated stormwater per foot width of buffer strip was begun by creating an assumed fixed buffer width. Similar to the calculation of trapping efficiency, in this particular analysis, the width of the buffer was again set to 328 feet (i.e., ten times the pixel size, or 10 cells) for each side of the stream.

The same location that was used for the sediment trapping efficiency simulation was used for this simulation (Figure 43).

4.4.2 Calculating runoff velocity, V

Similar to the demonstration of sediment trapping efficiency calculation, in this particular analysis the runoff velocity layer developed previously was used in this simulation (Figure 44).

4.4.3 Creating flow direction

For this simulation, the flow direction layer from the normal DEM was used for the simulation area (Figure 29). Flow direction for the simulation area is shown in Figure 47.

4.4.4 Minimum infiltration rate, f_c

The minimum infiltration rates layer developed previously (Figure 25) was also used to calculate the volume of stormwater infiltrated. The minimum infiltration rates for the simulation area are shown in Figure 48.

4.4.5 Calculating incremental travel time, T_t

The calculation of incremental travel time for individual cell was performed by overlaying the 328-fixed buffer layer (Figure 43) and runoff velocity layer (Figure 44) utilizing Equation 5. This typical calculation was conducted in ArcMap by using the 'Raster Calculator' function in the Spatial Analyst menu. The resultant layer of this calculation can be seen in Figure 49. From Figure 49, one can see that travel time varies from 0.5 to 4.7 minutes following random patterns, perhaps due to variation in the slope.

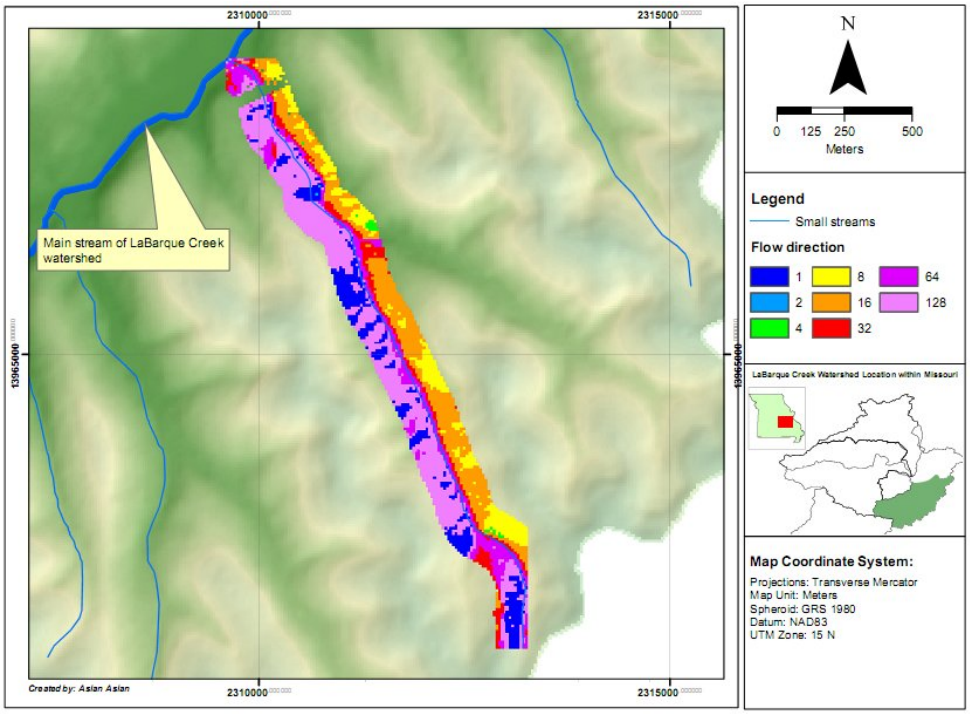

Figure 47. Flow direction layer for the simulation area within the LaBarque Creek watershed.

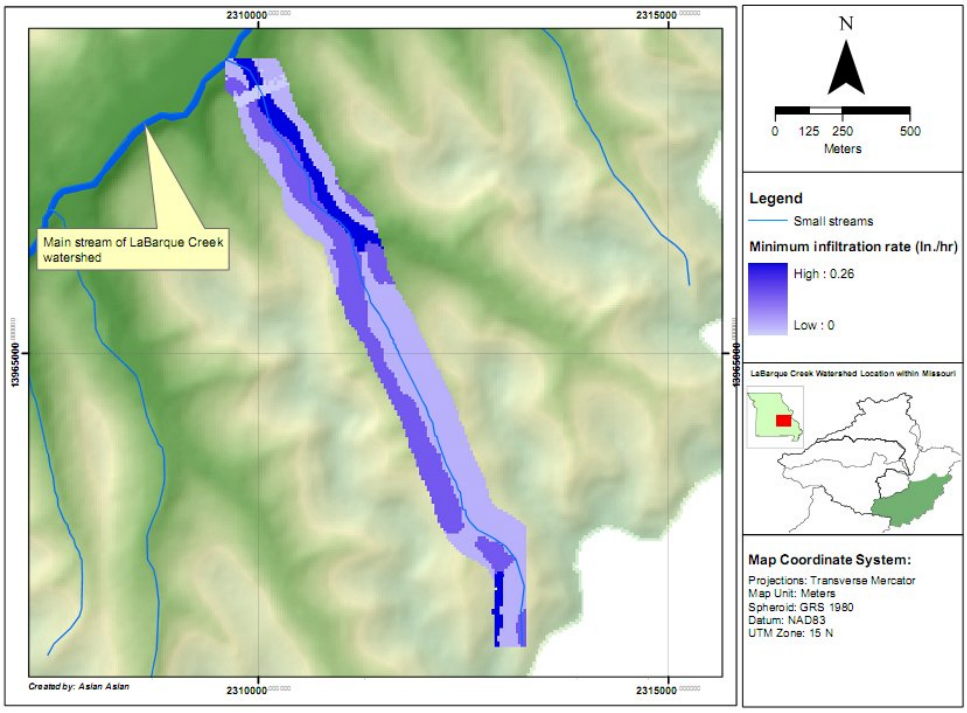

Figure 48. Minimum infiltration rates layer for the simulation area within the LaBarque Creek watershed.

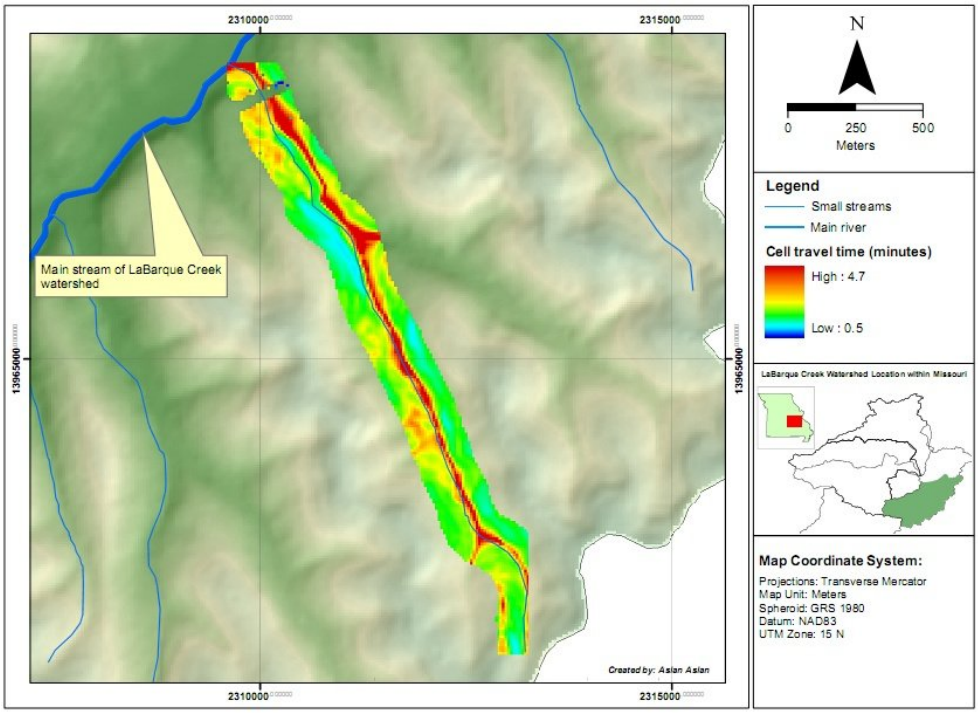

Figure 49. Travel time layer for the simulation area within the LaBarque Creek watershed.

4.4.6 Calculating volume of stormwater infiltration, V_L

Equation 6 was used to determine the volume of stromwater infiltration for each cell within the 328 foot of fixed buffer. The calculation was performed by overlaying the incremental travel time layer for individual cell (Figure 49), the minimum infiltration rates layer (Figure 48), and the 328 foot fixed buffer layer (Figure 43). The resulting layer of this calculation can be seen in Figure 50.

Based on Figure 50, it can be seen that the volume of stormwater infiltration varies from 0.0008 to 0.55 (ft^3/ft). The greater volumes of infiltrated water mostly occur in downstream locations due to the greater minimum infiltration rates (Fc) of the soils as compared to the smaller Fc values in upstream locations (see Figure 48).

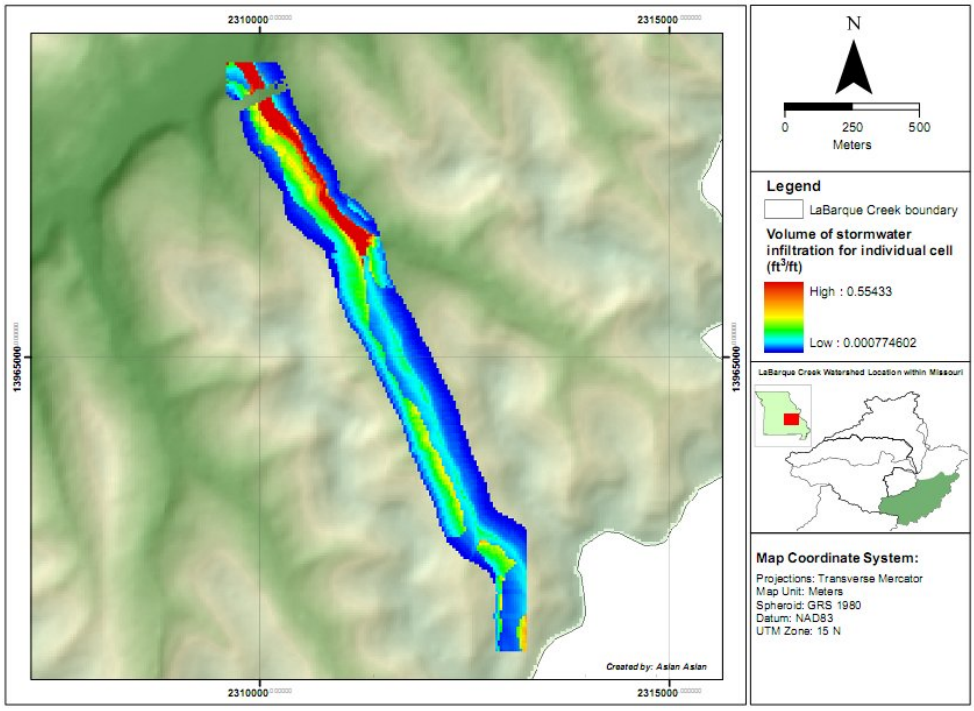

Figure 50. Incremental cell contribution of volume of stormwater infiltration per foot width of buffer strip for the simulation area within the LaBarque Creek watershed.

4.4.7 Calculating cumulative volume of stormwater infiltration

The calculation of cumulative volume of infiltrated water from each cell in this simulation was conducted by using the 'Flow Accumulation' function in ArcGIS following the weighted principle. In this particular case, two layers were used as inputs: (1) the flow direction layer (Figure 47) and (2) the cell contribution of volume of stormwater infiltration layer (Figure 50). This is an iterative process with the objective of calculating the final cumulative volume of stormwater infiltration by accumulating volumes of infiltrated water from one cell to another along the flow path and assuming that the centerline of streams will be the lowest point. The resultant layer from this process can be seen in Figure 51.

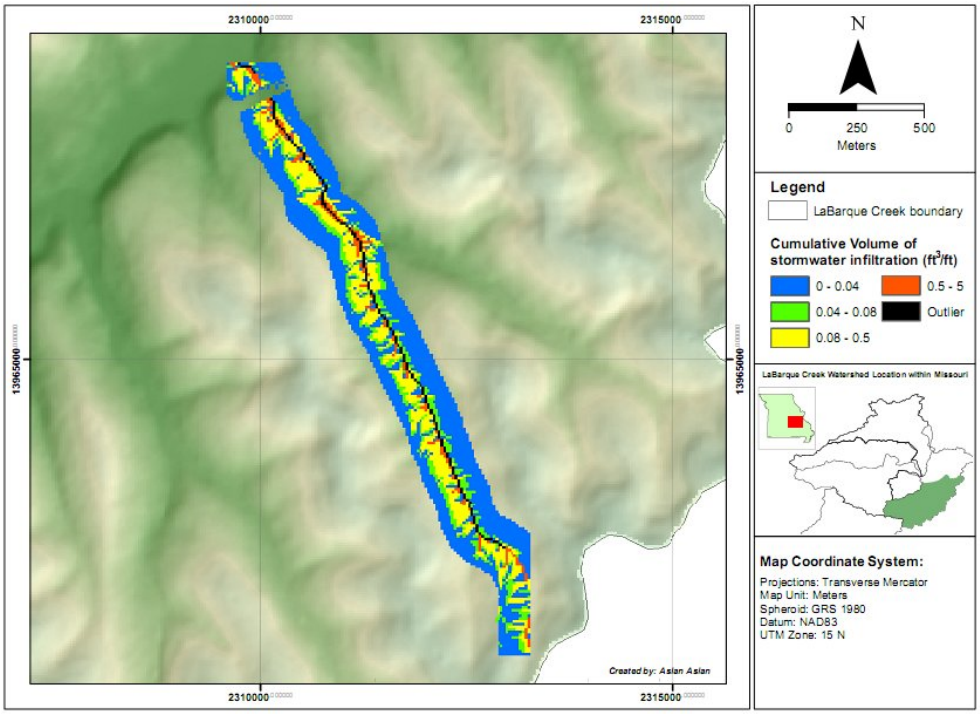

Figure 51. Cumulative volume of stormwater infiltration per foot width of buffer strip for the simulation area within the LaBarque Creek watershed.

Based on Figure 51, one can see that when stormwater enters the upper limits of the buffer, water will infiltrate at rates between 0 and 0.04 ft^3/ft gradually increasing until it finally reaches the rates of 0.5-5 ft^3/ft in the areas near the stream. This phenomenon may occur because of two factors: slope and soil type/texture. Normally, slopes in the floodplain near the stream are milder than in the areas near the upper bound of the buffer zones, causing the velocity of overland flow during rainfall events to be less when near streams as compared to uphill areas, resulting in higher volumes of stormwater infiltrated. In addition, one can see from Figure 18, that most of the areas near the stream within the LaBarque Creek watershed are categorized as group B soils according to the NRCS classification compared to the group C and D soils in the uphill areas. As was stated previously, group B soils tend to have a moderately low runoff potential and have moderately fine to moderately coarse textures, while group C and D soils have a

moderately to high runoff potential and moderately fine to fine texture. Consequently, more water will be infiltrated in the areas near streams as compared to uphill areas (i.e., close to the upper bounds of the buffers) due to overland.

4.5 Chapter summary

This chapter began with an overview of how GIS can assist decision makers in determining the most beneficial place to install buffers on a landscape. The chapter then discussed the implementation of GIS methodology by using raster data analysis for the three different scenarios in according to developed models that were derived in Chapter 3.

The GIS simulation analysis began with a set of procedures to delineate the required buffer width considering physical inputs parameter for the LaBarque Creek watershed. In this particular section, another simulation was also performed with the objective of comparing the buffer sizes derived from the model and a fixed width buffer. A second GIS simulation was performed via spatial analysis in order to obtain a map of sediment trapping efficiency based on a given buffer width for a selected tributary of LaBarque Creek. Finally, the GIS simulation ends with the series of spatial calculations to determine the volume of infiltrated water per foot width for a fixed buffer strip in the selected tributary of LaBarque Creek.

Chapter 5:
CONCLUSIONS AND RECOMMENDATIONS

5.1 Conclusions

This research has focused on the development and implementation of empirical models for buffer width delineation and the assessment of buffer effectiveness efficiencies in removing NPS pollutants and infiltrating stormwater using GIS analysis based upon a series of nomographs developed by Wong and McCuen (1982). In this particular study, GIS analysis has been shown to be a valuable tool to demonstrate the developed empirical models for three different scenarios: (1) utilization of GIS for delineating buffer widths; (2) utilization of GIS for calculating the trapping efficiencies for sediment in a given buffer; and (3) utilization of GIS for determining the volume of infiltrated stormwater per foot width of a specific buffer strip.

The concept of using incremental and cumulative contributions of each cell within a buffer in GIS analysis is a new approach in transforming the methodology from a graphical–based to a GIS-based solution to determine required buffer widths for specific locations. This method is unique and could be used for any developed vegetative buffer model in order for the model to be applied in a GIS fashion. Additionally, because these vegetative buffer strip models were developed based upon the conditions of a rainfall factor (R-factor) of 175 or equal to the average annual precipitation of 32.65 in/year, special circumstances may apply when considering the performance in other climatic conditions or for an individual storm (Wong and McCuen 1982; Renard et al. 1994). For example, high rates of runoff (from high-intensity rainfall events) from a contributing

watershed entering a buffer may cause the performance of the buffers to be less effective than expected on an individual storm basis. Consequently, the combination of buffers with other stormwater management techniques from best management practices (e.g., detention basins) may be necessary. Moreover, one needs to consider the influence of the R-factor on the modeled effectiveness of buffers. The R-factor value in St. Louis, MO (i.e., near the study area) is 210 or equal to an average annual precipitation of 39.18 in/year. The annual precipitation in St. Louis is 6.53 in/year higher than the annual precipitation found in Maryland where the initial model was developed. This fact means that a larger buffer maybe required to produce the results as in Maryland. However, this finding will have to be investigated further.

In addition to the simulation results on a mathematical basis, the developed models have been shown to be applicable for utilizing GIS technology over a continuous surface (i.e., raster data format) for a site-specific location (i.e., the LaBarque Creek watershed). The results have also shown that the required widths identified by a variable buffer delineation were different compared to the width of a fixed buffer according to the change in the physical characteristics of the study site.

In term of runoff velocity calculations, the Manning's n factor has been shown to be an important part of this model, because small changes in Manning's n values result in large differences in the runoff velocities. The variability seen in the required width of buffers (responding to changes in the physical characteristics of the study site along the different orders of streams/rivers) are consistent with the common recommendation of existing stream buffers ordinance (i.e., buffers should be wider for lower order streams).

Finally, the successful achievement in transforming and applying the GIS methodology developed in this research to determine required buffer widths and their efficiency in removing NPS pollutants and infiltrating water, will help decision makers implement the methodology as a guideline for individual sites based on their specific physical characteristics input as well as assist them in formulating stream buffer ordinances.

5.2 Recommendations

The results of this research have led to the following recommendation for future research on the issue of improving the models.

1. In this research, all the scenarios were successfully demonstrated within the study areas; however, the results of these simulation scenarios have not yet been proven based upon water quality with real data for a specific case (i.e., from soil erosion). Therefore, additional investigation may be needed in order to verify the effectiveness of the models with specific data, particularly where the conditions are different from those in Maryland.
2. The developed models may need to include other parameters in order to obtain maximum performance of the buffers; for example, the location of the floodplain. Floodplain areas are important because they represent the transition zones between land and stream where materials exchange rapidly between land and streams. According to Wenger (1999), whenever possible, the width of buffers should be extended to the edge of the 100-year floodplain.

3. Due to the fact that one of the limitation of these models is their development from Manning's n values ranging from 0.2 to 0.8 and the fact that not all land cover classes can be used in this model, future work should extend the bounds of applicable Manning's n values based on other vegetative covers.

REFERENCES

Abu-Zreig, M., Rudra, R. P., Whiteley, H.R., Lalonde, M.N., and Kaushik, N.K. (2003). "Phosphorus removal in vegetated filter strips." Journal of Environmental Quality **32**: 613-619.

Bajwa S.H, Tim U.S. (2002). Toward Immersive Virtual Environments for GIS-based Floodplain Modeling and Visualization. ESRI User Conference Proceedings. http://gis.esri.com/library/userconf/proc02/pap0723/p0723.htm.

Baker, J. L., Mickelson, S.K., Hatfield, J.L., Fawcett, R., Hoffman, D.W., Franti, T.G., Peter, C.J., and Tierney, D.P. (1995). Reducing herbicide runoff: role of best management practices. Brighton Crop Protection Conference, Brighton, England.

Bennett, H.H. (1939). Soil Conservation. New York, McGraw-Hill Book Company Inc.

Binford, M.W., and M.J. Buchenau. (1993). Riparian greenways and water resource. Pp 69-104 in D.S. Smith and P.C. Hellmund eds., Ecology of greenways: design and function of linear conservation areas. University of Minnesota Press, Minneapolis, MN.

Blinn, C. R. and M. A. Kilgore. (2001). "Riparian Management Practices A Summary of State Guidelines." Journal of Forestry **99**(8): 11-17.

Borin, M. and E. Bigon (2002). "Abatement of NO3-N concentration in agricultural waters by narrow buffer strips." Environmental Pollution **117**: 165-168.

Castelle, A. J., A. W. Johnson, and C.Conolly. (1994). "Wetland and Stream Buffer Size Requirements A Review." Journal of Environmental Quality **23**(5): 878-882.

City of Columbia, Missouri (2009). https://www.gocolumbiamo.com/PublicWorks/StormWater/. (Site last visited June 2009)

Clinnick, P. F. (1985)."Buffer strip management in forest operations: A review." Australian Forestry **48** (1): 34-45.

Corley, C. J., Frasier, G.W., Trlica, M.J., Smith, F.M., and Taylor, E.M. (1999). "Nitrogen and phosphorus in runoff from two montane riparian communities." Journal of Range Management **52**: 600-605.

Correll, D. L. (1996). Buffer Zones and Water Quality Protection: General Principles. The International Conference on Buffer Zones, Harpenden, Hertfordshire, England, Quest Environmental.

Dangermond, J. (1988). Introduction and Overview of GIS. Geographic Information Systems Seminar: Data sharing-Myth or reality. Ontario, Canada, Ministry of Natural Resources.

Davis, A. P. and R. H. McCuen (2005). Stormwater Management for Smart Growth. New York, Springer.

Dillaha, T. A., R. B. Reneau, et al. (1989). "Vegetation Filter Strips for Agricultural Non-Point Source Pollution Control." Transactions of the American Society of Agricultural Engineers **32**: 513-519.

Digital Globe. (2006). www.digitalglobe.com

Dosskey, M. G. (2001). "Toward quantifying water pollution abatement in response to installing buffers on crop land." Environmental Management **28**(5): 577-598.

Dosskey, M. G., M. J. Helmers, et al. (2005). "Establishing Conservation Buffers Using Precision Information." Journal of Soil and Water Conservation **60**(6): 349-353.

Dosskey, M. G., M. J. Helmers, et al. (2008). "A Design Aid for Determining Width of Filter Strips." Journal of Soil and Water Conservation **63**(4): 232-241.

Engman, E.T. (1986). Roughness coefficients for routing surface runoff. Journal of Irrigation and Drainage Engineering. **112**(1): 39-53.

ESRI, GIS and Mapping Software, ArcGIS. (2009). http://www.esri.com/ (Site last visited June 2009)

Fennessy, M. S. and J. K. Cronk (1997). "The effectiveness and restoration potential of riparian ecotones for the management of nonpoint source pollution, particularly nitrate." Critical Reviews in Environmental Science and Technology **27**: 285-317.

Fischer, R. A., Martin, C.O., and Fischenich, J.C. (2000). Improving Riparian Buffer Strips and Corridors for Water Quality and Wildlife. *In* P.J. Wingington and R.L. Beschta. American Water Resources Association International Conference on Riparian Ecology and Management in Multi-Land Use Watersheds Proceedings. Portland, OR.

Flanagan, D. C., Foster, G.R., Neiblig, W.H., and Burt, J.P. (1989). "Simplified equations for filter strip design." Transactions of the ASAE **32**(6): 2001-2007.

Freeman, R. E. and R. O. Ray (2001). "Landscape ecology practice by small scale river conservation groups." Landscape and Urban Planning **56**: 171-184.

Geyer, D. J., Keller, C.K., Smith, J.L., and Johnstone, D.L.. (1992). "Subsurface fate of nitrate as a function ofdepth and landscape position in Missouri Flat Creek watershed, USA." Journal of Contaminant Hydrology **11**: 127-147.

Gilliam, J. W. (1994). "Riparian wetlands and water quality." Journal of Environmental Quality **23**: 896-900.

Goodchild, M. F. (1996). The application of advanced information technology in assessing environmental impacts. Applications of GIS to the Modeling of Non-Point Source Pollutants in the Vadose Zone. D. L. Corwin and K. Loague. Madison, WI, SSSA Special Publication No. 48**:** pp. 1–18. [262].

Goodchild, M. F., Steyaert, L.T., parks, B.O., Johnston, C., Maidment, D.R., Glendinning, S., and Crane, M. (1996). GIS and Environmental Modeling: Progress and Research Issues. New York, John Wiley and Sons.

Halley, J. M. (2002). Watershed management and riparian buffer analyses using remotely sensed data. Raleigh, North Carolina State University. Master's Thesis**:** 120.

Herron, N. F. and P. B. Hairsine (1998). "A scheme for evaluating the effectiveness of riparian zones in reducing overland flow to streams." Australian Journal of Soil Research **36**: 683-698.

Hickey, R., Burns, E., Bolte, J., and D. Walker. (2005). Development of a Statewide Erosion Vulnerability Screening Tool for Oregon. Retrieved: June 19, 2009 from http://www.siue.edu/geography/online/Hickey05.pdf.

Hollabaugh, E. M. (2006). Field Performance of Instrumentation for Monitoring Effects of Timber Harvesting on Water Quality. Civil and Environmental Engineering Department. Columbia, University of Missouri. Master's Thesis: 169.

J. F. O'Callaghan, and D. M. Mark. (1984). "The Extraction of Drainage Networks From Digital Elevation Data," Comp. Vision, Graphics Image Process. vol. 28, pp. 328-344.

Johnson, L. E. (2009). Geographic Information Systems in Water Resources Engineering Boca Raton, FL CRC Press. Tylor & Francis Group.

Karr, J. R. and IJ. Schlosser. (1977). Impact of nearstream vegetation and stream morphology on water quality and stream biota. U.S. Environmental Protection Agency, Report EPA - 60013 -77 - 097, Athens, GA.

Karr, J. R. and I. J. Schosser (1978). "Water Resources and the Land-Water Interface." Science **201**: 229-234.

Knisel, W. G. (1980). CREAMS: A Field-scale Model for Chemicals, Runoff, and Erosion from Agricultural Management Systems. Conservation Research Report. Washington, DC, USDA. **No. 26**.

Kohnke, H. and A. R. Bertrand (1959). Soil Conservation. New York, McGraw-Hill Book Company, Inc.

Lavalle, N. M. (2007). Improving Hawaii's Water Quality: Selecting Sites for Riparian Restoration in a GIS. Environment and Earth Sciences, Duke University. Master's Thesis.

Lee, K. H., Isenhart, T. M., Schultz, R.C., and Mickelson, S.K. (2000). "Multispecies riparian buffers trap sediment and nutrients during rainfall simulations." Journal of Environmental Quality **29**: 1200-1205.

Lim, T. T., Edwards, D. R., Workman, S.R., Larson, B.T., and Dunn, L. (1998). "Vegetated filter strip removal of cattle manure constituents in runoff." Transactions of the ASAE **41**: 1375-1381.

Line, D. E., Harman, W. A., Jennings, G.D., Thompson, E.J., and Osmond, D.L. (2000). "Nonpoint-source pollutant load reductions associated with livestock exclusion." Journal of Environmental Quality **29**: 1882-1890.

Lowrance, R. R., Leonard, R., and Sheridan, J.M. (1985). "Managing Riparian Ecosystems to Control Nonpoint Pollution." Journal of Soil and Water Conservation **40**: 87-91.

Lowrance, R., Altier, L.S., Williams, R.G., Imadar, S.P., Bosch, D.D., Sheridan, J.M., Thomas, D.L., and Hubbard, R.K. (1998). The Riparian Ecosystem Management Model: Simulator for ecological processes in riparian zones. Proceedings of the First Federal Interagency Hydrologic Modeling Conference.

Magette, W. L., Brinsfield, R.B., Palmer, R.E., and Wood, J.D. (1989). "Nutrient and sediment removal by vegetated filter strips." Transactions of the American Society of Agricultural Engineers **32**: 663-667.

Mannering, J.V. and C.B. Johnson. (1974). Report on simulated rainfall phase. Appendix No. 9. First Annual Report, Black Creek Study Project, Allen County, Indiana, Indiana Soil and Water Conservation District. Fort Wayne, IN.

McCuen, R. H. (2005). Hydrologic Analysis and Design. Third Edition. Upper Saddle River, New Jersey, Pearson Prentice Hall.

Melcher, C. P. and S. K. Skagen (2005). Grass Buffers for Playas in Agricultural Landscapes: A Literature Synthesis, U.S Geological Survey, Biological Resource Discipline**:** Open-File Report 2005-1220, 35p.

Missouri Spatial Data Information Service (MSDIS). (2009). http://www.msdis.missouri.edu/

Missouri Department of Conservation. (2007). LaBarque Creek Watershed Conservation Opportunity Area. http://mdc4.mdc.mo.gov/Documents/17990.pdf.

Morgan, T. R. and D. G. Polcari (1991). Get set! Go for mapping, modeling, and facility management. Proceedings of Computers in the Water Industry Conference, Houston, TX, AWWA.

Muñoz-Carpena, R. and J. E. Parsons (2004). "A design procedure for vegetative filter strips using VFSMOD-W." Transactions of the ASAE **47**(6): 1933-1941.

National Wetlands Mitigation Action Plan. (2009). Retrieved June 14, 2009, from http://www.mitigationactionplan.gov/

NRC (2002). Riparian Areas: Functions and Strategies for Management. Washington, D.C, National Academy Press.

NOAA. (2009). http://www.nws.noaa.gov/oh/hrl/gis/data.html

NRCS. (2004). Soil Survey Geographic (SSURGO) Database. http://soils.usda.gov/survey/geography/ssurgo/ Site last visited June 2009

Osborne, L. L. and D. A. Kovacic (1993). "Riparian vegetated buffer strips in water quality restoration and stream management." Freshwater Biology **29**: 243-258.

Parkyn, S. (2004). Review of Riparian Buffer Zone Effectiveness. Wellington, New Zealand, Ministry of Agriculture and Forestry.

Pearce, R., Trlica, M., Leininger, W., Smith, J., and Frasier, G. (1997). "Efficiency of Grass Buffer Strips and Vegetation Height on Sediment Filtration in Laboratory Rainfall Simulations." Journal of Environmental Quality **26**: 139-144

Phillips, J. D. (1989). "An evaluation of the factors determining the effectiveness of water quality buffer zones." Journal of Hydrology **107**(1-4): 133-145.

Prakash, A. (2004). Water resources engineering: handbook of essential methods and design. ASCE Press. Reston, VA.

Presler, H. H. (2006). "Successful Implementation of Riparian Buffer Program: Designing a Program to Protect Water Quality." Retrieved March 19, 2009.

Renard, K.G., G.R. Foster, D.C. Yoder, and D.K. McCool. (1994). RUSLE revisited: Status, questions, answer, and the future." Journal of Soil Water Conservation **49 (3)**: 213-220.

Schueler, T. (1995). "The Architecture of Stream Buffers." Watershed Protection Techniques, Center for Watershed Protection. **1 (4):** 155-165.

Shamsi, U. M. (2005). GIS Applications for Water, Wastewater, and Stormwater Systems. Boca Raton, FL, CRC. Press Tylor & Francis Group.

Sharpley, A. N., P. Kleinman, et al. (2001). "Innovative management of agricultural phosphorus to protect soil and water resources." Communications in Soil Science and Plant Analysis **32**: 1071-1100.

Slagter, J. P. and G. M. Yoakum. (2002). Reconciling Recent Regulatory Takings And Development Moratoria Decisions. *In*: *Build On This.*

Tollner, E. W., Barfield, B.J., Haan, C.T., Kao, T.Y. (1976). "Suspended Sediment Filtration Capacity of Simulated Vegetation." ASAE **19**: 678-682.

Trimble, G. R. and R. S. Sartz (1957). "How far from a stream should a logging road be located?" Journal of Forestry **55**: 339-341.

U.S. Census Bureau. (2000). http://www.census.gov/geo/www/relate/rel_tract.html.

USEPA. "Model Ordinances to Protect Local Resources." Retrieved February 13, 2009, from http://www.epa.gov/owow/nps/ordinance/buffers.htm.

USEPA (1976). Erosion and Sediment Control, Surface Mining in the Eastern U.S. Washington, DC, United States Environmental Protection Agency. **I:** EPA 625/3-76-006.

USEPA (2005). Stormwater Phase II Final Rule Fact Sheet 2.3: Public Education and Outreach Minimum Control Measure Washington, D.C, United States Environmental Protection Agency. Publication EPA 833-F00-005.

Vought, L. B. M., Pinay, G., Fuglsang, A., and Ruffinoni, C. (1995). "Structure and function of buffer strips from a water quality perspective in agricultural landscapes." Landscape and Urban Planning **31**(1-3): 323-331.

Welsch, D. J. (1991). Riparian forest buffers. Radnor, PA, USDA Forest Service. NA-PR-07-91.

Wang, X., and P. Cui. (2005). Support Soil Conservation Practices by Identifying Critical Erosion Areas within an American Watershed Using the GIS-AGNPS Model. Retrieved: June 14, 2009 from http://www.spatialhydrology.com/journal/paper/soil_conservation/AGNPS.pdf.

Weng, Q. (2001). "Modeling Urban Growth Effects on Surface Runoff with the Integration of Remote Sensing and GIS " Environmental Management **28**(6): 737-748.

Wenger, S. (1999). A Review of the Scientific Literature on Riparian Buffer Width, Extent, and Vegetation. Athens, Institute of Ecology, University of Georgia**:** 59.

Wong, S. L. and R. H. McCuen (1982). The Design of Vegetative Buffer Strips for Runoff and Sediment Control. Stormwater Management in Coastal Areas, Appendix J, ed. R.H. McCuen. College Park, MD, University of Maryland Department of Civil Engineering.

Xiang, W.-N. (1993). "A GIS method for riparian water quality buffer generation." International Journal of Geographical Information Science **7**(1): 57 - 70-57 - 70.

Xiang, W.-N. (1996). "GIS-based riparian buffer analysis: injecting geographic information into landscape planning." Landscape and Urban Planning **34**(1): 1-10.

Xiang, W.-N. and W. L. Stratton (1996). "Technical Note The b-function and variable stream buffer mapping: a note on 'A GIS method for riparian water quality buffer generation." International Journal of Geographical Information Science **10**(4): 499-510.

Young, R. A., T. Huntrods, et al. (1980). "Effectiveness of vegetated buffer strips in controlling pollution from feedlot runoff." Journal of Environmental Quality **9**: 483-487.

APPENDICES

Appendix A: Data recorded from digitizing Manning's n values

A.1 n = 0.2

ID	Velocity (ft/sec)	Slope (%)	ID	Velocity (ft/sec)	Slope (%)	ID	Velocity (ft/sec)	Slope (%)
1	0.020	-0.018	36	0.548	2.934	71	0.970	8.540
2	0.036	-0.009	37	0.561	3.078	72	0.980	8.725
3	0.052	0.007	38	0.574	3.221	73	0.991	8.911
4	0.069	0.032	39	0.587	3.365	74	1.001	9.096
5	0.085	0.061	40	0.600	3.508	75	1.011	9.282
6	0.101	0.096	41	0.613	3.651	76	1.022	9.467
7	0.117	0.133	42	0.626	3.794	77	1.032	9.651
8	0.133	0.179	43	0.639	3.937	78	1.043	9.834
9	0.149	0.224	44	0.652	4.082	79	1.053	10.017
10	0.165	0.269	45	0.665	4.230	80	1.064	10.200
11	0.181	0.335	46	0.678	4.378	81	1.074	10.383
12	0.197	0.402	47	0.691	4.526	82	1.085	10.566
13	0.212	0.480	48	0.704	4.677	83	1.095	10.750
14	0.228	0.558	49	0.716	4.835	84	1.106	10.933
15	0.243	0.636	50	0.728	4.992	85	1.115	11.130
16	0.259	0.719	51	0.741	5.149	86	1.124	11.326
17	0.274	0.804	52	0.753	5.306	87	1.133	11.522
18	0.289	0.889	53	0.765	5.464	88	1.143	11.718
19	0.304	0.982	54	0.777	5.621	89	1.152	11.914
20	0.319	1.082	55	0.790	5.778	90	1.162	12.108
21	0.334	1.181	56	0.802	5.935	91	1.171	12.302
22	0.349	1.281	57	0.814	6.092	92	1.180	12.501
23	0.364	1.381	58	0.827	6.249	93	1.189	12.705
24	0.379	1.486	59	0.839	6.406	94	1.197	12.909
25	0.393	1.591	60	0.851	6.572	95	1.206	13.112
26	0.408	1.696	61	0.862	6.749	96	1.214	13.316
27	0.422	1.807	62	0.873	6.926	97	1.223	13.520
28	0.436	1.929	63	0.884	7.103	98	1.231	13.724
29	0.451	2.051	64	0.895	7.283	99	1.240	13.928
30	0.465	2.174	65	0.905	7.462	100	1.248	14.131
31	0.479	2.297	66	0.916	7.642			
32	0.493	2.421	67	0.927	7.821			
33	0.507	2.545	68	0.938	8.001			
34	0.521	2.668	69	0.949	8.180			
35	0.535	2.792	70	0.959	8.360			

Appendix A: Data recorded from digitizing Manning's n values

A.2 n = 0.35

ID	Velocity (ft/sec)	Slope (%)	ID	Velocity (ft/sec)	Slope (%)	ID	Velocity (ft/sec)	Slope (%)
1	0.018	-0.007	36	0.370	3.702	71	0.592	9.272
2	0.031	0.022	37	0.377	3.849	72	0.597	9.440
3	0.043	0.058	38	0.385	3.996	73	0.603	9.609
4	0.055	0.119	39	0.393	4.144	74	0.608	9.778
5	0.067	0.187	40	0.400	4.295	75	0.613	9.947
6	0.078	0.258	41	0.407	4.449	76	0.618	10.115
7	0.090	0.329	42	0.414	4.603	77	0.623	10.284
8	0.102	0.404	43	0.421	4.757	78	0.628	10.452
9	0.113	0.484	44	0.428	4.911	79	0.634	10.620
10	0.124	0.565	45	0.435	5.064	80	0.639	10.788
11	0.135	0.655	46	0.442	5.218	81	0.644	10.955
12	0.146	0.745	47	0.448	5.375	82	0.649	11.123
13	0.157	0.840	48	0.455	5.533	83	0.655	11.291
14	0.168	0.942	49	0.462	5.690	84	0.660	11.460
15	0.178	1.045	50	0.468	5.848	85	0.665	11.629
16	0.189	1.147	51	0.475	6.006	86	0.669	11.801
17	0.199	1.256	52	0.481	6.166	87	0.674	11.971
18	0.209	1.368	53	0.487	6.328	88	0.679	12.143
19	0.219	1.479	54	0.493	6.490	89	0.684	12.313
20	0.229	1.588	55	0.499	6.651	90	0.688	12.486
21	0.240	1.698	56	0.505	6.813	91	0.692	12.660
22	0.249	1.814	57	0.511	6.975	92	0.696	12.835
23	0.259	1.936	58	0.517	7.137	93	0.701	13.009
24	0.268	2.058	59	0.523	7.299	94	0.705	13.182
25	0.278	2.184	60	0.529	7.461	95	0.710	13.353
26	0.287	2.311	61	0.535	7.625	96	0.714	13.525
27	0.296	2.439	62	0.541	7.788	97	0.718	13.700
28	0.305	2.574	63	0.547	7.952	98	0.722	13.875
29	0.313	2.709	64	0.553	8.115	99	0.726	14.050
30	0.322	2.844	65	0.559	8.278	100	0.730	14.225
31	0.330	2.979	66	0.565	8.442			
32	0.339	3.119	67	0.571	8.606			
33	0.346	3.264	68	0.576	8.770			
34	0.354	3.410	69	0.582	8.937			
35	0.362	3.556	70	0.587	9.104			

Appendix A: Data recorded from digitizing Manning's n values

A.3 n = 0.8

ID	Velocity (ft/sec)	Slope (%)	ID	Velocity (ft/sec)	Slope (%)	ID	Velocity (ft/sec)	Slope (%)
1	0.0139	0.0541	36	0.1857	4.6813	71	0.2640	9.8766
2	0.0210	0.1655	37	0.1885	4.8277	72	0.2658	10.0263
3	0.0282	0.2752	38	0.1913	4.9741	73	0.2675	10.1765
4	0.0356	0.3827	39	0.1941	5.1206	74	0.2690	10.3269
5	0.0428	0.4928	40	0.1969	5.2671	75	0.2706	10.4773
6	0.0494	0.6099	41	0.1997	5.4136	76	0.2722	10.6276
7	0.0560	0.7286	42	0.2025	5.5600	77	0.2737	10.7780
8	0.0623	0.8499	43	0.2053	5.7065	78	0.2753	10.9283
9	0.0684	0.9726	44	0.2080	5.8535	79	0.2768	11.0788
10	0.0741	1.1000	45	0.2105	6.0012	80	0.2783	11.2293
11	0.0798	1.2275	46	0.2130	6.1489	81	0.2798	11.3797
12	0.0855	1.3548	47	0.2154	6.2968	82	0.2814	11.5302
13	0.0914	1.4798	48	0.2179	6.4445	83	0.2829	11.6807
14	0.0974	1.6048	49	0.2204	6.5923	84	0.2844	11.8312
15	0.1033	1.7297	50	0.2227	6.7406	85	0.2859	11.9817
16	0.1081	1.8652	51	0.2250	6.8889	86	0.2874	12.1320
17	0.1127	2.0016	52	0.2273	7.0373	87	0.2889	12.2827
18	0.1173	2.1378	53	0.2295	7.1858	88	0.2901	12.4338
19	0.1219	2.2741	54	0.2318	7.3343	89	0.2913	12.5848
20	0.1265	2.4105	55	0.2341	7.4827	90	0.2925	12.7359
21	0.1312	2.5468	56	0.2364	7.6312	91	0.2937	12.8870
22	0.1358	2.6832	57	0.2384	7.7802	92	0.2949	13.0381
23	0.1404	2.8195	58	0.2403	7.9297	93	0.2961	13.1892
24	0.1445	2.9593	59	0.2422	8.0792	94	0.2972	13.3404
25	0.1483	3.1010	60	0.2442	8.2288	95	0.2984	13.4915
26	0.1520	3.2429	61	0.2461	8.3783	96	0.2995	13.6427
27	0.1558	3.3848	62	0.2480	8.5278	97	0.3007	13.7939
28	0.1596	3.5265	63	0.2498	8.6775	98	0.3018	13.9450
29	0.1633	3.6684	64	0.2516	8.8273	99	0.3029	14.0963
30	0.1669	3.8115	65	0.2534	8.9772	100	0.3041	14.2475
31	0.1704	3.9546	66	0.2551	9.1271			
32	0.1740	4.0976	67	0.2569	9.2770			
33	0.1773	4.2419	68	0.2587	9.4268			
34	0.1801	4.3883	69	0.2605	9.5767			
35	0.1829	4.5347	70	0.2622	9.7266			

Appendix B: Data recorded from digitizing trapping efficiency

B.1 TR = 75%

ID	Velocity (ft/sec)	BW (ft)	ID	Velocity (ft/sec)	BW (ft)	ID	Velocity (ft/sec)	BW (ft)
1	0.267	5.168	36	0.589	45.169	71	0.878	112.853
2	0.276	5.344	37	0.598	46.699	72	0.886	114.945
3	0.286	5.475	38	0.607	48.225	73	0.894	117.038
4	0.296	6.098	39	0.615	49.755	74	0.902	119.126
5	0.305	6.926	40	0.624	51.285	75	0.910	121.219
6	0.315	7.755	41	0.633	53.003	76	0.918	123.311
7	0.324	8.516	42	0.642	54.754	77	0.926	125.400
8	0.334	9.248	43	0.650	56.505	78	0.934	127.493
9	0.343	9.979	44	0.659	58.313	79	0.942	129.585
10	0.353	10.796	45	0.667	60.195	80	0.950	131.678
11	0.362	11.846	46	0.675	62.081	81	0.958	133.766
12	0.372	12.896	47	0.684	63.968	82	0.966	135.859
13	0.381	13.950	48	0.692	65.850	83	0.974	137.951
14	0.390	15.000	49	0.700	67.736	84	0.982	140.040
15	0.399	16.106	50	0.709	69.623	85	0.990	142.133
16	0.409	17.216	51	0.717	71.535	86	0.998	144.225
17	0.418	18.326	52	0.725	73.564	87	1.006	146.314
18	0.427	19.436	53	0.733	75.593	88	1.014	148.406
19	0.437	20.591	54	0.741	77.621	89	1.022	150.499
20	0.446	21.881	55	0.750	79.654	90	1.030	152.591
21	0.455	23.171	56	0.758	81.683	91	1.038	154.826
22	0.464	24.465	57	0.766	83.711	92	1.046	157.091
23	0.473	25.826	58	0.774	85.740	93	1.053	159.356
24	0.482	27.315	59	0.782	87.799	94	1.061	161.621
25	0.491	28.800	60	0.790	89.884	95	1.069	163.890
26	0.500	30.285	61	0.798	91.973	96	1.076	166.155
27	0.509	31.725	62	0.806	94.058	97	1.084	168.420
28	0.518	33.169	63	0.814	96.143	98	1.091	170.685
29	0.527	34.609	64	0.822	98.228	99	1.099	172.950
30	0.536	36.049	65	0.830	100.316	100	1.107	175.215
31	0.545	37.556	66	0.838	102.401			
32	0.553	39.079	67	0.846	104.486			
33	0.562	40.601	68	0.854	106.579			
34	0.571	42.120	69	0.862	108.671			
35	0.580	43.643	70	0.870	110.760			

Appendix B: Data recorded from digitizing trapping efficiency

B.2 TR = 80%

ID	Velocity (ft/sec)	BW (ft)	ID	Velocity (ft/sec)	BW (ft)	ID	Velocity (ft/sec)	BW (ft)
1	0.251	13.856	36	0.604	70.511	71	0.919	153.146
2	0.262	14.708	37	0.614	72.386	72	0.927	155.903
3	0.273	15.593	38	0.624	74.261	73	0.935	158.655
4	0.283	16.706	39	0.634	76.140	74	0.943	161.408
5	0.294	17.820	40	0.644	78.015	75	0.952	164.164
6	0.305	18.945	41	0.653	79.890	76	0.960	166.916
7	0.315	20.074	42	0.663	81.769	77	0.968	169.669
8	0.326	21.206	43	0.673	83.678	78	0.976	172.421
9	0.336	22.436	44	0.682	85.830	79	0.984	175.271
10	0.347	23.880	45	0.692	87.979	80	0.992	178.144
11	0.357	25.320	46	0.701	90.131	81	1.000	181.013
12	0.367	26.764	47	0.711	92.280	82	1.008	183.885
13	0.378	28.208	48	0.720	94.433	83	1.016	186.758
14	0.388	29.895	49	0.729	96.581	84	1.024	189.630
15	0.398	31.669	50	0.739	98.768	85	1.032	192.555
16	0.408	33.446	51	0.748	101.141	86	1.039	195.506
17	0.417	35.220	52	0.757	103.519	87	1.047	198.458
18	0.427	36.994	53	0.766	105.893	88	1.055	201.413
19	0.437	38.768	54	0.775	108.266	89	1.062	204.364
20	0.447	40.549	55	0.784	110.640	90	1.070	207.315
21	0.457	42.364	56	0.793	113.014	91	1.078	210.270
22	0.467	44.179	57	0.802	115.388	92	1.085	213.221
23	0.477	45.998	58	0.811	117.941	93	1.093	216.173
24	0.487	47.813	59	0.819	120.563	94	1.101	219.128
25	0.497	49.628	60	0.828	123.184	95	1.109	222.079
26	0.507	51.443	61	0.836	125.809	96	1.116	225.030
27	0.517	53.258	62	0.845	128.430	97	1.124	227.981
28	0.526	55.140	63	0.853	131.111	98	1.132	230.936
29	0.536	57.071	64	0.861	133.868	99	1.139	233.888
30	0.546	59.003	65	0.869	136.620	100	1.147	236.839
31	0.556	60.934	66	0.878	139.376			
32	0.565	62.865	67	0.886	142.133			
33	0.575	64.796	68	0.894	144.885			
34	0.585	66.728	69	0.902	147.641			
35	0.595	68.633	70	0.910	150.394			

Appendix B: Data recorded from digitizing trapping efficiency

B.3 TR = 85%

ID	Velocity (ft/sec)	BW (ft)	ID	Velocity (ft/sec)	BW (ft)	ID	Velocity (ft/sec)	BW (ft)
1	0.247	23.130	36	0.618	101.010	71	0.928	209.764
2	0.259	24.866	37	0.628	103.556	72	0.936	213.218
3	0.270	26.606	38	0.638	106.103	73	0.944	216.671
4	0.281	28.343	39	0.648	108.649	74	0.952	220.125
5	0.292	30.120	40	0.659	111.199	75	0.960	223.579
6	0.303	32.085	41	0.669	113.745	76	0.968	227.033
7	0.314	34.050	42	0.678	116.569	77	0.975	230.569
8	0.325	36.019	43	0.688	119.464	78	0.983	234.221
9	0.336	37.984	44	0.697	122.363	79	0.990	237.870
10	0.347	39.990	45	0.706	125.258	80	0.997	241.519
11	0.358	42.090	46	0.716	128.160	81	1.005	245.171
12	0.369	44.186	47	0.725	131.258	82	1.012	248.820
13	0.380	46.286	48	0.734	134.355	83	1.019	252.469
14	0.390	48.386	49	0.743	137.453	84	1.026	256.121
15	0.401	50.483	50	0.751	140.546	85	1.034	259.770
16	0.412	52.620	51	0.760	143.644	86	1.041	263.419
17	0.422	54.964	52	0.769	146.760	87	1.048	267.064
18	0.433	57.304	53	0.778	149.985	88	1.056	270.686
19	0.443	59.648	54	0.787	153.210	89	1.063	274.309
20	0.454	61.988	55	0.795	156.439	90	1.071	277.935
21	0.464	64.331	56	0.804	159.664	91	1.078	281.595
22	0.475	66.671	57	0.812	162.889	92	1.085	285.405
23	0.485	69.015	58	0.821	166.118	93	1.091	289.215
24	0.495	71.359	59	0.829	169.354	94	1.098	293.025
25	0.506	73.796	60	0.838	172.658	95	1.105	296.846
26	0.516	76.241	61	0.846	175.958	96	1.111	300.671
27	0.526	78.683	62	0.855	179.261	97	1.118	304.493
28	0.537	81.124	63	0.863	182.561	98	1.124	308.314
29	0.547	83.569	64	0.871	185.861	99	1.131	312.139
30	0.557	86.010	65	0.880	189.195	100	1.138	315.960
31	0.567	88.455	66	0.888	192.611			
32	0.578	90.896	67	0.896	196.031			
33	0.588	93.368	68	0.904	199.448			
34	0.598	95.914	69	0.912	202.864			
35	0.608	98.460	70	0.920	206.310			

Appendix B: Data recorded from digitizing trapping efficiency

B.4 TR = 90%

ID	Velocity (ft/sec)	BW (ft)	ID	Velocity (ft/sec)	BW (ft)	ID	Velocity (ft/sec)	BW (ft)
1	0.203	28.133	36	0.649	168.180	71	0.959	355.313
2	0.219	30.158	37	0.660	172.943	72	0.967	360.893
3	0.235	32.629	38	0.671	177.784	73	0.974	366.499
4	0.250	35.100	39	0.682	182.764	74	0.982	372.128
5	0.265	37.751	40	0.692	187.740	75	0.989	377.756
6	0.280	40.725	41	0.702	192.814	76	0.997	383.385
7	0.295	43.725	42	0.712	197.936	77	1.005	389.010
8	0.309	47.239	43	0.721	203.059	78	1.012	394.665
9	0.323	50.753	44	0.731	208.185	79	1.019	400.384
10	0.337	54.266	45	0.741	213.330	80	1.026	406.103
11	0.351	57.795	46	0.750	218.565	81	1.033	411.821
12	0.364	61.631	47	0.760	223.800	82	1.040	417.540
13	0.378	65.471	48	0.769	229.035	83	1.047	423.259
14	0.391	69.308	49	0.778	234.289	84	1.055	428.978
15	0.404	73.148	50	0.787	239.621	85	1.062	434.696
16	0.417	77.205	51	0.796	244.950	86	1.069	440.415
17	0.430	81.375	52	0.805	250.283	87	1.076	446.134
18	0.442	85.541	53	0.814	255.611	88	1.083	451.864
19	0.455	89.711	54	0.823	260.944	89	1.089	457.740
20	0.467	94.151	55	0.831	266.441	90	1.095	463.620
21	0.479	98.610	56	0.840	271.969	91	1.101	469.500
22	0.491	103.065	57	0.848	277.496	92	1.107	475.380
23	0.503	107.524	58	0.856	283.020	93	1.113	481.275
24	0.514	112.088	59	0.864	288.566	94	1.119	487.204
25	0.526	116.651	60	0.872	294.113	95	1.124	493.133
26	0.537	121.215	61	0.880	299.659	96	1.130	499.054
27	0.549	125.779	62	0.888	305.205	97	1.136	504.964
28	0.561	130.343	63	0.896	310.748	98	1.142	510.870
29	0.572	134.974	64	0.904	316.294	99	1.148	516.780
30	0.583	139.710	65	0.912	321.840	100	1.154	522.686
31	0.594	144.443	66	0.920	327.413			
32	0.605	149.179	67	0.927	332.993			
33	0.616	153.911	68	0.935	338.573			
34	0.627	158.651	69	0.943	344.153			
35	0.638	163.414	70	0.951	349.733			

Appendix B: Data recorded from digitizing trapping efficiency

B.5 TR = 95%

ID	Velocity (ft/sec)	BW (ft)	ID	Velocity (ft/sec)	BW (ft)	ID	Velocity (ft/sec)	BW (ft)
1	0.160	36.773	36	0.678	369.653	71	0.950	745.706
2	0.183	44.164	37	0.687	380.164	72	0.956	756.608
3	0.205	51.690	38	0.697	390.754	73	0.962	767.531
4	0.226	59.535	39	0.705	401.486	74	0.968	778.455
5	0.245	67.834	40	0.712	412.215	75	0.973	789.379
6	0.265	76.155	41	0.720	422.948	76	0.979	800.303
7	0.285	84.563	42	0.728	433.680	77	0.985	811.223
8	0.304	93.060	43	0.737	444.386	78	0.991	822.146
9	0.321	102.004	44	0.745	455.066	79	0.996	833.070
10	0.339	110.948	45	0.753	465.743	80	1.002	843.994
11	0.357	119.891	46	0.762	476.423	81	1.008	854.918
12	0.375	128.835	47	0.770	487.118	82	1.014	865.841
13	0.391	138.116	48	0.778	497.865	83	1.019	876.765
14	0.407	147.593	49	0.786	508.616	84	1.025	887.693
15	0.422	157.054	50	0.793	519.364	85	1.031	898.620
16	0.438	166.500	51	0.801	530.111	86	1.037	909.548
17	0.454	175.943	52	0.809	540.859	87	1.042	920.475
18	0.469	185.498	53	0.817	551.610	88	1.048	931.403
19	0.484	195.101	54	0.824	562.358	89	1.054	942.326
20	0.499	204.705	55	0.832	573.105	90	1.060	953.254
21	0.512	214.661	56	0.840	583.853	91	1.065	964.181
22	0.524	224.798	57	0.848	594.604	92	1.071	975.109
23	0.537	234.968	58	0.855	605.370	93	1.076	986.066
24	0.549	245.160	59	0.863	616.140	94	1.081	997.031
25	0.560	255.353	60	0.870	626.910	95	1.087	1007.993
26	0.572	265.583	61	0.878	637.680	96	1.092	1018.958
27	0.584	275.843	62	0.885	648.446	97	1.097	1029.923
28	0.595	286.166	63	0.893	659.216	98	1.102	1040.884
29	0.606	296.546	64	0.901	669.986	99	1.107	1051.849
30	0.616	306.926	65	0.908	680.756	100	1.113	1062.810
31	0.627	317.306	66	0.916	691.526			
32	0.638	327.690	67	0.923	702.364			
33	0.648	338.115	68	0.929	713.201			
34	0.658	348.626	69	0.936	724.035			
35	0.668	359.141	70	0.943	734.873			

Appendix C: Comparison of slope calculations between modeled and observed values for Manning's n

C.1 n = 0.2

ID	Slope Model (%)	Slope Observe (%)	Percentage differences	ID	Slope Model (%)	Slope Observe (%)	Percentage differences	ID	Slope Model (%)	Slope Observe (%)	Percentage differences
1	0.02	-0.02	188.89	36	2.73	2.93	6.92	71	8.06	8.54	5.62
2	0.04	-0.01	488.89	37	2.85	3.08	7.31	72	8.22	8.73	5.84
3	0.06	0.01	714.29	38	2.98	3.22	7.51	73	8.39	8.91	5.84
4	0.08	0.03	162.50	39	3.11	3.37	7.67	74	8.56	9.10	5.93
5	0.11	0.06	86.89	40	3.24	3.51	7.70	75	8.73	9.28	5.93
6	0.15	0.10	55.21	41	3.37	3.65	7.64	76	8.90	9.47	6.02
7	0.19	0.13	41.35	42	3.51	3.79	7.51	77	9.07	9.65	6.01
8	0.23	0.18	28.49	43	3.65	3.94	7.34	78	9.25	9.83	5.90
9	0.28	0.22	23.66	44	3.79	4.08	7.18	79	9.43	10.02	5.89
10	0.33	0.27	21.93	45	3.93	4.23	7.07	80	9.61	10.20	5.78
11	0.38	0.34	13.73	46	4.08	4.38	6.92	81	9.80	10.38	5.59
12	0.44	0.40	-9.20	47	4.22	4.53	6.72	82	9.98	10.57	5.58
13	0.50	0.48	-3.96	48	4.37	4.68	6.59	83	10.17	10.75	5.40
14	0.56	0.56	-0.90	49	4.52	4.84	6.62	84	10.36	10.93	5.22
15	0.63	0.64	0.79	50	4.66	4.99	6.59	85	10.53	11.13	5.39
16	0.70	0.72	2.36	51	4.81	5.15	6.51	86	10.70	11.33	5.56
17	0.78	0.80	3.48	52	4.97	5.31	6.39	87	10.87	11.52	5.64
18	0.85	0.89	3.94	53	5.12	5.46	6.26	88	11.04	11.72	5.80
19	0.94	0.98	4.79	54	5.28	5.62	6.07	89	11.22	11.91	5.79
20	1.02	1.08	5.91	55	5.44	5.78	5.85	90	11.40	12.11	5.86
21	1.10	1.18	6.52	56	5.60	5.94	5.61	91	11.58	12.30	5.85
22	1.19	1.28	6.79	57	5.77	6.09	5.33	92	11.75	12.50	6.00
23	1.29	1.38	6.73	58	5.94	6.25	5.02	93	11.92	12.70	6.14
24	1.38	1.49	6.93	59	6.11	6.41	4.70	94	12.08	12.91	6.43
25	1.48	1.59	6.79	60	6.27	6.57	4.61	95	12.25	13.11	6.56
26	1.59	1.70	6.54	61	6.42	6.75	4.82	96	12.42	13.32	6.76
27	1.69	1.81	6.47	62	6.58	6.93	4.98	97	12.59	13.52	6.88
28	1.79	1.93	7.00	63	6.74	7.10	5.11	98	12.76	13.72	7.00
29	1.90	2.05	7.26	64	6.90	7.28	5.29	99	12.93	13.93	7.18
30	2.01	2.17	7.45	65	7.06	7.46	5.41	100	13.10	14.13	7.29
31	2.13	2.30	7.44	66	7.22	7.64	5.52				
32	2.24	2.42	7.39	67	7.38	7.82	5.59				
33	2.36	2.55	7.23	68	7.55	8.00	5.65				
34	2.48	2.67	6.90	69	7.72	8.18	5.66				
35	2.61	2.79	6.52	70	7.89	8.36	5.67				

Appendix C: Comparison of slope calculation between modeled and observed values for Manning's n

C.2 n=0.35

ID	Slope Model (%)	Slope Observe (%)	Percentage Differences	ID	Slope Model (%)	Slope Observe (%)	Percentage Differences	ID	Slope Model (%)	Slope Observe (%)	Percentage Differences
1	0.04	-0.01	500.00	36	3.82	3.70	3.24	71	9.10	9.27	1.83
2	0.08	0.02	300.00	37	3.96	3.85	2.86	72	9.25	9.44	2.01
3	0.13	0.06	116.67	38	4.11	4.00	2.75	73	9.40	9.61	2.19
4	0.18	0.12	50.00	39	4.26	4.14	2.90	74	9.55	9.78	2.35
5	0.23	0.19	21.05	40	4.40	4.30	2.33	75	9.70	9.95	2.51
6	0.29	0.26	11.54	41	4.54	4.45	2.02	76	9.85	10.12	2.67
7	0.36	0.33	9.09	42	4.69	4.60	1.96	77	10.01	10.28	2.63
8	0.43	0.40	7.50	43	4.83	4.76	1.47	78	10.16	10.45	2.78
9	0.51	0.48	6.25	44	4.98	4.91	1.43	79	10.32	10.62	2.82
10	0.59	0.57	3.51	45	5.13	5.06	1.38	80	10.49	10.79	2.78
11	0.68	0.66	3.03	46	5.28	5.22	1.15	81	10.65	10.96	2.83
12	0.77	0.75	2.67	47	5.43	5.38	0.93	82	10.82	11.12	2.70
13	0.87	0.84	3.57	48	5.58	5.53	0.90	83	10.98	11.29	2.75
14	0.97	0.94	3.19	49	5.72	5.69	0.53	84	11.14	11.46	2.79
15	1.07	1.04	2.88	50	5.88	5.85	0.51	85	11.30	11.63	2.84
16	1.18	1.15	2.61	51	6.03	6.01	0.33	86	11.45	11.80	2.97
17	1.29	1.26	2.38	52	6.18	6.17	0.16	87	11.61	11.97	3.01
18	1.40	1.37	2.19	53	6.32	6.33	0.16	88	11.76	12.14	3.13
19	1.52	1.48	2.70	54	6.47	6.49	0.31	89	11.92	12.31	3.17
20	1.64	1.59	3.14	55	6.62	6.65	0.45	90	12.07	12.49	3.36
21	1.77	1.70	4.12	56	6.77	6.81	0.59	91	12.20	12.66	3.63
22	1.90	1.81	4.97	57	6.92	6.98	0.86	92	12.34	12.83	3.82
23	2.02	1.94	4.12	58	7.07	7.14	0.98	93	12.48	13.01	4.07
24	2.16	2.06	4.85	59	7.23	7.30	0.96	94	12.63	13.18	4.17
25	2.29	2.18	5.05	60	7.38	7.46	1.07	95	12.79	13.35	4.19
26	2.42	2.31	4.76	61	7.53	7.62	1.18	96	12.95	13.52	4.22
27	2.56	2.44	4.92	62	7.69	7.79	1.28	97	13.09	13.70	4.45
28	2.70	2.57	5.06	63	7.85	7.95	1.26	98	13.23	13.87	4.61
29	2.83	2.71	4.43	64	8.00	8.11	1.36	99	13.37	14.05	4.84
30	2.97	2.84	4.58	65	8.16	8.28	1.45	100	13.51	14.22	4.99
31	3.12	2.98	4.70	66	8.32	8.44	1.42				
32	3.26	3.12	4.49	67	8.48	8.61	1.51				
33	3.40	3.26	4.29	68	8.65	8.77	1.37				
34	3.53	3.41	3.52	69	8.80	8.94	1.57				
35	3.67	3.56	3.09	70	8.95	9.10	1.65				

Appendix C: Comparison of slope calculation between modeled and observed values for Manning's n

C.3 n=0.8

ID	Slope Model (%)	Slope Observe (%)	Percentage Differences	ID	Slope Model (%)	Slope Observe (%)	Percentage Differences	ID	Slope Model (%)	Slope Observe (%)	Percentage Differences
1	0.15	0.05	200.00	36	5.46	4.68	16.67	71	9.99	9.88	1.11
2	0.24	0.17	41.18	37	5.60	4.83	15.94	72	10.11	10.03	0.80
3	0.35	0.28	25.00	38	5.74	4.97	15.49	73	10.22	10.18	0.39
4	0.47	0.38	23.68	39	5.88	5.12	14.84	74	10.33	10.33	0.00
5	0.60	0.49	22.45	40	6.03	5.27	14.42	75	10.43	10.48	0.48
6	0.73	0.61	19.67	41	6.17	5.41	14.05	76	10.54	10.63	0.85
7	0.86	0.73	17.81	42	6.32	5.56	13.67	77	10.65	10.78	1.21
8	1.00	0.85	17.65	43	6.47	5.71	13.31	78	10.75	10.93	1.65
9	1.14	0.97	17.53	44	6.61	5.85	12.99	79	10.86	11.08	1.99
10	1.28	1.10	16.36	45	6.75	6.00	12.50	80	10.96	11.23	2.40
11	1.43	1.23	16.26	46	6.89	6.15	12.03	81	11.07	11.38	2.72
12	1.59	1.35	17.78	47	7.02	6.30	11.43	82	11.17	11.53	3.12
13	1.76	1.48	18.92	48	7.16	6.44	11.18	83	11.28	11.68	3.42
14	1.93	1.60	20.63	49	7.30	6.59	10.77	84	11.39	11.83	3.72
15	2.12	1.73	22.54	50	7.44	6.74	10.39	85	11.50	11.98	4.01
16	2.27	1.87	21.39	51	7.57	6.89	9.87	86	11.60	12.13	4.37
17	2.42	2.00	21.00	52	7.70	7.04	9.38	87	11.71	12.28	4.64
18	2.58	2.14	20.56	53	7.83	7.19	8.90	88	11.80	12.43	5.07
19	2.74	2.27	20.70	54	7.97	7.33	8.73	89	11.88	12.58	5.56
20	2.91	2.41	20.75	55	8.10	7.48	8.29	90	11.97	12.74	6.04
21	3.08	2.55	20.78	56	8.24	7.63	7.99	91	12.06	12.89	6.44
22	3.26	2.68	21.64	57	8.36	7.78	7.46	92	12.14	13.04	6.90
23	3.44	2.82	21.99	58	8.48	7.93	6.94	93	12.23	13.19	7.28
24	3.60	2.96	21.62	59	8.60	8.08	6.44	94	12.31	13.34	7.72
25	3.76	3.10	21.29	60	8.72	8.23	5.95	95	12.40	13.49	8.08
26	3.92	3.24	20.99	61	8.83	8.38	5.37	96	12.48	13.64	8.50
27	4.08	3.38	20.71	62	8.95	8.53	4.92	97	12.57	13.79	8.85
28	4.24	3.53	20.11	63	9.07	8.68	4.49	98	12.65	13.95	9.32
29	4.40	3.67	19.89	64	9.18	8.83	3.96	99	12.74	14.10	9.65
30	4.56	3.81	19.69	65	9.30	8.98	3.56	100	12.82	14.25	10.04
31	4.73	3.95	19.75	66	9.41	9.13	3.07				
32	4.89	4.10	19.27	67	9.53	9.28	2.69				
33	5.05	4.24	19.10	68	9.64	9.43	2.23				
34	5.18	4.39	18.00	69	9.76	9.58	1.88				
35	5.32	4.53	17.44	70	9.87	9.73	1.44				

Appendix D: Comparison of buffer width determinations between modeled and observed values for trapping efficiency

D.1 TR = 75%

ID	BW Model (ft)	BW Observe (ft)	Percentage Differences	ID	BW Model (ft)	BW Observe (ft)	Percentage Differences	ID	BW Model (ft)	BW Observe (ft)	Percentage Differences
1	14.11	5.17	172.95	36	53.77	45.17	19.05	71	112.63	112.85	0.20
2	14.71	5.34	175.17	37	55.21	46.70	18.23	72	114.66	114.95	0.25
3	15.39	5.48	181.10	38	56.67	48.23	17.52	73	116.71	117.04	0.28
4	16.13	6.10	164.58	39	58.15	49.76	16.88	74	118.79	119.13	0.28
5	16.94	6.93	144.54	40	59.66	51.29	16.32	75	120.89	121.22	0.27
6	17.79	7.76	129.44	41	61.13	53.00	15.34	76	123.02	123.31	0.23
7	18.70	8.52	119.60	42	62.62	54.75	14.37	77	125.17	125.40	0.18
8	19.65	9.25	112.52	43	64.13	56.51	13.49	78	127.35	127.49	0.11
9	20.64	9.98	106.87	44	65.64	58.31	12.57	79	129.55	129.59	0.02
10	21.66	10.80	100.65	45	67.15	60.20	11.56	80	131.78	131.68	0.08
11	22.69	11.85	91.55	46	68.69	62.08	10.64	81	134.03	133.77	0.20
12	23.75	12.90	84.15	47	70.24	63.97	9.80	82	136.31	135.86	0.33
13	24.83	13.95	77.99	48	71.81	65.85	9.05	83	138.61	137.95	0.48
14	25.93	15.00	72.87	49	73.40	67.74	8.36	84	140.95	140.04	0.65
15	27.05	16.11	67.95	50	75.01	69.62	7.74	85	143.30	142.13	0.82
16	28.19	17.22	63.74	51	76.64	71.54	7.13	86	145.69	144.23	1.01
17	29.35	18.33	60.13	52	78.25	73.56	6.37	87	148.09	146.31	1.22
18	30.52	19.44	57.04	53	79.88	75.59	5.66	88	150.53	148.41	1.43
19	31.71	20.59	54.00	54	81.52	77.62	5.03	89	152.99	150.50	1.65
20	32.90	21.88	50.35	55	83.19	79.65	4.44	90	155.48	152.59	1.89
21	34.10	23.17	47.18	56	84.89	81.68	3.92	91	157.90	154.83	1.99
22	35.33	24.47	44.40	57	86.60	83.71	3.45	92	160.33	157.09	2.06
23	36.55	25.83	41.54	58	88.33	85.74	3.02	93	162.79	159.36	2.15
24	37.78	27.32	38.31	59	90.08	87.80	2.59	94	165.27	161.62	2.26
25	39.02	28.80	35.49	60	91.83	89.88	2.17	95	167.77	163.89	2.37
26	40.28	30.29	32.99	61	93.61	91.97	1.78	96	170.30	166.16	2.50
27	41.56	31.73	30.99	62	95.41	94.06	1.44	97	172.86	168.42	2.63
28	42.86	33.17	29.20	63	97.23	96.14	1.13	98	175.44	170.69	2.78
29	44.17	34.61	27.62	64	99.08	98.23	0.87	99	178.04	172.95	2.94
30	45.50	36.05	26.22	65	100.95	100.32	0.63	100	180.67	175.22	3.12
31	46.84	37.56	24.71	66	102.83	102.40	0.42				
32	48.19	39.08	23.31	67	104.75	104.49	0.25				
33	49.56	40.60	22.06	68	106.68	106.58	0.10				
34	50.94	42.12	20.95	69	108.64	108.67	0.03				
35	52.35	43.64	19.95	70	110.62	110.76	0.12				

Appendix D: Comparison of buffer width determinations between modeled and observed values for trapping efficiency

D.2 TR = 80%

ID	BW Model (ft)	BW Observe (ft)	Percentage Differences	ID	BW Model (ft)	BW Observe (ft)	Percentage Differences	ID	BW Model (ft)	BW Observe (ft)	Percentage Differences
1	16.57	13.86	19.58	36	69.82	70.51	0.98	71	152.75	153.15	0.26
2	17.18	14.71	16.83	37	71.85	72.39	0.74	72	155.49	155.90	0.27
3	17.95	15.59	15.12	38	73.90	74.26	0.48	73	158.26	158.66	0.25
4	18.84	16.71	12.77	39	75.99	76.14	0.19	74	161.07	161.41	0.21
5	19.84	17.82	11.35	40	78.11	78.02	0.13	75	163.91	164.16	0.15
6	20.94	18.95	10.55	41	80.27	79.89	0.47	76	166.78	166.92	0.08
7	22.13	20.07	10.23	42	82.45	81.77	0.83	77	169.69	169.67	0.01
8	23.38	21.21	10.27	43	84.66	83.68	1.17	78	172.63	172.42	0.12
9	24.70	22.44	10.07	44	86.82	85.83	1.15	79	175.52	175.27	0.14
10	26.03	23.88	9.02	45	89.01	87.98	1.17	80	178.41	178.14	0.15
11	27.42	25.32	8.31	46	91.23	90.13	1.22	81	181.34	181.01	0.18
12	28.85	26.76	7.80	47	93.49	92.28	1.31	82	184.31	183.89	0.23
13	30.32	28.21	7.48	48	95.78	94.43	1.42	83	187.30	186.76	0.29
14	31.78	29.90	6.30	49	98.10	96.58	1.57	84	190.32	189.63	0.37
15	33.26	31.67	5.02	50	100.44	98.77	1.69	85	193.33	192.56	0.40
16	34.76	33.45	3.94	51	102.73	101.14	1.57	86	196.34	195.51	0.43
17	36.30	35.22	3.06	52	105.06	103.52	1.49	87	199.38	198.46	0.46
18	37.86	36.99	2.34	53	107.41	105.89	1.44	88	202.44	201.41	0.51
19	39.44	38.77	1.74	54	109.81	108.27	1.42	89	205.55	204.36	0.58
20	41.05	40.55	1.24	55	112.23	110.64	1.44	90	208.67	207.32	0.66
21	42.68	42.36	0.73	56	114.69	113.01	1.48	91	211.84	210.27	0.75
22	44.33	44.18	0.33	57	117.18	115.39	1.55	92	215.03	213.22	0.85
23	46.00	46.00	0.00	58	119.61	117.94	1.41	93	218.26	216.17	0.96
24	47.70	47.81	0.24	59	122.03	120.56	1.21	94	221.51	219.13	1.09
25	49.42	49.63	0.43	60	124.48	123.18	1.05	95	224.80	222.08	1.23
26	51.16	51.44	0.55	61	126.96	125.81	0.91	96	228.12	225.03	1.37
27	52.93	53.26	0.61	62	129.47	128.43	0.81	97	231.48	227.98	1.53
28	54.71	55.14	0.77	63	131.98	131.11	0.66	98	234.86	230.94	1.70
29	56.51	57.07	0.99	64	134.46	133.87	0.44	99	238.28	233.89	1.88
30	58.32	59.00	1.15	65	136.98	136.62	0.26	100	241.72	236.84	2.06
31	60.17	60.93	1.26	66	139.53	139.38	0.11				
32	62.04	62.87	1.31	67	142.11	142.13	0.02				
33	63.94	64.80	1.33	68	144.72	144.89	0.11				
34	65.86	66.73	1.30	69	147.37	147.64	0.19				
35	67.82	68.63	1.18	70	150.04	150.39	0.23				

Appendix D: Comparison of buffer width determinations between modeled and observed values for trapping efficiency

D.3 TR = 85%

ID	BW Model (ft)	BW Observe (ft)	Percentage Differences	ID	BW Model (ft)	BW Observe (ft)	Percentage Differences	ID	BW Model (ft)	BW Observe (ft)	Percentage Differences
1	22.19	23.13	4.06	36	98.41	101.01	2.57	71	211.05	209.76	0.61
2	22.98	24.87	7.60	37	101.29	103.56	2.19	72	214.69	213.22	0.69
3	24.01	26.61	9.77	38	104.22	106.10	1.77	73	218.38	216.67	0.79
4	25.24	28.34	10.94	39	107.19	108.65	1.34	74	222.10	220.13	0.89
5	26.64	30.12	11.55	40	110.21	111.20	0.89	75	225.87	223.58	1.02
6	28.17	32.09	12.22	41	113.28	113.75	0.41	76	229.68	227.03	1.17
7	29.82	34.05	12.42	42	116.23	116.57	0.29	77	233.39	230.57	1.22
8	31.57	36.02	12.35	43	119.17	119.46	0.24	78	236.96	234.22	1.17
9	33.42	37.98	12.01	44	122.16	122.36	0.16	79	240.57	237.87	1.14
10	35.35	39.99	11.60	45	125.20	125.26	0.05	80	244.22	241.52	1.12
11	37.32	42.09	11.33	46	128.27	128.16	-0.09	81	247.90	245.17	1.11
12	39.35	44.19	10.95	47	131.23	131.26	0.02	82	251.62	248.82	1.13
13	41.44	46.29	10.48	48	134.24	134.36	0.09	83	255.38	252.47	1.15
14	43.58	48.39	9.94	49	137.30	137.45	0.11	84	259.17	256.12	1.19
15	45.76	50.48	9.35	50	140.39	140.55	0.11	85	263.00	259.77	1.24
16	47.98	52.62	8.82	51	143.53	143.64	0.08	86	266.87	263.42	1.31
17	50.18	54.96	8.70	52	146.69	146.76	0.05	87	270.79	267.06	1.40
18	52.41	57.30	8.53	53	149.80	149.99	0.13	88	274.79	270.69	1.51
19	54.69	59.65	8.32	54	152.94	153.21	0.18	89	278.82	274.31	1.64
20	57.00	61.99	8.05	55	156.13	156.44	0.20	90	282.89	277.94	1.78
21	59.34	64.33	7.76	56	159.37	159.66	0.18	91	286.93	281.60	1.89
22	61.72	66.67	7.42	57	162.64	162.89	0.15	92	290.68	285.41	1.85
23	64.14	69.02	7.07	58	165.96	166.12	0.10	93	294.47	289.22	1.82
24	66.59	71.36	6.68	59	169.31	169.35	0.02	94	298.29	293.03	1.80
25	69.05	73.80	6.44	60	172.63	172.66	0.02	95	302.11	296.85	1.77
26	71.54	76.24	6.16	61	176.00	175.96	0.02	96	305.97	300.67	1.76
27	74.06	78.68	5.87	62	179.41	179.26	0.08	97	309.85	304.49	1.76
28	76.62	81.12	5.55	63	182.86	182.56	0.16	98	313.77	308.31	1.77
29	79.22	83.57	5.21	64	186.36	185.86	0.27	99	317.72	312.14	1.79
30	81.86	86.01	4.83	65	189.87	189.20	0.35	100	321.71	315.96	1.82
31	84.54	88.46	4.43	66	193.31	192.61	0.36				
32	87.26	90.90	4.00	67	196.79	196.03	0.39				
33	90.01	93.37	3.60	68	200.31	199.45	0.43				
34	92.77	95.91	3.27	69	203.88	202.86	0.50				
35	95.56	98.46	2.95	70	207.45	206.31	0.55				

Appendix D: Comparison of buffer width determinations between modeled and observed values for trapping efficiency

D.4 TR = 90%

ID	BW Model (ft)	BW Observe (ft)	Percentage Differences	ID	BW Model (ft)	BW Observe (ft)	Percentage Differences	ID	BW Model (ft)	BW Observe (ft)	Percentage Differences
1	34.23	28.13	21.69	36	168.76	168.18	0.34	71	353.83	355.31	0.42
2	33.62	30.16	11.47	37	173.95	172.94	0.58	72	359.72	360.89	0.32
3	33.94	32.63	4.01	38	179.10	177.78	0.74	73	365.55	366.50	0.26
4	35.11	35.10	0.03	39	184.12	182.76	0.74	74	371.37	372.13	0.20
5	37.02	37.75	1.93	40	189.24	187.74	0.80	75	377.25	377.76	0.14
6	39.47	40.73	3.09	41	194.25	192.81	0.75	76	383.19	383.39	0.05
7	42.41	43.73	3.02	42	199.25	197.94	0.66	77	389.19	389.01	0.05
8	45.55	47.24	3.58	43	204.33	203.06	0.63	78	395.15	394.67	0.12
9	48.99	50.75	3.47	44	209.49	208.19	0.62	79	400.87	400.38	0.12
10	52.67	54.27	2.95	45	214.68	213.33	0.63	80	406.65	406.10	0.14
11	56.54	57.80	2.18	46	219.76	218.57	0.54	81	412.47	411.82	0.16
12	60.42	61.63	1.96	47	224.92	223.80	0.50	82	418.35	417.54	0.19
13	64.44	65.47	1.57	48	230.16	229.04	0.49	83	424.29	423.26	0.24
14	68.58	69.31	1.05	49	235.42	234.29	0.48	84	430.29	428.98	0.31
15	72.83	73.15	0.44	50	240.59	239.62	0.40	85	436.34	434.70	0.38
16	77.03	77.21	0.23	51	245.82	244.95	0.36	86	442.45	440.42	0.46
17	81.24	81.38	0.17	52	251.12	250.28	0.34	87	448.60	446.13	0.55
18	85.54	85.54	0.00	53	256.50	255.61	0.35	88	454.79	451.86	0.65
19	89.92	89.71	0.23	54	261.96	260.94	0.39	89	460.17	457.74	0.53
20	94.14	94.15	0.01	55	267.01	266.44	0.21	90	465.59	463.62	0.42
21	98.42	98.61	0.19	56	272.06	271.97	0.03	91	471.05	469.50	0.33
22	102.77	103.07	0.29	57	277.17	277.50	0.12	92	476.54	475.38	0.24
23	107.20	107.52	0.30	58	282.34	283.02	0.24	93	481.99	481.28	0.15
24	111.59	112.09	0.45	59	287.52	288.57	0.36	94	487.26	487.20	0.01
25	116.06	116.65	0.51	60	292.75	294.11	0.46	95	492.57	493.13	0.11
26	120.60	121.22	0.51	61	298.05	299.66	0.54	96	497.96	499.05	0.22
27	125.22	125.78	0.45	62	303.41	305.21	0.59	97	503.48	504.96	0.29
28	129.92	130.34	0.32	63	308.83	310.75	0.62	98	509.04	510.87	0.36
29	134.62	134.97	0.26	64	314.32	316.29	0.62	99	514.64	516.78	0.41
30	139.26	139.71	0.32	65	319.88	321.84	0.61	100	520.27	522.69	0.46
31	143.99	144.44	0.31	66	325.40	327.41	0.61				
32	148.80	149.18	0.25	67	330.96	332.99	0.61				
33	153.68	153.91	0.15	68	336.58	338.57	0.59				
34	158.65	158.65	0.00	69	342.27	344.15	0.55				
35	163.66	163.41	0.15	70	348.02	349.73	0.49				

Appendix D: Comparison of buffer width determinations between modeled and observed values for trapping efficiency

D.5 TR = 95%

ID	BW Model (ft)	BW Observe (ft)	Percentage Differences	ID	BW Model (ft)	BW Observe (ft)	Percentage Differences	ID	BW Model (ft)	BW Observe (ft)	Percentage Differences
1	86.07	36.77	134.05	36	388.77	369.65	5.17	71	740.81	745.71	0.66
2	77.68	44.16	75.89	37	399.05	380.16	4.97	72	750.41	756.61	0.82
3	72.85	51.69	40.93	38	408.77	390.75	4.61	73	759.60	767.53	1.03
4	71.77	59.54	20.55	39	417.33	401.49	3.95	74	768.87	778.46	1.23
5	73.95	67.83	9.02	40	425.99	412.22	3.34	75	778.22	789.38	1.41
6	78.87	76.16	3.57	41	434.77	422.95	2.79	76	787.64	800.30	1.58
7	85.94	84.56	1.63	42	443.64	433.68	2.30	77	797.14	811.22	1.74
8	94.59	93.06	1.64	43	452.88	444.39	1.91	78	806.71	822.15	1.88
9	103.70	102.00	1.66	44	4 62.55	455.07	1.65	79	816.36	833.07	2.01
10	113.67	110.95	2.45	45	472.35	465.74	1.42	80	826.09	843.99	2.12
11	124.32	119.89	3.69	46	482.29	476.42	1.23	81	835.89	854.92	2.23
12	135.54	128.84	5.20	47	492.16	487.12	1.03	82	845.77	865.84	2.32
13	146.33	138.12	5.95	48	501.54	497.87	0.74	83	855.73	876.77	2.40
14	156.97	147.59	6.35	49	511.06	508.62	0.48	84	865.71	887.69	2.48
15	167.95	157.05	6.94	50	520.67	519.36	0.25	85	875.74	898.62	2.55
16	179.27	166.50	7.67	51	530.41	530.11	0.06	86	885.84	909.55	2.61
17	190.88	175.94	8.49	52	540.26	540.86	0.11	87	896.02	920.48	2.66
18	202.39	185.50	9.11	53	550.23	551.61	0.25	88	906.29	931.40	2.70
19	213.99	195.10	9.68	54	560.32	562.36	0.36	89	916.62	942.33	2.73
20	225.86	204.71	10.33	55	570.53	573.11	0.45	90	927.04	953.25	2.75
21	236.49	214.66	10.17	56	580.87	583.85	0.51	91	937.53	964.18	2.76
22	246.56	224.80	9.68	57	591.32	594.60	0.55	92	948.09	975.11	2.77
23	256.64	234.97	9.22	58	601.63	605.37	0.62	93	957.95	986.07	2.85
24	266.79	245.16	8.82	59	612.05	616.14	0.66	94	967.69	997.03	2.94
25	277.12	255.35	8.52	60	622.57	626.91	0.69	95	977.52	1007.99	3.02
26	287.45	265.58	8.23	61	633.22	637.68	0.70	96	987.39	1018.96	3.10
27	297.77	275.84	7.95	62	644.00	648.45	0.69	97	997.33	1029.92	3.16
28	307.88	286.17	7.59	63	654.88	659.22	0.66	98	1007.35	1040.88	3.22
29	317.82	296.55	7.17	64	665.90	669.99	0.61	99	1017.42	1051.85	3.27
30	327.91	306.93	6.84	65	677.04	680.76	0.55	100	1027.57	1062.81	3.32
31	338.17	317.31	6.57	66	688.26	691.53	0.47				
32	348.60	327.69	6.38	67	698.56	702.36	0.54				
33	358.88	338.12	6.14	68	708.98	713.20	0.59				
34	368.69	348.63	5.75	69	719.48	724.04	0.63				
35	378.66	359.14	5.43	70	730.09	734.87	0.65				

Appendix E: Double Mass Plot between modeled and observed values for Manning's n

E.1 n = 0.2

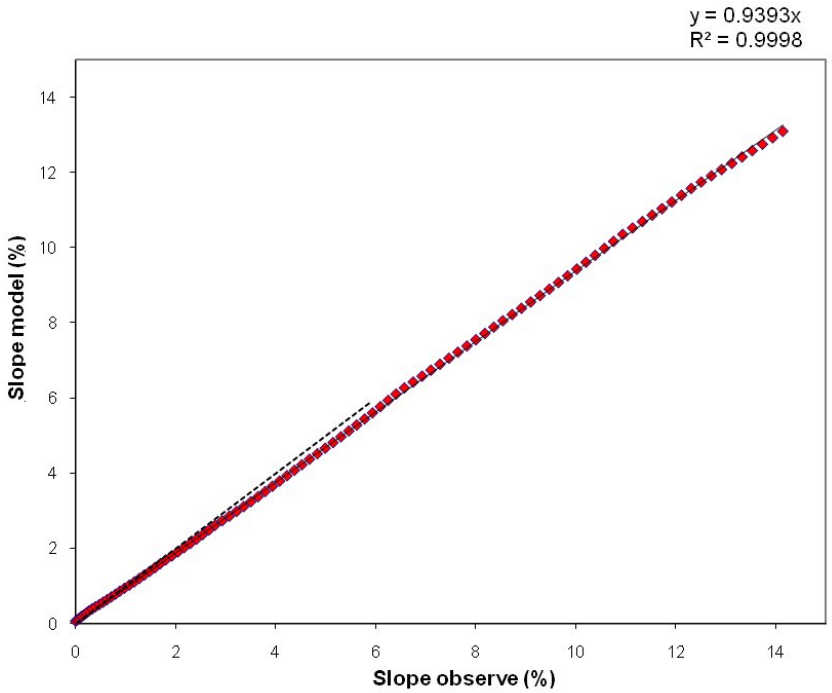

E.2 n = 0.35

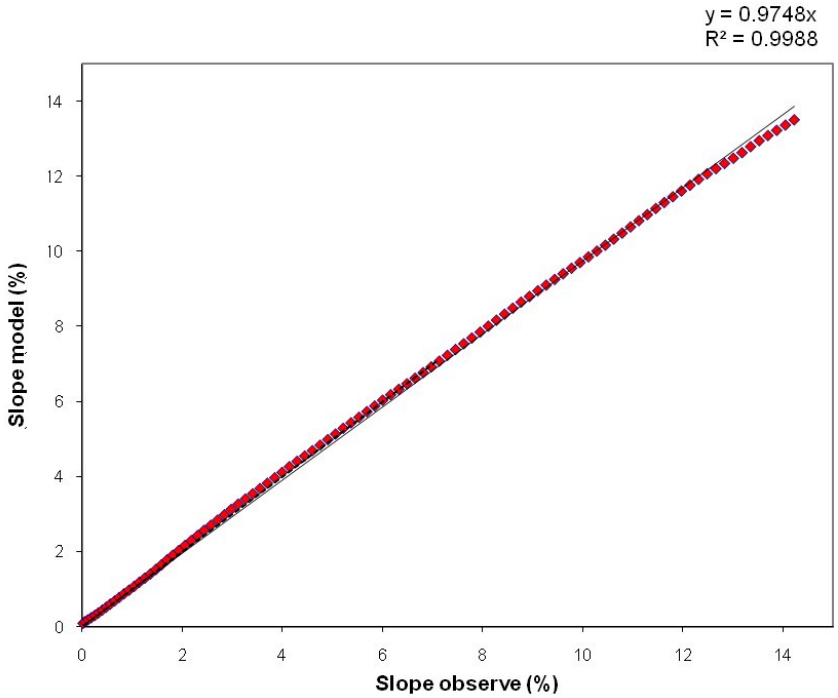

Appendix E: Double Mass Plot between modeled and observed values for Manning's n

E.3 n = 0.8

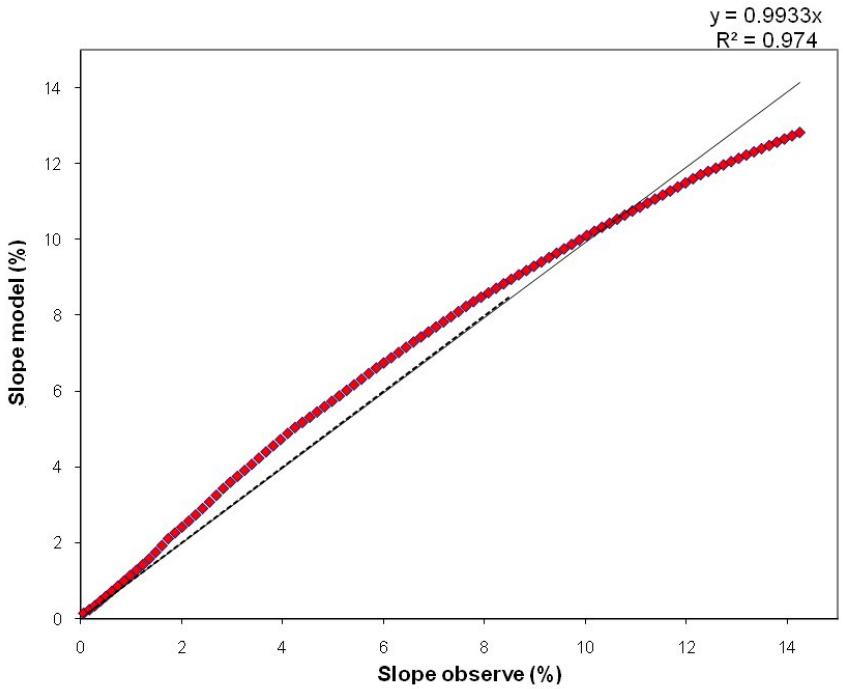

Appendix F: Double Mass Plot between modeled and observed values for trapping efficiency

F.1 TR = 75%

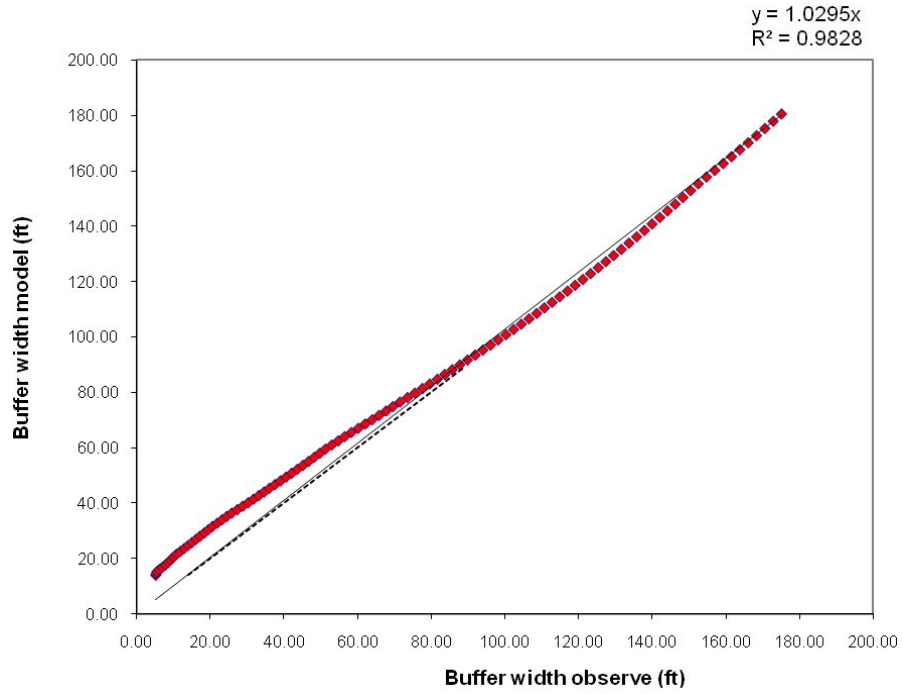

F.2 TR = 80%

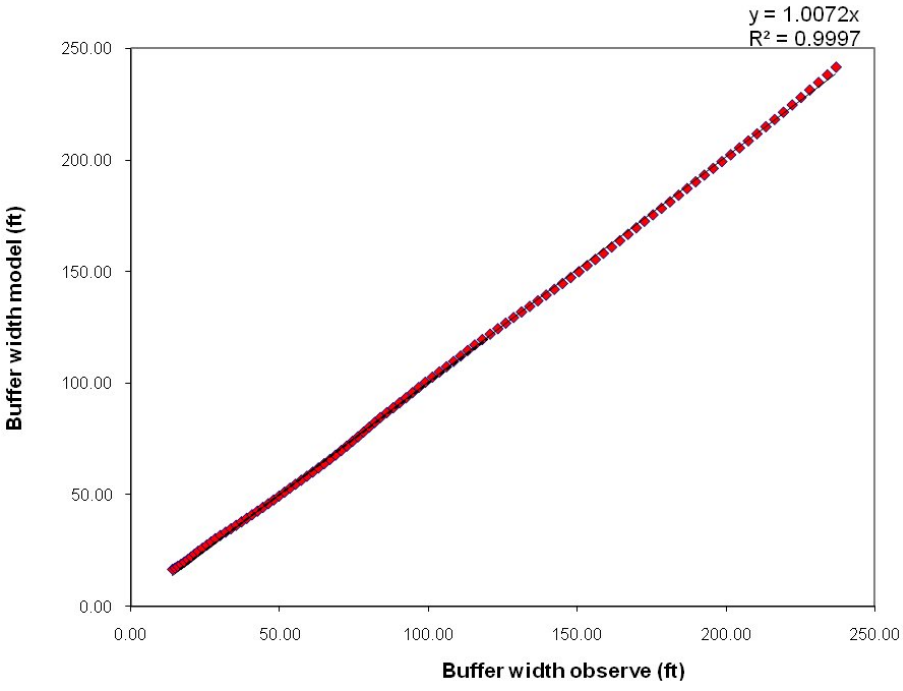

Appendix F: Double Mass Plot between modeled and observed values for trapping efficiency

F.3 TR = 85%

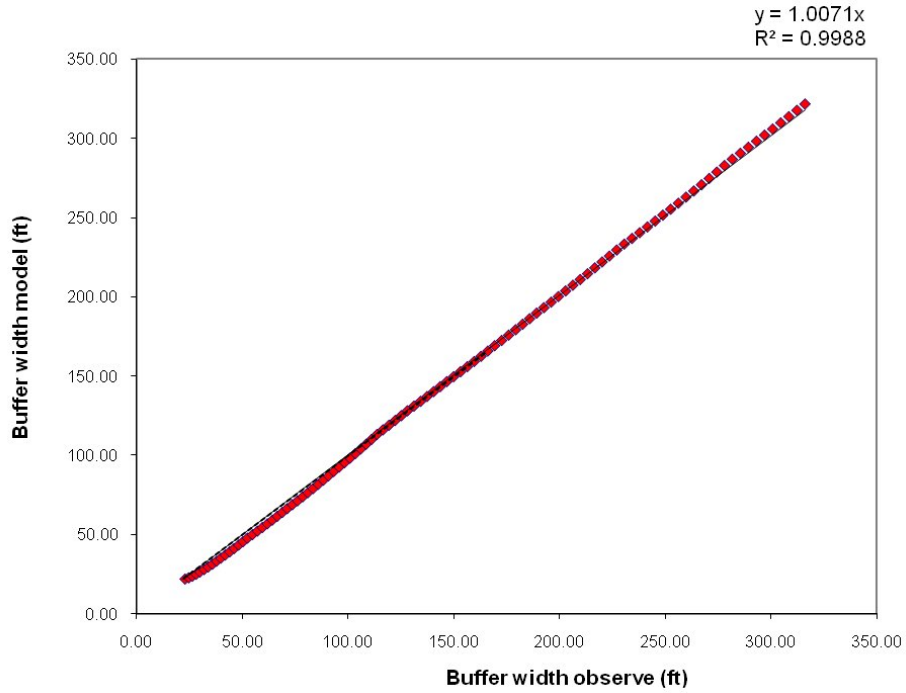

F.4 TR = 90%

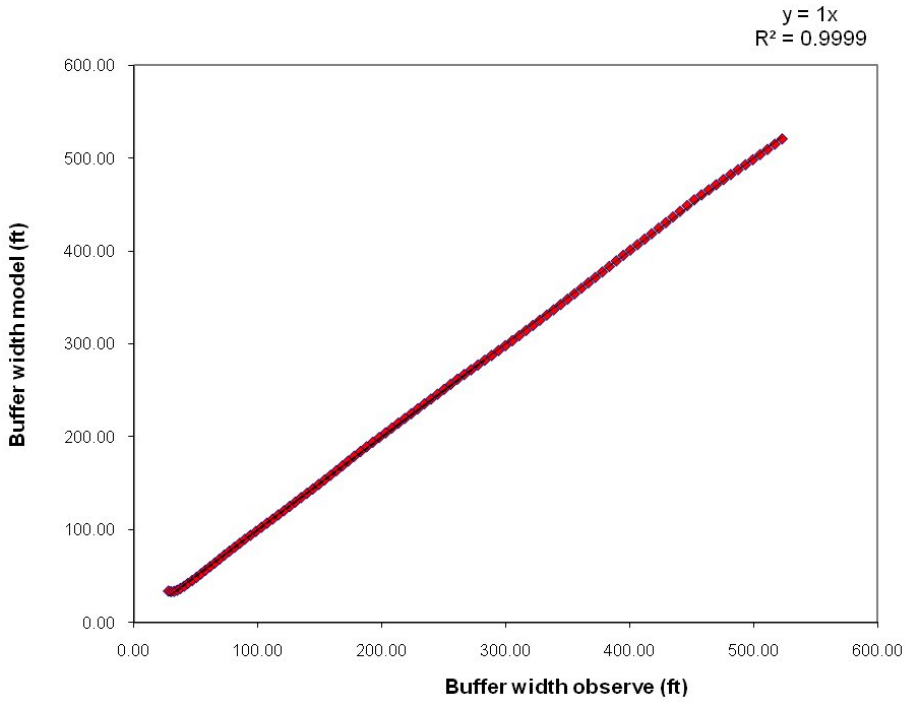

Appendix F: Double Mass Plot between modeled and observed values for trapping efficiency

F.5 TR = 95%

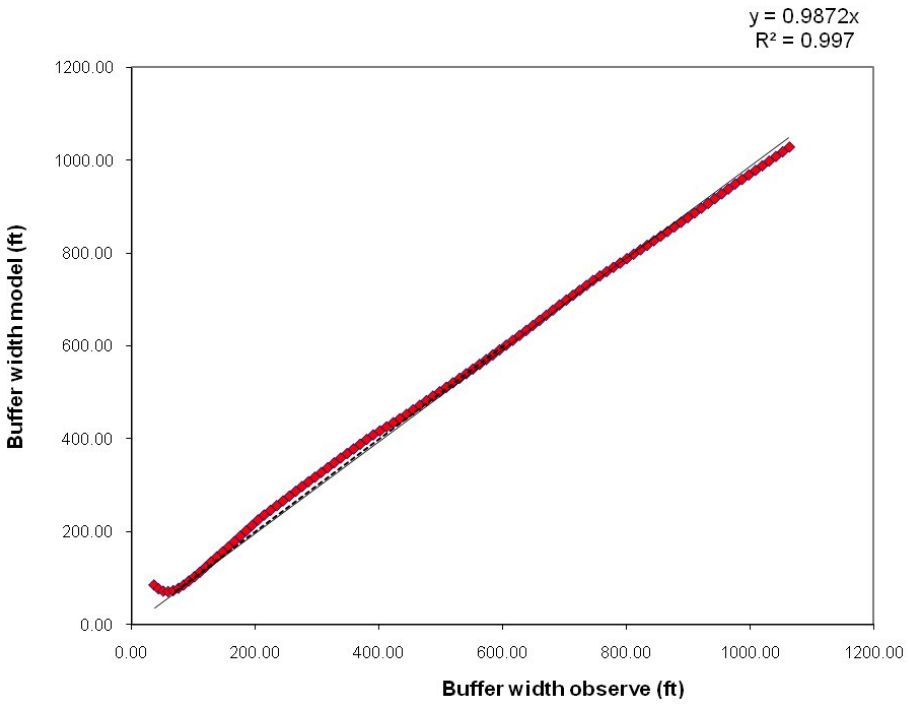

Appendix G: Trapping efficiency from 75% to 95% and its corresponding gradient values

ID	Trapp Efficiency (%)	Gradient of Trapp Efficiency	ID	Trapp Efficiency (%)	Gradient of Trapp Efficiency	ID	Trapp Efficiency (%)	Gradient of Trapp Efficiency
1	75.00	0.251	37	79.50	0.302	72	83.00	0.373
2	75.10	0.251	38	79.60	0.304	73	83.10	0.375
3	75.20	0.251	39	79.70	0.306	74	83.20	0.378
4	75.30	0.251	40	79.80	0.308	75	83.30	0.380
5	75.40	0.251	41	79.90	0.310	76	83.40	0.382
6	75.50	0.251	42	80.00	0.311	77	83.50	0.384
7	75.60	0.251	43	80.10	0.313	78	83.60	0.387
8	75.70	0.252	44	80.20	0.315	79	83.70	0.389
9	75.80	0.252	45	80.30	0.317	80	83.80	0.391
10	75.90	0.252	46	80.40	0.319	81	83.90	0.394
11	76.00	0.253	47	80.50	0.321	82	84.00	0.396
12	76.10	0.254	48	80.60	0.323	83	84.10	0.399
13	76.20	0.254	49	80.70	0.325	84	84.20	0.401
14	76.30	0.255	50	80.80	0.327	85	84.30	0.404
15	76.40	0.256	51	80.90	0.329	86	84.40	0.406
16	76.50	0.257	52	81.00	0.331	87	84.50	0.409
17	76.60	0.258	53	81.10	0.333	88	84.60	0.411
18	76.70	0.259	54	81.20	0.335	89	84.70	0.414
19	76.80	0.260	55	81.30	0.337	90	84.80	0.416
20	76.90	0.261	56	81.40	0.339	91	84.90	0.419
21	77.00	0.262	57	81.50	0.341	92	85.00	0.422
22	78.00	0.276	58	81.60	0.344	93	85.10	0.425
23	78.10	0.277	59	81.70	0.346	94	85.20	0.427
24	78.20	0.279	60	81.80	0.348	95	85.30	0.430
25	78.30	0.281	61	81.90	0.350	96	85.40	0.433
26	78.40	0.282	62	82.00	0.352	97	85.50	0.436
27	78.50	0.284	63	82.10	0.354	98	85.60	0.439
28	78.60	0.286	64	82.20	0.356	99	85.70	0.442
29	78.70	0.287	65	82.30	0.358	100	85.80	0.445
30	78.80	0.289	66	82.40	0.360	101	85.90	0.448
31	78.90	0.291	67	82.50	0.362	102	86.00	0.452
32	79.00	0.293	68	82.60	0.365	103	86.10	0.455
33	79.10	0.294	69	82.70	0.367	104	86.20	0.458
34	79.20	0.296	70	82.80	0.369	105	86.30	0.462
35	79.30	0.298	71	82.90	0.371	106	86.40	0.465
36	79.40	0.300				107	86.50	0.469

Appendix G: Trapping efficiency from 75% to 95% and its corresponding gradient values

ID	Trapp Efficiency (%)	Gradient of Trapp Efficiency	ID	Trapp Efficiency (%)	Gradient of Trapp Efficiency	ID	Trapp Efficiency (%)	Gradient of Trapp Efficiency
108	86.60	0.472	144	90.20	0.679	180	93.80	1.155
109	86.70	0.476	145	90.30	0.687	181	93.90	1.174
110	86.80	0.480	146	90.40	0.696	182	94.00	1.193
111	86.90	0.484	147	90.50	0.705	183	94.10	1.213
112	87.00	0.488	148	90.60	0.715	184	94.20	1.234
113	87.10	0.492	149	90.70	0.724	185	94.30	1.255
114	87.20	0.496	150	90.80	0.734	186	94.40	1.276
115	87.30	0.500	151	90.90	0.744	187	94.50	1.298
116	87.40	0.505	152	91.00	0.754	188	94.60	1.320
117	87.50	0.509	153	91.10	0.764	189	94.70	1.342
118	87.60	0.514	154	91.20	0.775	190	94.80	1.365
119	87.70	0.518	155	91.30	0.786	191	94.90	1.389
120	87.80	0.523	156	91.40	0.797	192	95.00	1.413
121	87.90	0.528	157	91.50	0.809			
122	88.00	0.533	158	91.60	0.820			
123	88.10	0.538	159	91.70	0.832			
124	88.20	0.543	160	91.80	0.844			
125	88.30	0.548	161	91.90	0.857			
126	88.40	0.554	162	92.00	0.870			
127	88.50	0.560	163	92.10	0.883			
128	88.60	0.565	164	92.20	0.896			
129	88.70	0.571	165	92.30	0.910			
130	88.80	0.577	166	92.40	0.924			
131	88.90	0.583	167	92.50	0.938			
132	89.00	0.590	168	92.60	0.953			
133	89.10	0.596	169	92.70	0.968			
134	89.20	0.603	170	92.80	0.983			
135	89.30	0.610	171	92.90	0.998			
136	89.40	0.617	172	93.00	1.014			
137	89.50	0.624	173	93.10	1.031			
138	89.60	0.631	174	93.20	1.047			
139	89.70	0.639	175	93.30	1.064			
140	89.80	0.646	176	93.40	1.082			
141	89.90	0.654	177	93.50	1.099			
142	90.00	0.662	178	93.60	1.117			
143	90.10	0.670	179	93.70	1.136			